

A Thesis Submitted for the Degree of PhD at the University of Warwick

Permanent WRAP URL:

<http://wrap.warwick.ac.uk/134763>

Copyright and reuse:

This thesis is made available online and is protected by original copyright.

Please scroll down to view the document itself.

Please refer to the repository record for this item for information to help you to cite it.

Our policy information is available from the repository home page.

For more information, please contact the WRAP Team at: wrap@warwick.ac.uk

**Crystal Fields for Er^{3+} in Gold and Zero-Field Splittings for Gd^{3+} in
Lanthanum Ethylsulphate**

Fotios Christodoulos, MSc

A thesis submitted for the degree of Doctor of Philosophy

*University of Warwick
Department of Physics*

August 1987

Table of Contents

Table of Contents	i
List of Tables	vi
List of Figures	x
Acknowledgements	xii
Declaration	xiii
Summary	xiv
Dedication	xv
<u>PREFACE</u>	1
<u>AN OUTLINE HISTORY OF CRYSTAL FIELD THEORY</u>	7
<u>CHAPTER 1: DESCRIPTION AND DETERMINATION OF CRYSTAL FIELDS</u>	10
1.1 Free Ion Hamiltonian	10
1.2 Ions in a Crystalline Environment	16
1.3 Parametrisation of the Crystal Field Interaction	20
1.3.1 The Point Charge Model	21
1.4 Experimental Determination of Crystal Fields	28
<u>CHAPTER 2: MORE SOPHISTICATED CRYSTAL FIELD MODELS FOR METAL- LIC SYSTEMS</u>	30
2.1 Introduction	30
2.2 Phenomenological Treatments of the Conduction Electrons	31
2.3 Free Electron Screening Model	35
2.4 The σ - and π -bonding Approach for RE Compounds	36

2.5 Towards a Unified Treatment of Crystal Fields for Rare Earth Doped Compounds	40
2.5.1 Criticisms of Crystal Field Theory	40
2.5.2 The Perturbation Scheme of Stevens	41
2.5.3 First Order Perturbation Theory - Example for non-S-state RE ions	46
2.6 The Determination of Crystal Fields Using a Recently Developed Unified Scheme	50
2.6.1 Introduction	50
2.6.2 Incorporation of Screening	51
2.6.3 The screening constant k_s and the screening function $F(k_s r)$	52
2.6.4 First Order of the DW Model	55
CHAPTER 3: CONTRIBUTIONS TO CRYSTAL FIELD PARAMETERS FOR	
$Er^{3+}:Au$ FROM LIGAND ELECTRONS AND NUCLEI	61
3.1 Introduction	61
3.2 Procedures to be Adopted for Calculations	63
3.3 Wavefunctions	65
3.4 Contributions to the CFPs from the Direct Coulomb Term without Screening	66
3.5 Contributions to the CFPs from the Exchange Term without Screening	70
3.6 Conclusion and Discussion of Chapter 3	74
CHAPTER 4: SCREENING EFFECTS ON THE 4f/LIGAND MECHANISM FOR	
$Er^{3+}:Au$	75
4.1 Introduction	75
4.2 Justification of Approximation made in Section 4.1	76
4.3 Calculation	78
4.4 Approximate Evaluation of the Screening Constant k_s	79

4.5 Results and Comparison with Earlier Work	81
4.6 Conclusion for Chapter 4	83
CHAPTER 5: CONTRIBUTIONS TO CRYSTAL FIELD PARAMETERS FOR	
$Er^{3+}:A_{23}$ FROM A 5d VIRTUAL BOUND STATE	
5.1 Introduction	85
5.2 Preliminaries	86
5.3 Contributions of the 4f/5d(vbs) Mechanism to the CFPs when the 5d-vbs Free Ion Wavefunction of Equation (4.11) is Used	87
5.4 Corrections to the Contributions Obtained in Section 5.3 Due to Orthogonalisation of the Free 5d-vbs to Neighbouring Sites	90
5.5 Conclusion and Discussion of Chapter 5	98
CHAPTER 6: A QUALITATIVE ESTIMATION OF CONTRIBUTIONS TO CFPs	
FOR $Er^{3+}:A_{23}$ AND $Er^{3+}:A_{81}$ FROM A SPLIT OFF STATE FROM THE MAJORITY	
CONDUCTION BAND	
6.1 Introduction	99
6.2 Direct contributions	103
6.3 Exchange contributions	105
6.4 Conclusion and Discussion of Chapter 6	107
CHAPTER 7: ZERO-FIELD SPLITTINGS FOR S-STATE IONS	
7.1 Introduction-First Order Perturbation for S-state Ions: $P_0 H P_0$	109
7.2 Review of Intra-site Mechanisms Resulting in the ZFS of Gd^{3+}	114
7.2.1 Hutchison, Judd and Pope Mechanism	114
7.2.2 Judd Mechanism	115
7.2.3 Third-order Spin-Spin Interaction Mechanism	115
7.2.4 Second-order Spin-Spin Interaction Mechanism	115

7.2.5 Second-order Relativistic Mechanism	115
7.2.6 Crystal Field Configuration Mixing Mechanism	116
7.2.7 Electrostatically Correlated Crystal Fields	116
7.2.8 Fifth-order Configuration Interaction Mechanism	116
7.2.9 Sixth-order Mechanisms	117
7.2.10 Lulek's Mechanism	117
7.2.11 Spin Correlated Crystal Fields	118
7.3 Conclusion and Discussion of Chapter 7	119
CHAPTER 8: INTER-SITE CONTRIBUTIONS TO SCCF AND ZFS FOR Gd^{3+} IN LANTHANUM ETHYLSULPHATE	121
8.1 The Crystal Structure of Lanthanum Ethylsulphate	121
8.2 Preliminaries, Perturbation Theory and Empty States	122
8.3 Categorising of Excitations	129
8.4 An Effective Inter-site Operator	130
8.4.1 Second Quantised Effective Operators	130
8.4.2 Conversion to Effective Spin and Orbital Operators	132
8.5 Evaluation of the Coefficient μ	135
8.6 The Effects of Overlaps	137
8.7 Results and Comparison with the Experiment	138
8.8 Conclusion and Discussion of Chapter 7	140
CHAPTER 9: CONCLUDING REMARKS	142
9.1 CFP's for $Er^{3+}:Am$	142
9.2 ZFS for Gd^{3+} in Lanthanum Ethylsulphate	147
APPENDIX A: Generalised Wannier Functions	149
APPENDIX B: Analytical Expressions for the Radial Wavefunctions Used in Chapter 3	

.....	150
1 Radial Wavefunctions of Neutral-Gold Electronic Orbitals	150
2 The 4f Radial Wavefunction of Er^{3+}	156
3 The 5d (vbs) Radial Wavefunction of Er^{3+}	157
APPENDIX C: Expansion of the Screened Coulomb Interaction in Legendre Polynomials	
als	158
APPENDIX D: A method for the Expansion of Off-site Functions	
.....	160
APPENDIX E: Values of the F_{λ}^{μ} (4f, 5d, 5d⁴ⁿ) radial integrals of Chapter 5, in e^2/a_0	
units for $n=4, 6$	162
APPENDIX F: Data Used for the Calculation of Chapter 8	
.....	163
APPENDIX G: RAPW energy bands of Silver and Gold	
.....	168
1 RAPW band structure of Gold	168
2 RAPW band structure of Silver	168
REFERENCES	169

List of Tables

Table 1.1: Energy levels in cm^{-1} for Er^{3+} (Dieke 1968).	18
Table 1.2: Comparison between experimental results obtained from EPR, inelastic neutron scattering and susceptibility measurements on samples of RE ions in Ag and Au and theoretical results obtained from a lattice sum PC calculation. All measurements have been performed on dilute alloys except those of ref.[d] which refer to the intermetallic compound.	26
Table 2.1: CFP (in cm^{-1}) calculated in the framework of the π model approach for the RE intermetallics with the $CsCl$ structure. a_0 stands for a lattice constant of cubic unit cell. References in the last column concern only experimental data.	39
Table 2.2: Values of β^{AA} , β^P , β^{CP} for Al, Li and Na. r_s is in units of a_0 .	55
Table 4.1: Comparison between theory and experiment	82
Table 5.1: Values of 4f-5d(vbs) Slater integrals for $Er^{3+}:Au$. k_z is in a_0^{-1} units and the Slater integrals in cm^{-1} .	89
Table 5.2: Values of various contributions to C_4 in cm^{-1} for $Er^{3+}:Au$ due to the direct and exchange terms of the 4f-5d(vbs) interaction. k_z is in units of a_0^{-1} .	89
Table 5.3: Polar coordinates of the twelve nearest neighbours of the RE site.	92
Table 6.1: The parameters C_i and Z_i which define the 6s radial wavefunction of Gold given by equation (6.4).	101
Table 6.2: The parameters C_i and Z_i which define the 6s radial wavefunction of Silver given by equation (6.5).	102
Table 6.3: Values of the F direct radial integrals defined in equation (6.11), in e^2/a_0 .	105

Table 6.4: CFPs derived from the direct $4f/4d$ interaction for $Er^{3+}:Au$ and $Er^{3+}:Ag$ in cm^{-1} .	105
Table 6.5: Values of the G exchange radial integrals defined in equation (6.16), in e^2/a_0 .	107
Table 6.6: CFPs derived from the exchange $4f/4d$ interaction for $Er^{3+}:Au$ and $Er^{3+}:Ag$ in cm^{-1} .	107
Table 7.1: Calculated values (by using non-relativistic wavefunctions) for the contributions of various ground-state splitting mechanisms for $E(\pm 7/2) \rightarrow E(\pm 1/2)$ transitions (Buckmaster et al 1972, Wybourne 1966).	118
Table 8.1: Parameters for the 1s and 2s Oxygen wavefunctions	127
Table 8.2: Overlaps and sum of squares of overlaps S	128
Table 8.3: Energy of $ \phi_n^s\rangle$, in e^2/a_0 , for a range of values of Z_{eff} and A	129
Table 8.4: Values of the total μ (in cm^{-1}) as a function of A and Z_{eff}	139
Table 9.1: The CFPs from the three components of DW's first order perturbation theory, in comparison with an unscreened PCM with all neighbouring charges equal to +1, and experiment.	143
Table B.1: The parameters C_i and Z_i which define the 1s radial wavefunction of Gold.	150
Table B.2: The parameters C_i and Z_i which define the 2s radial wavefunction of Gold.	150
Table B.3: The parameters C_i and Z_i which define the 2p radial wavefunction of Gold.	151
Table B.4: The parameters C_i and Z_i which define the 3s radial wavefunction of Gold.	151
Table B.5: The parameters C_i and Z_i which define the 3p radial wavefunction of Gold.	152

Table B.6: The parameters C_i and Z_i which define the 3d radial wavefunction of Gold	152
Table B.7: The parameters C_i and Z_i which define the 4s radial wavefunction of Gold	153
Table B.8: The parameters C_i and Z_i which define the 4p radial wavefunction of Gold	153
Table B.9: The parameters C_i and Z_i which define the 4d radial wavefunction of Gold	154
Table B.10: The parameters C_i and Z_i which define the 4f radial wavefunction of Gold	154
Table B.11: The parameters C_i and Z_i which define the 5s radial wavefunction of Gold	155
Table B.12: The parameters C_i and Z_i which define the 5p radial wavefunction of Gold	155
Table B.13: The parameters C_i and Z_i which define the 5d radial wavefunction of Gold	156
Table B.14: The parameters C_i and Z_i which define the 4f radial wavefunction of Er^{3+}	156
Table B.15: The parameters C_i and Z_i which define the 5d(vbs) radial wavefunction of Er^{3+}	157
Table E.1: F_L^{+2} (4f, 5d $^{E+}$, 5d $^{A+}$) radial integrals defined by (5.15), in e^2/a_0	162
Table F.1: Parameters of the 4f-radial wavefunction for Gd^{3+}	163
Table F.2: Values of the 6j-symbol $\left\{ \begin{matrix} 3 & 2 & 1 \\ 3 & 2 & 1 \end{matrix} \right\}$	163
Table F.3: Values of the $\langle l Y_L l \rangle$	163
Table F.4: Values of Δ , KE and PE components of $P(R_1)$ for $Z_{eff} = 10$ varying with	

A for $R_1 = 4.4785a_0$	164
Table F.5: Values of KE and PE components of $P(R_2)$ for $Z_{eff} = 10$ varying with A for $R_2 = 4.7619a_0$	164
Table F.6: Values of $R(lL)$ in cm as A varies and for $Z_{eff} = 0$. Columns headed (lL)	165
Table F.7: Values of $Q(lLR)$ in e^2a_0 for $R_1 = 4.4785a_0$ as A varies. Columns headed (lL).	165
Table F.8: Values of $Q(lLR)$ in e^2a_0 for $R_2 = 4.7619a_0$ as A varies. Columns headed (lL).	166
Table F.9: The $\langle g_{3s}(r) g_{3s}(r - R) \rangle$ overlap. All R_{ij} are in a_0 units.	166
Table F.10: Radial integral of the $\langle f_{4f}(r) g_{3s}(r - R) \rangle$ overlap.	167

List of Figures

Figure 1: Observed energy levels of the RE ions. The thickness of each level represents the total CF splitting in $LaCl_3$. A pendant semicircle indicates that this level fluoresces in the $LaCl_3$ structure (from Dieke 1968 p.142).	19
Figure 2: Comparison of energy levels of Er^{3+} from theory (intermediate coupling); experiment - free ion; crystal spectra - $Er(C_2H_5SO_4)_3 \cdot 9H_2O$; approximate theory (RS-coupling). For instructive purposes a few examples are shown (from Hüfner 1978 p.17).	20
Figure 3: Schematic picture explaining the idea of the classical and modified PCM models. The black circles represent the charge of the ligands, open circles the positive charge of the RE ion (Zolnieriek 1984)	37
Figure 4: The full curve represents the function $F(k_e r)$ of equation (2.27) and the broken curve the function $\exp(-k_e r)$	53
Figure 5: Comparison of the unscreened Coulomb interaction e^2/r with $(e^2/r) F(k_e r)$ and $(e^2/r) \exp(-k_e r)$	53
Figure 6: Interaction between a $4f(RE)$ and a ligand electron. Co-ordinate system used for the calculation of the <u>direct</u> part of V_{direct} (see equation 2.33).	64
Figure 7: Interaction between a $4f(RE)$ and a ligand electron. Co-ordinate system used for the calculation of the <u>exchange</u> part of V_{direct} (see equation 2.33).	65
Figure 8: p_σ parameter as a function of internuclear distance for $Er^{3+}Au$. Contributions solely from the Direct Coulomb term have been considered.	69
Figure 9: The Hermann-Skillman 5d radial wavefunction of Gold, $P_{5d}(r)$, given in the Appendix (full curve) and the approximation used, given by equation (3.18),	

for the estimation of the exchange contribution (dotted curve).	73
Figure 10: Variation of the 5d-vbs energy (in e^2/a_0) with the value of k_e (in a_0^{-1})	81
Figure 11 : Variation of C_s (in cm^{-1}) with k_e (in a_0^{-1}). Only nearest neighbour contributions with charges of +1 have been taken into account	83
Figure 12: The twelve nearest neighbours (labelled as 1,2, ..., 12 of the fcc structure of $Er^{3+}:Al$. The impurity site is labelled as 0.	91
Figure 13: Diagram showing the geometrical configuration (not to scale) of the nearest neighbours surrounding a RE ion in an ethylsulphate crystal. R_1 to R_9 label Oxygen sites.	122

ACKNOWLEDGEMENTS

I should firstly like to express my gratitude to Dr J M Dixon, my research supervisor, for introducing me to the subject of Crystal Fields, excellent supervision, generous encouragement and unbounded enthusiasm throughout the course of this work.

Special thanks are due to several friends: George Galanakis who has a similar appreciation of life to myself. Dave Holton, Mike Kearney, Ian Stroud and Graham Warren with whom I shared many enjoyable moments.

I also thank the academic staff of the Physics Department of the University of Warwick for the experience I have gained with them.

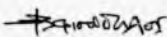
For financial support, I thank:

- [1] the "*Alexander S Onassis Public Benefit Foundation*" for a 22-month studentship.
- [2] the "*Vice-Chancellor Fund*" committee of the University of Warwick for partial support of my studies.
- [3] the "*Institute of Physics*" and the "*Department of Physics/University of Warwick*" for supporting my participation in the "Annual Solid State Conference" at Imperial College/London 1986.
- [4] the "*MacMillan Memorial Fund*" committee of the Department of Physics/University of Warwick for sustaining attendance at the "Heavy Fermion Compounds" Conference in London 1987.
- [5] the "*Barber Trust Fund*" committee of the Institute of Physics, the "*European Physical Society*" and the "*Department of Physics/University of Warwick*" for providing grants towards my participation in the 7-th General Conference of the European Physical Society at Helsinki-Finland 1987.

DECLARATION

This thesis is submitted to the University of Warwick in support of my application for admission to the degree of Doctor of Philosophy. It contains an account of my work carried out at the Department of Physics of the University of Warwick in the period October 1985 to May 1987 under the supervision of Dr J M Dixon. The work described is the result of my own independent research except where specifically acknowledged in the text. No part of this thesis has been submitted in respect of a degree to this or any other University. Some parts of this work are or will be published or presented at a Conference as detailed below:

- [1] F Christodoulos, J M Dixon and C H A Fitzpatrick 1986, *J Phys C: Solid State Phys* **19**, 5863-83. "Inter-site Contributions to Correlated Crystal Fields and Zero-Field Splittings for Gd^{3+} in Lanthanum Ethylsulphates"
- [2] F Christodoulos and J M Dixon 1987, *J Phys C: Solid State Phys*, accepted for publication. "Comment on a Recent Paper Entitled: Inter-site Contributions to ..."
- [3] F Christodoulos and J M Dixon 1987, *J Phys C: Solid State Phys*, accepted for publication. "The Effects of Screening on the Crystalline Electric Fields for Er^{3+} in Gold"
- [4] F Christodoulos and J M Dixon 1987, *Phys Lett A*, accepted for publication. "A Reassessment of the Role Played by a 5d Virtual Bound State in the Determination of Crystal Fields for Heavy Rare Earth Ions in Gold and Silver"
- [5] J M Dixon and F Christodoulos 1987, *Physica B*, accepted for publication. "Contributions to Crystal Field Parameters for $Er^{3+}:Au$ from Ligand Electrons and Nuclei"
- [6] F Christodoulos and J M Dixon 1987, presented at the "7-th General Conference of the European Physical Society" at Helsinki-Finland 1987. "4f Ligand Penetration & Screening Due to Conduction Electron Effects on the Crystal Fields for Er^{3+} in Gold"


Fotios Christodoulos
August 1987

SUMMARY

In the first and dominant part of the thesis, a recently developed theory for Crystal Fields (CFs) in metals has been used, in its first order, to investigate the microscopic origin of CF splittings for the dilute $Er^{3+}:Au$ alloy. To first order there are three contributions to the CF splitting of the Rare Earth (RE) $4f$ -electron ground state. One is due to penetration effects with ligand ions, another due to a $5d$ semi-localised state about the RE site, the so called *virtual bound state* (vbs), and the third arises from the interaction of the $4f(RE)$ electrons with a discrete band state, denoted by $|c\rangle$, which is split off from the s -like majority conduction band of Gold. The coupling between the $5d$ -vbs and the conduction band has been assumed weak. We find, within the limitations of our calculations, that the model used is quite capable of explaining the CF splitting of the ground level for $Er^{3+}:Au$. In particular we have found that the penetration effects, in the limit of no screening, considerably enhance the Crystal Field Parameters (CFPs) over their Point Charge Model (PCM) values, which consist of a fourth order CFP of the wrong sign, three times smaller than the experimental value and a sixth order CFP of the right sign but five times smaller than the observed. Contributions to CFPs directly from neighbours may be described in terms of a Coulomb interaction using different effective total charges (which we call pseudo-Point Charges) on the ligands for the fourth and sixth order CFPs. The sixth order CFP is much more affected by such effects. When screening is introduced, in an approximate way, we find that it tends to increase (over the unscreened PCM values) the magnitude of the CFPs by as much as 20% principally by screening out the sizable contribution, of opposite sign, from the next nearest neighbours. We also find that the probability of having a reversal in sign for the fourth order CFP, with respect to PCM values, is small since in the regime of the screening constant where we might expect this effect the energy of the $5d$ -vbs is negative corresponding to a bound state. We also estimate the CFPs of $Er^{3+}:Ag$, within the same model. It becomes clear that the model fails to explain the observed CFPs, at least within the approximations made in our first order investigation, unless a basic assumption, concerning the nature of the conduction band, is modified.

In the second part of the thesis we study the Zero Field Splitting (ZFS) of Gd^{3+} -doped lanthanum ethylsulphate. On-site excitations of the Gd^{3+} in this particular salt have recently been shown to produce a Spin Correlated Crystal Field (SCCF) which results in a ZFS of the same sign as those from experiment but, approximately, two times too large. Inter-site one-electron excitations have been invoked to produce additional contributions to the SCCF and so produce a ZFS which compensates the ZFS of the on-site mechanisms to finally produce ZFS in good agreement with experiment. The resultant ZFS is thus a delicate balance between a number of on-site mechanisms i.e. from the Gd^{3+} ion itself, and a contribution from the host in which it is embedded.

To my Parents and Grandmother

PREFACE

The Crystal Field (CF) splitting of otherwise degenerate low-lying ion states significantly modifies the low-temperature magnetic and thermal properties of solids containing such ions (for instance Van Vleck 1932, Bleaney and Stevens 1953). A determination of the CF states is an essential prerequisite for the analysis of low-temperature heat capacity, magnetic susceptibility, electron paramagnetic resonance and inelastic neutron scattering experiments. In spite of the importance of the CF splitting in the above cases and its practical importance in general (for instance rare earth lasers, Prokhorov 1986) very little is known about the physical origin of the Rare Earth (RE) CF splitting in metals. Many efforts have been undertaken in the last few decades (see for instance the proceedings of the five international conferences on CF effects listed in the beginning of the References section) to study such CF splittings. Most of these are based on phenomenological arguments and pay a great deal of attention to the local symmetry by specifying that 4f-electrons are localised about particular sites. Such treatments do not reveal much about the origin of CFs and also their physical validity is questionable since they distinguish electrons (see our discussion in section 2.5.1). In order to circumvent the latter problem and to clarify the microscopic origin of a seemingly unrelated problem namely exchange interactions in mag-

netic insulators, Stevens (1976) developed a specific method of calculating such interactions. The method is very general and may be applied not only to study exchange interactions but also other physical phenomena, like CF interactions (see section 2.5).

Recently, Dixon and Wardlaw (1986a, hereafter DW) used the ideas of Stevens to develop a model for substitutionally dissolved REs in non-magnetic metals. The starting point of DW's investigation was a very *general* Hamiltonian of interacting electrons and nuclei. They performed a series of unitary transformations on the starting Hamiltonian and, with the aid of a particular form of operator degenerate perturbation theory, second quantisation techniques and a separate study of conduction band states (Dixon and Wardlaw 1986b), they were able to incorporate a type of *dynamic screening* (Raimes 1957), the many-body character of the problem and calculate Crystal Field Parameters (CFPs) building in all the rotational and other symmetries of the general starting Hamiltonian.

The objective of this thesis is twofold. The *first* and dominant part is a study of the microscopic origin of CFs for a particular heavy RE dilute in a non-magnetic metal, namely $Er^{3+}:\text{Au}$. We have chosen Er^{3+} since it has both a simple stable configuration (eleven 4f electrons) and a sufficiently large spin-orbit interaction to make the effects of intermediate coupling generally small (section 1.1). As a non-magnetic host, we have chosen Gold since the CFPs for dilute Er^{3+} in Gold are some of the most accurately determined from experiment (Williams and Hirst 1969) and the fcc structure of Gold considerably simplifies calculations. We discuss, within DW's first-order perturbation theory, some possible contributions to CF splittings for the simple case where one Er^{3+} magnetic heavy RE ion is substitutionally dissolved and surrounded by a rigid regular array of non-magnetic Gold ions in an otherwise perfectly periodic metallic host. *Secondly*, using similar techniques, an attempt has been made to improve agreement between theory and experiment for the observed Zero Field Splitting (ZFS) of the S-state ion Gd^{3+} substitutionally dissolved in lanthanum ethylsulphate. To do this we have first calculated the magnitude of the Spin Correlated Crystal Field (SCCF), a mechanism proposed by Newman (1970), and then the resulting ZFS. This is a long standing problem and it is only recently that Tuszyński et al (1984,1986) have calculated this ZFS and obtained a result of the correct sign. However they

found a value which was a factor of two times too large when compared with experiment.

One factor which is common in these seemingly unrelated investigations is the use they both make of methods developed by Stevens (1976). For Gd^{3+} we have used the second order of a particular projector form of degenerate perturbation theory (Bates et al 1968) whereas for $Er^{3+}:Au$ we have only so far incorporated the first order components of DW. Both also study energy splittings of REs in their particular hosts. In the Gadolinium doped lanthanum ethylsulphate the energy separations are within the intermediate coupling (sometimes called spin-orbit mixed coupling) ground state whereas in the other investigation they are splittings of the ground total angular momentum manifold by "crystal fields", arising from a number of sources, in a non-magnetic metal.

The thesis begins with an outline history of CF studies. In the subsequent two chapters an account is presented of the background literature on which the investigation in the thesis depends.

In CHAPTER 1 we present a brief description of free ion spectra and the idea of CFs is introduced for ions in solids. By assuming, for simplicity, a Point Charge Model (PCM) some qualitative aspects of CFs are discussed. The failure of the PCM, at least for CFs in metals, becomes clear and by recalling and discussing some of the assumptions made by the PCM we point out possible improvements of it and consider some of the origins of CFs in solids.

In CHAPTER 2 the main features of various theoretical models for calculating CFPs are represented and the validity of the different approaches is briefly discussed. A large portion of this chapter is devoted to the method of Stevens (1976). This enables the reader to understand how effective operators are found using this method and why in its original form at least, it is valid only within a particular configuration of electrons. The CF operator is shown to be a particular form of such an effective operator. When the method is applied to REs in metals the DW model results and this is described and first order results are given.

From Chapter 3 to Chapter 8 we present and discuss our calculations. For the first part of the thesis we are working within DW's first-order perturbation theory, as we have already mentioned earlier, which involves three interactions. These are the interaction of the RE 4f-electrons

with: (i) the ligand electrons and nuclei, (ii) a 5d virtual bound state (vbs) and (iii) an A_1 -like state split off from the majority conduction band states denoted by $|c_0\rangle$. For purposes of comparison we use the theoretically predicted PCM values of CFPs which give a fourth order CFP for $Er^{3+}:Au$ which is of the wrong sign and about three times smaller than the experimental value and a sixth order CFP of the right sign but about five times too small in comparison with experiment.

In CHAPTER 3 we discuss the interaction (in the limit of no screening) between the RE 4f-electrons with the ligand Gold ions, treated as ionic entities with extended charge distributions. It is shown that the ligand Gold ions can be effectively treated as pseudo-Point Charges (pseudo-PCs) different for each of the fourth and sixth order CFPs. The values of these pseudo-PCs are determined by comparing contributions to CFPs from the 4f/ligand penetration mechanism and a naive PCM. In comparison with unscreened PCM values we find a considerable improvement in the agreement with experiment for the sixth order CFP but the fourth order CFP does not change sign and its magnitude enhances by about 21%.

In CHAPTER 4 approximative methods, which are used to investigate the effect of screening on the above 4f/ligand interaction, are introduced and discussed (since computational difficulties arise in the exact calculation of screening). We conclude that screening of the 4f/ligand interaction does not significantly affect the magnitude of the CFPs resulting from this particular mechanism. We also find that the probability that this interaction will produce a reversal in sign of the fourth order CFP is small. As a consequence, because we did not include screening in Chapter 3, the use of the pseudo-PCs, which we introduced there, should still be reasonably accurate even when screening is incorporated.

In CHAPTER 5 the contribution from a 5d-vbs (its existence is discussed in section 2.2) to CFPs is studied. In a cubic environment such a state splits into two e_g and three t_{2g} states and subsequently, via the interaction between the 4f electrons and the 5d-vbs, the 4f splitting reflects the cubic symmetry. A partial occupancy of the low lying t_{2g} 5d-states is assumed following a number of authors in the literature. We find that good agreement for the fourth order CFP with experiment can be obtained, especially when screening effects are taken into account. Mixing of

the 5d-vbs with neighbouring 5d(Au) ligand orbitals has been found quantitatively insignificant as far as contributions to CFPs are concerned although a qualitatively interesting contribution to the sixth order CFP is found. At this stage a short qualitative comparison between the fourth order CFP of $Er^{3+}:Ag$ and the fourth order CFP of $Er^{3+}:Au$ is presented and discussed.

In CHAPTER 6 estimations of the contributions to CFPs from the interaction between the RE 4f-electrons and a split off discrete state from the s-like majority conduction band of Gold are presented. Only admixtures of 6s states on ligands were considered in $|c_0\rangle$ although smaller contributions might be expected from the 5d, 5p and 5s ligand states and further admixtures from the rest of the band states. The overlap between the 6s on the central site and these 5d, 5p and 5s states is smaller than the $\langle 6s^{eff} | 6s^{eff} \rangle$ overlap but not small enough to be neglected entirely. Terms incorporating admixtures from the rest of the band states have been dropped, for $Er^{3+}:Au$, because we expect their effect to be small. The numerical computation necessary to incorporate these soon becomes far too time consuming. However, results using the $\langle 6s^{eff} | 6s^{eff} \rangle$ overlap produces small contributions to both the fourth and sixth CFPs so components, which are expected to be smaller because of smaller overlaps from 5d, 5p and 5s have not been fully considered.

In CHAPTER 7 we begin the study of ZFS of the S-state Gd^{3+} ion which is assumed to enter substitutionally into the host lanthanum ethylsulphate. By considering each of the most important components of the Hamiltonian H in turn, in second quantised form, it becomes apparent, when applying Stevens's first order perturbation theory, that the ZFS of the studied Gd^{3+} ion cannot be explained. We point out the difficulties involved in obtaining a complete theoretical understanding of the ZFS. A brief review of the most important mechanisms contributing towards the ZFS of this particular Gd^{3+} -doped salt is given and the importance of Newman's (1970) SCCF mechanism is remarked.

In CHAPTER 8 we extend the intra-site mechanism of Tuszyński et al (1984,1986) to include inter-site contributions to the SCCF and subsequently to the ZFS for Gd^{3+} in lanthanum ethylsulphate. We find that by adding our contribution to all other different mechanisms, the

agreement with experiment is improved. We conclude that our inter-site mechanism could play an important role for the determination of ZFSs of S-state ions in various hosts.

In the CHAPTER 9 we briefly present our concluding remarks. We find that the DW model, in first order, is quite capable of accounting for both size and sign of the CFPs of $Er^{3+}:Al$. It is also clear that it cannot explain the size of the observed CFPs for $Er^{3+}:Ag$, at least within the assumptions made in our calculations of the DW's first order components. A specific mechanism is proposed towards the explanation of the observed C_4 CFP for $Er^{3+}:Ag$ namely, a further admixture of conduction band states to the $|c_0\rangle$, used in Chapter 6. A formula is proposed for the calculation of CFPs which incorporates the results from the DW model. Remarkably, it is similar in form with one given earlier in the literature (for instance Dixon 1973 and section 2.2) from a phenomenological OPW model where different contributions to the CFPs were difficult to interpret physically but which provided agreement with a wide range of experiments (see relevant discussion in section 2.2). The current study enables a specific physical interpretation to be given for the different components arising.

We have shown that if inter-site parts of the SCCF are incorporated as well as components from all other mechanisms, including the important on-site Tuszyński et al (1984,1986) mechanism, it is possible to obtain quite good agreement with experiment. This strongly supports the idea that the ZFS of Gd^{3+} are made up of on-site components delicately balanced by inter-site ones thus explaining why in some hosts of a similar structure the ZFS may be opposite in sign (Newman and Urban 1972 and references therein). The importance of our inter-site contributions to the SCCFs and so to the ZFSs of S-state ions dissolved in various hosts is discussed.

AN OUTLINE HISTORY OF CRYSTAL FIELD THEORY

The birth of CF theory must be credited to Becquerel (1929) and Bethe (1929). Becquerel in a review article on RE spectra in 1929 proposed that an ion dissolved in a crystal is subjected to an electric field originating from the ligands. The same year, in a now classic paper, Bethe formulated this proposal into an exact theory. In particular, he showed how the observed splitting of the electronic terms of an ion in the CF is connected with the symmetry of this field. In so doing, he laid down the foundation for all further work in this field.

Another decisive step towards the understanding of the observed phenomena was taken by Kramers (1930) who succeeded in proving that in the presence of any electric field the electronic levels in molecules containing an odd number of electrons must retain an even degeneracy provided that no magnetic field is present. This is called *Kramers degeneracy*.

The first application of the new theory was made by Van Vleck (1932a) who was able to account quantitatively for the behaviour of the susceptibility of various ions in the 3d group. By realising that the quenching of the orbital angular momentum would be a consequence of the CF model, he succeeded in explaining why the paramagnetism of complexes of the first transition series corresponds to a "spin-only" value. Furthermore, the CF model was able to predict those

cases in which there would be small deviations from this empirical rule (Van Vleck 1932b). Schlapp and Penney (1932) and Jordahl (1934) applied the theory in detail to a number of salts and directly confirmed the basic idea of the CF approach. A note by Gorter (1932), in which it is shown that the CF from ligands forming a regular tetrahedron will produce the same levels as those produced by a regular octahedron but with the level order inverted concluded the pioneer papers.

Little reliable quantitative experimental work on the REs could be carried out at that time. The main limitation in the work of the pre-war period was to be found in the fact that, as we see now, the purity of the REs available then was considerably less than assumed at the time. However, several qualitative steps were taken. Freed (1931) identified the optical spectroscopic transitions in trivalent REs as transitions between levels within the 4f configuration. Tomaschek and Deutschein (1933), Joos (1938), Spedding (1940) and Tomaschek (1942) contributed considerably to the understanding of absorption spectra phenomena.

Since RE CFs appear as small perturbations on the free ion levels, a theoretical interpretation of free ion spectra was a necessary prerequisite to the development of CF theory. This interpretation was provided by Condon and Shortley (1935), but was cumbersome for systems having more than two electrons in a *f*-shell. Racah (1942a,b, 1943, 1949) provided the theoretical techniques to deal with more complicated structures. He developed a virtually complete classification scheme of the states of *fⁿ*-configurations.

Just before the outbreak of World War II considerable progress in obtaining good optical spectra of open shell ions in crystals was made by K H Hellwege (for instance Hellwege 1939a,b) at Darmstadt. This effort was continued after the war (for instance Hellwege 1947) and concentrated mainly on REs. At about the same time (early fifties) Bleaney's electron spin resonance group at Oxford began to work on the properties of RE ions (for instance Bleaney and Stevens 1953, Elliot and Stevens 1952, 1953a,b, Bleaney et al 1954). This quickly stimulated a new theoretical approach, the so-called "*Stevens's operator equivalens*" method (Stevens 1952). A little later Judd (1955) began to employ optical spectra to determine RE Crystal Field Parameters

(CFPs). Meanwhile, G H Dieke started to develop an important Laboratory for optical spectroscopy at Johns Hopkins University. The work of this school has been presented in a monograph (Dieke 1968). In the meantime the theoretical methods of Stevens, Elliot and Judd were used to reduce the raw data to CFPs.

This brings us to the present period of CF studies. The period of CFs in RE metals, dilute RE alloys and intermetallics. RE metallic compounds have received little attention compared with the large amount of work which exists for insulators. One reason perhaps was that conduction electrons were thought to bring about inherent difficulties in the theoretical analysis. Another reason may lie in the fact that optical absorption and fluorescence techniques which were used for RE insulators cannot be easily used for metallic compounds (Fulde 1979). The first experimental results for metallic RE compounds were reported in the late sixties (for instance Griffiths and Coles 1966, Ulrich and Barnes 1967, Hirst et al 1968, Rainford et al 1968, Vogt and Cooper 1968, Williams and Hirst 1969).

Progress in both theoretical and experimental studies was rapid and as result five International Conferences on Crystal Field effects (ICCF) have been held up to 1985 (ICCF-1 in Montreal 1974, ICCF-2 in Zürich 1976, ICCF-3 in Philadelphia 1979, ICCF-4 in Wrocław 1981 and ICCF-5 in Sendai 1985) and another one is planned for 1988 in Germany. The current stage of CF studies in RE metals, dilute RE alloys and intermetallics recognises that the conduction-4f electron mixing (hereafter c-f mixing) plays a vital role in determining the CF splittings. Depending on the degree of this c-f mixing some very interesting classes of compounds, with rather exotic properties may result e.g. the Heavy Fermion Compounds (for instance Stewart 1984).

CHAPTER 1

DESCRIPTION AND DETERMINATION OF CRYSTAL FIELDS

1.1. Free Ion Hamiltonian

Because RE CFs appear as small perturbations on the free ion energy levels a brief resume of free ion spectra is instructive.

A Hamiltonian operator designed to describe the behaviour of any "outer" (single electron moving outside closed core shells) electron is given by:

$$H_{one} = -\frac{\hbar^2}{2m} \nabla^2 - \frac{Z_{eff} e^2}{r} \quad (1.1)$$

i.e. a sum of its kinetic energy and its potential energy. Z_{eff} is an effective charge which attempts to take into account the screening of the nuclear charge by the core electrons. The solutions of this one-electron Hamiltonian (including spin) are called *spin-orbitals*. The situation becomes more difficult to analyse in the more general case of n-electrons outside the core. In this case an interelectronic coupling between electrons becomes important which arises from the electrostatic interaction between electrons and is called the Coulomb Term (H_e). For n-electrons this is conventionally written as:

$$H_e = \sum_{i < j}^n \frac{e^2}{|r_i - r_j|} \quad (1.2)$$

In the one-electron case an additional potential energy arises, magnetic in origin, which is called *spin-orbit coupling*. This interaction derives from a relativistic treatment of the electrons (Dirac 1958) and arises as a consequence of the fact that the magnetic field produced by the orbital motion of a single charged particle interacts with the spin of the same particle. For one electron it takes the form $\xi \mathbf{l} \cdot \mathbf{s}$ where \mathbf{l} and \mathbf{s} are the orbital and spin angular momentum operators for the electron and ξ is a quantity, with units of energy, called the *one-electron spin-orbit coefficient*. For n -electrons this is conventionally written as:

$$H_{so} = \sum_{i=1}^n \xi_i(r_i) \mathbf{l}_i \cdot \mathbf{s}_i \quad (1.3)$$

with $\xi_i(r_i)$ the spin-orbit coefficient for the i -th electron. By inclusion of these two coupling mechanisms we obtain the dominant terms in the free ion Hamiltonian. For the n -outer electrons of an ion it takes the form:

$$H_{main} = -\frac{\hbar^2}{2m} \sum_{i=1}^n \nabla_i^2 - Ze^2 \sum_{i=1}^n \frac{1}{r_i} + H_c + H_{so} \quad (1.4)$$

where m is the electron mass. It is useful exercise (in view of later perturbation methods) to have an approximate quantitative picture of the hierarchy of splittings due to the terms appearing in H_{main} . The sum of the kinetic energy term and the attraction to the nucleus term -which is usually called *shell energy* (Orton 1968)- leads to a classification of the gross structure of the energy levels in which different shells have energy separations between 10^4 and 10^6 cm^{-1} (for instance Orton 1968, Herman and Skillman 1963). The Coulomb repulsion term H_c is a smaller effect and will result in a splitting of the "shell energies" to new components with energy separations of the order of 10^4 - 10^5 cm^{-1} (Orton 1968). Finally, the spin-orbit interaction H_{so} splits each of the H_c -split energy components into further additional components whose separations are of the order of 10 - 10^3 cm^{-1} (Orton 1968). For REs the spin-orbit coupling is typically of the order of 10^3 cm^{-1} while for the $3d$ -transition ions is of the order of 10^2 cm^{-1} (Abragam and Bleaney 1970). Of course this scheme of the order of magnitudes just given is not always as clear-cut as we have made out, but it is realistic enough to give us a starting point for the application of perturbation

(*) $219520 \text{ cm}^{-1} = 1 (e^2/a_0) = 2 \text{ Rydberg} = 27.2 \text{ eV}$

methods.

In atomic theory there are two limiting cases for the relative size of the electrostatic interaction between the electrons H_e and the spin-orbit interaction H_{so} terms of the Hamiltonian (1.4). When the spin-orbit interaction H_{so} is much weaker than the electrostatic interaction between the electrons (H_e) the appropriate coupling scheme is the one called *Russell-Saunders(RS) coupling* (Russell and Saunders 1925, Schiff 1968 p.434, Atkins 1983 p.241). This is based on the view that if the spin-orbit interaction is weak it is effective only when all the orbital angular momenta are operating in concert similarly to all spin angular momenta. Therefore the orbital angular momenta of the individual electrons are supposed first to couple into the *total orbital angular momentum* \underline{L} and the spin angular momenta of the individual electrons to some overall *total spin angular momentum* \underline{S} , and only then do these two momenta interact by the H_{so} interaction to form the final *total angular momentum* \underline{J} . Strictly speaking, this coupling is appropriate for light elements (e.g. ions of the first transition series) and begins to fail quantitatively as we move to heavier elements.

In the other limiting case the electrostatic interaction between electrons H_e is much weaker than the spin-orbit interaction H_{so} . Now the orbital and spin angular momenta of individual electrons, \underline{l} 's and \underline{s} 's, couple together and give rise to resultant angular momenta \underline{j} 's. These resultants interact weakly via electrostatic coupling between the electrons they represent and so form a resultant \underline{J} . This is the so-called *jj-coupling* scheme (for instance Schiff 1968 p. 436). This coupling scheme is appropriate wherever $H_{so} \gg H_e$. However, nowhere in the periodic table of elements does the use of *jj-coupling* offer a marked advantage over the RS-coupling. It is simply an empirical fact that the RS-coupling picture provides a reasonably accurate basis for discussion throughout so much of the periodic table (Abragam and Bleaney 1970 p.593). Both of them are qualitatively correct but quantitatively are just limiting cases. The wavefunctions resulting from the coupling schemes (RS and *jj*) yield eigenfunctions for J^2 and J_z but otherwise differ from one another in the intermediate stages of coupling.

In the case of REs the electrostatic interaction between the electrons H_e and the spin-orbit

interaction H_{so} can be much closer in magnitude which makes both coupling schemes quantitatively inappropriate (except sometimes when we are interested in the Ground Level where the RS-coupling can be used). It is therefore not difficult to see that an energy level calculation, in this case, is mathematically more involved since a matching up procedure is required between the two coupling schemes; this situation is called *intermediate coupling*. Before explaining this coupling scheme it is instructive to clarify what is meant by the names: Spin-orbital, Configuration, free-ion Term, free-ion Level, State and list Hund's rules.

A *Spin-orbital* of an atom or ion is any eigenfunction of the appropriate one-electron Hamiltonian operator -see equation (1.1)- whose spin and space parts are both included.

The *Configuration* of an atom or ion is the specification of the orbitals the electrons occupy. For n electrons in a shell characterised by the principal quantum number n and the orbital angular momentum quantum number l we use the notation: $n l^x$. So the configuration of Gd^{3+} is: $1s^2 2s^2 2p^6 3s^2 3p^6 3d^{10} 4s^2 4p^6 4d^{10} (4f^7) 5s^2 5p^6$. For reasons of convenience, we normally omit all filled shells and we write down only the open shells i.e. in this description the configuration of Gd^{3+} is represented by $4f^7$.

A free ion *Term*, within RS-coupling, is a set of many-electron wavefunctions sharing common total spin S and total orbital angular momentum L . A term is represented by either $1L, S >$ or ^{2S+1}L . For historical reasons the term symbol ^{2S+1}L is used. The term ^{2S+1}L is $(2S+1)(2L+1)$ -fold degenerate. In some configurations there will be more than one term having the same S and L values and additional quantum numbers must be introduced to distinguish these terms (for instance, such a classification scheme has been derived by Racah (1949) for any f^n configuration). Usually, when we introduce spin-orbit coupling the degeneracy of a Term is lifted. The resultant components are now characterised by J . Customarily, each component $1L, S, J >$ or $^{2S+1}L_J$ of the Term ^{2S+1}L is called a *Level* (Condon and Shortley 1935 p.122). For historical reasons a Level is represented by $^{2S+1}L_J$ and is $(2J+1)$ -fold degenerate with

respect to M_J .

States are one-electron or many-electron wavefunctions that are completely specified by the eigenvalues of a complete set of commuting observables e.g. within the RS-coupling a state is labelled by total spin S , total orbital L , the resultant J , the z -component M_J of the total angular momenta J and any other necessary labels (see discussion by Wybourne 1965 p.12).

We can now give *Hund's rules*. These rules concern the determination of the *Ground Level* of an atom or ion, whose configuration is given, within RS-coupling. According to these rules, the Ground Level is characterised by performing the following procedure *in order* (Kittel 1976 p.442):

- [1] Form the maximum value of the sum S of the spin angular momentum components m_s , $S = \sum m_s$, allowed by the Pauli's principle (Atkins 1983 p.230).
- [2] With the maximum value of S fixed by [1] maximise the sum L of the orbital angular momentum components m_l , $L = \sum m_l$, consistent again with Pauli's principle. The resulting total spin S and total orbital L angular momentum determine the Ground Term.
- [3] The value J of the total angular momentum J is equal to $|L-S|$ when the shell is less than half full and to $L+S$ when the shell is more than half full. When the shell is just half full, the application of the first rule gives $L=0$ so that $J=S$.

Consider two examples of the Hund's rules: The ion Gd^{3+} has an electronic configuration $4f^7$. From the first rule we have $S = \sum m_s = 7 \times \frac{1}{2}$ as the maximum value of S consistent with Pauli's principle. The second rule then gives $L = \sum m_l = 3+2+1+0-1-2-3 = 0$. The third rule gives $J=S=\frac{7}{2}$. So the Ground Level of $Gd^{3+}:4f^7$ within the RS-coupling is represented by $^8S_{7/2}$. Similarly, for $Er^{3+}:4f^{11}$ we find that the Ground Level is given by $^4I_{15/2}$.

We are now able to give a brief description of the intermediate coupling scheme. To calculate the energy levels in the intermediate coupling scheme we have to calculate the matrix elements (MEs) for $H_c + H_{so}$ in a well defined basis scheme (usually the RS-coupling scheme).

These MEs are then rearranged in energy submatrices one for each value of J , since H_{so} is diagonal in J (Wybourne 1965 p.38) and H_c is independent of J (Wybourne 1965 p.17) i.e. $H_c + H_{so}$ is diagonal in J . These submatrices are such that the number of rows (or columns) is equal to the number of states within the specific configuration that interests us - having the same *total* angular momentum J but different L and S . These submatrices are now diagonalised to yield a set of eigenvalues and their corresponding eigenvectors. A theoretical energy level scheme may then be constructed. The eigenvectors will indicate the different admixtures of the basis states of the well defined basis coupling scheme used to construct the submatrices (for details see Wybourne 1965 p.36-39). For example the Ground Level wavefunction of Gd^{3+} (Wybourne 1966) and Er^{3+} (Dieke 1968 p.74) is now, in the intermediate coupling approximation:

$$Er^{3+} : |^4I_{15/2}\rangle = 0.982|^4I_{15/2}\rangle - 0.186|^2K_{15/2}\rangle + \text{smaller admixtures}$$

$$Gd^{3+} : |^2S_{7/2}\rangle = 0.987|^2S_{7/2}\rangle + 0.162|^6P_{7/2}\rangle + \text{smaller admixtures}$$

where the $|\dots\rangle$ symbol denotes the intermediate coupling wavefunction and the $|\dots\rangle$ denotes the RS-coupling wavefunction. In the above cases we see that the intermediate coupling Ground Level wavefunctions are mainly spanned by the pure RS Ground Level wavefunctions. We shall see later that the admixtures are very important for Gd^{3+} (S-state ions) whereas, for our purposes at any rate, of little significance for Er^{3+} (non S-state ions). This is not the case for the excited terms, for instance (Dieke 1968 p.74):

$$\begin{aligned} Er^{3+} : |^4F_{9/2}\rangle = & -0.416|^4F_{9/2}\rangle - 0.342|^2G_{9/2}\rangle + 0.276|^2G_{9/2}\rangle \\ & - 0.219|^2H_{9/2}\rangle + 0.438|^2H_{9/2}\rangle + 0.627|^4F_{9/2}\rangle \\ & + \text{smaller admixtures.} \end{aligned}$$

where $^2G_{9/2}$ and $^2H_{9/2}$ Levels for the $4f^{11}$ configuration.

In this section we have attempted to provide a brief description of the dominant interactions which determine the free ion spectra. There are several texts on this subject e.g. Woodgate (1980), Gerloch (1986). A thorough analysis has recently been given in an excellent review arti-

cle by Judd (1985) and references therein.

1.2. Ions in a Crystalline Environment

So far we have considered free ions i.e. the environment of these ions has been assumed *isotropic* (for instance ions in a gas at very low pressure). When an ion enters a crystal it either occupies an interstitial or substitutional position. In this thesis we shall consider that the ion substitutes for another in the host and it is well separated from any other ion of the same type. The environment is no longer isotropic but has the point symmetry of the substituted ion provided the substitute does not distort its environment to lower this symmetry. As a result, a further splitting of the free-ion energy levels is expected. The order of magnitude of this further splitting depends on the ion dissolved in the crystal and also the host in which it is embedded.

In the case of RE ions the CF interaction H_{CF} is quite small in comparison with the spin-orbit interaction H_{so} and the electrostatic interaction between the electrons H_e . This case ($H_{CF} < H_{so} < H_e$) is called the *weak crystal field case* and the total angular momentum J is a good quantum number to a very good degree of approximation (Abragam and Bleaney 1970 p.303, p.713). Actually, the CF interaction is of the order of 10^{-10}cm^{-1} . One reason for the small magnitude of the CF is that, at the commencement of the RE series, a deep potential develops near the nucleus and the *4f*-electrons are drawn from the outer part of the atom into the interior (Wybourne 1965a p.2). This effectively reduces the internuclear distances and hence considerably the CF interactions. This is actually an electrostatic argument and contributions to CFs can arise from other sources as we see later (for instance Chapter 2), but this gives a qualitative feel for why the CF becomes smaller in the RE series.

In the iron group the CF interaction is of the order of 10^4cm^{-1} , much stronger than that in the RE group. This can be qualitatively understood by noticing that the open *3d*-shell is the outermost shell and so experiences fully its environment. Note that here the H_{CF} is stronger than the H_{so} but not as strong as the H_e . This situation ($H_{so} < H_{CF} < H_e$) is called the *intermediate crystal field case* and J is not a good quantum number any more. Instead of the total angular momentum J , the total orbital L and total spin S angular momentum are good quantum

numbers (Abragam and Bleaney 1970 p.372).

In the Platinum and Palladium groups the H_{CF} interaction can be comparable or stronger than both H_m and H_c . This is known as the *strong crystal field case*. In this case, $H_m \ll H_{CF}$ and $H_c \ll H_{CF}$, none of the L , L_z , S provide good quantum numbers. Details can be found in Abragam and Bleaney 1970 p.377. Of course, there is no real distinction between the three cases; they go over into each other. For example iron group ions belong to the strong CF case, particularly in strongly covalent compounds such as Co^{2+} in TiO_2 and in Al_2O_3 (Orton 1968 p.15). The reason we distinguish between them is simply in order to specify our starting point.

In this thesis we shall concentrate on the RE group which belongs to the weak CF case. This implies that to a first approximation the free ion calculation is valid the CF being a small perturbation on the free ion energy levels. To clarify this we present observed energy levels (in RS-coupling formalism) together with the centers of gravity for Er^{3+} in a number of host materials in Table 1.1.

Table 1.1 : Energy levels* in cm^{-1} for Er^{3+} (Dieke 1968).

Level	Free ion	LaF_3	ErES^{**}	$\text{ErCl}_3 \cdot 6\text{H}_2\text{O}$	LaCl_3	LaBr_3	Y_2O_3
$^4I_{13/2}$	0.0	0.0	0.0	0.0	0.0	0.0	0.0
$^4I_{13/2}$	6486	6481	-	-	6482	6475	6458
$^4I_{11/2}$	10124	10123	10113	10109	10111	-	10073
$^4I_{9/2}$	12346	12351	12367	12349	12352	12339	12288
$^4F_{9/2}$	15183	15236	15207	15182	15176	15150	15071
$^4S_{3/2}$	18300	18353	18327	18284	18291	18261	18072
$^3H_{11/2}$	19011	-	19087	19056	-	-	18931
$^4F_{7/2}$	20494	20492	20458	20426	-	-	20268
$^4F_{5/2}$	22182	20162	22122	22078	22068	22022	21894
$^4F_{3/2}$	22453	22494	22461	22436	22409	22369	22208
$^3H_{9/2}$	24475	24527	24516	24464	24434	-	24304
$^4G_{11/2}$	26377	26369	26349	26298	26271	26180	26074
$^2G_{9/2}$	27319	27412	-	27285	-	27159	-
$^2K_{15/2}$	27585	-	-	27649	-	-	-
$^2G_{7/2}$	27825	28082	-	-	-	-	-
$^3P_{3/2}$	31414	31501	-	-	31385	31285	31186

* Since we are interested solely in relative splittings we put the energy of the Ground Level equal to 0 cm^{-1} .

** $\text{Er}(\text{C}_2\text{H}_5\text{SO}_4)_3 \cdot 9\text{H}_2\text{O}$

We note immediately from Table 1.1 that the positions of the free ion energy levels, in various ionic hosts, are approximately the same to within a few hundred wavenumbers (rarely more than 100 cm^{-1}). The same is true for all trivalent REs (Dieke 1968, Hüfner 1978). This finding had been anticipated from the electronic structure of the REs and is nicely confirmed by experiment. It means that the centers of gravity of the energy levels in a "typical" ionic host is representative of

that in all other ionic crystals. So a typical energy level scheme for trivalent RE ions in ionic crystals will be similar to that in Figure 1. A similar energy level scheme is also expected when a RE ion becomes part of any metallic matrix (for instance Fulde and Loewenkaupt 1986, p.591).

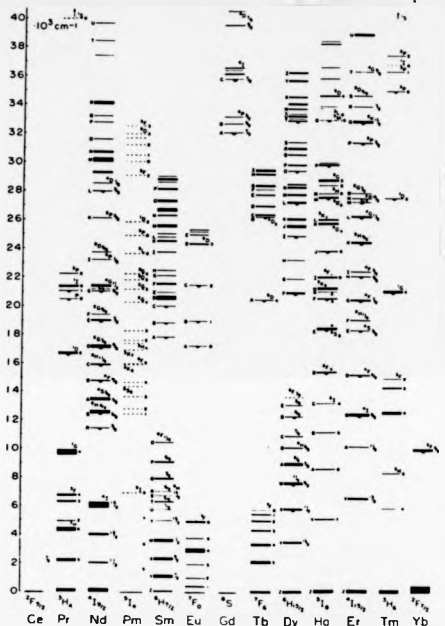


Figure 1: Observed energy levels of the RE ions. The thickness of each level represents the total CF splitting in LaCl_3 . A pendant semicircle indicates that this level fluoresces in the LaCl_3 structure (from Dieke 1968 p.142).

For a direct comparison between theory and experiment we present in Figure 2 the energy levels of Er^{3+} from: (i) an intermediate coupling theoretical calculation, (ii) a RS-coupling theoretical

calculation, (iii) experiment - free ion and (iv) experiment - $Er(C_2H_5SO_4)_3 \cdot 9H_2O$.

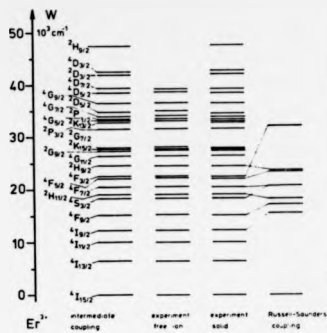


Figure 2: Comparison of energy levels of Er^{3+} from theory (intermediate coupling); experiment - free ion; crystal spectra - $Er(C_2H_5SO_4)_3 \cdot 9H_2O$; approximate theory (RS-coupling). For instructive purposes a few examples are shown (from Hüfner 1978 p.17).

Notice the very good agreement between intermediate coupling predictions and experiment for the whole range of the plotted energy (up to $50000 cm^{-1}$). It is worthwhile to note that the RS-coupling gives a quite reasonable description of the Ground Level $4I_{13/2}$ and the first excited Level $4I_{15/2}$ (as one should expect since $1^4I_{13/2} \approx 0.995 |1^4I_{13/2} + \text{smaller admixtures}\rangle$). The RS-coupling starts to break down as one moves to higher energy levels.

1.3. Parametrisation of the Crystal Field Interaction

Up to now we have attempted to give a qualitative insight of the CF interaction for REs. A quantitative calculation of CF splittings involves two considerations: the first concerns the number of levels into which the free ion energy levels are split and the second concerns the actual size of the CF splitting. Whereas the first topic is completely understood (for instance Tinkham

1964 p.67-78) the second is being actively researched and the various mechanisms that determine the magnitude of the CF splitting are by no means completely understood (for instance Newman 1971, Fulde 1979). As we have already pointed out in our outline history of CF studies the *Sievers's operator equivalents* parametrisation scheme has been, almost universally, adopted to characterise a measured CF spectrum. A remarkable tribute to the usefulness of the parametrisation scheme is illustrated by the fact that, for instance, it is possible to fit up to 100 CF levels to a four-parameter expression for the H_{CF} with a standard deviation as low as 1 cm^{-1} (e.g. see Rajnak and Krupke 1967, Dieke 1968). This remarkable success is due to the fact that in deriving the parametrisation scheme we make no specific assumptions about the origin of the CF, such as using a point charge model (see section 1.3.1), and only invoke the point symmetry of the substitutional ion. The two main restrictions entering the scheme are first that we assume that the CF acts on all $4f$ -electrons independently and equally, and second that the $4f$ -electrons are equivalent in the sense that they have the same radial dependence. Both these approximations seem justifiable for $4f$ -electrons and therefore make the scheme's success qualitatively understandable. Before going into the details of this method we would like to discuss the CF potential energy, V_{CF} . For the time being we shall discuss it in a very simple manner. The so-called *point charge model* (PCM).

1.3.1. The Point Charge Model

In this most naive picture, a crystal can be visualised as built up of point charges at the crystallographic positions of the ions. The potential energy V_{CF} at the site of the RE ion is then entirely due to the electrostatic field generated by the "point-ions" in the crystal. Without any loss of generality we suppose that our coordination system is sited on the RE ion site. So the $V_{CF}(\mathbf{r})$ of a charge q_j at a point \mathbf{r}_j near the origin, due to the surrounding point charges at \mathbf{R}_j is given by:

$$V_{CF}(\mathbf{r}) = \sum_j \frac{q_j q}{|\mathbf{R}_j - \mathbf{r}|} \quad (1.5)$$

where q_j is the charge at the j -th neighbouring ion at a distance R_j from the origin. This potential satisfies Laplace's equation $\nabla^2 V_{CF}(\mathbf{r}) = 0$ since it is produced by charges outside the region of interest (i.e. $r < R_j$). This implies that $V_{CF}(\mathbf{r})$ can be expanded in terms of spherical harmonics

$Y_n^m(\theta, \phi)$ (for the definition of spherical harmonics see Arfken 1970 p.569):

$$V_{CF}(L) = \sum_{n=0}^{\infty} \sum_{m=-n}^n K_n^m r^n Y_n^m(\theta, \phi) = \sum_{n,m} V_n^m \quad (1.6)$$

where

$$K_n^m = \frac{4\pi}{2n+1} \sum_j \frac{q_j}{R_j^{n+1}} Y_n^{m*}(\theta_j, \phi_j) \quad (1.7)$$

For a derivation of equation (1.7) see Hutchings (1964). It turns out that for the determination of the CF energy levels only a small number of terms in the infinite sum (1.7) are of significance. We firstly assume that the atomic orbitals involved are written, in polar coordinates, as $\psi_{nlm}(r, \theta, \phi) = R_{nl}(r) Y_l^m(\theta, \phi)$ where n, l, m are the principal, angular momentum and magnetic quantum numbers respectively. The radial function $R_{nl}(r)$ is not easy to compute. Freeman and Watson (1962) provide data for the trivalent free ions of the RE group but the orbits should be expected to be modified when the ions are situated in a crystal lattice. On this ground it is usual to regard $R_{nl}(r)$ as an undetermined function. We now determine which terms of the series in (1.7) are non-zero.

- [1] The triangular condition for the evaluation of MEs - which states that if in a ME an operator of rank n connects angular momenta l_1 and l_2 then the ME is non-zero only if the condition $||l_1 - l_2| \leq n \leq l_1 + l_2$ holds (Arfken 1970 p.586) - shows that for d -electrons $0 \leq n \leq 4$ and for f -electrons $0 \leq n \leq 6$.
- [2] All terms for which n is odd have zero MEs. This can be understood on the grounds of parity. The MEs of the potential terms V_n^m , which are of the form $\int \chi^* V_n^m \psi d\tau$ with χ, ψ being f (or d)-electron wavefunctions, should be invariant under a change in sign of all three coordinates x, y, z (principle of parity conservation). Since the product $\chi^* \psi$ has even parity it is necessary that the potential V_n^m should also have even parity in order to have non-zero ME.
- [3] The term for $n=0$ can also be dropped since it produces a constant shift in all energy levels and we are interested solely in their splittings by the CF.
- [4] The number of terms is further reduced by the symmetry of the environment. In general the

CF potential must be invariant under the operations of the point group of the surroundings of the substitutionally dissolved impurity ion. The terms occurring depend also on the choice of the quantisation axis. Prather (1961) has listed the non-vanishing terms for different point groups.

The CF Hamiltonian of all the $4f$ -electrons of a RE ion is then given by:

$$H_{CF} = \sum_i V_{CF}(r_i) \quad (1.8)$$

where the \sum_i is over all electrons in the open $4f$ -shell. We must now evaluate the MEs of the perturbing Hamiltonian H_{CF} between free ion states. The matrix thus formed can be diagonalised to find the energy levels and eigenfunctions of the ion in the CF. The free ion wavefunctions used will depend on the size of H_{CF} relative to the H_e and H_m , as we explained in detail in section 1.1 and 1.2. For the RE group, J is a good quantum number and we shall denote the free-ion wavefunctions by $|\alpha L S J J_z\rangle$, within RS-coupling, where α denotes any extra quantum numbers needed to characterise the state in a unique way. The most obvious way to obtain the sought MEs is by direct integration. The free ion wavefunctions are expanded into determinantal product states involving one-electron wavefunctions on which the corresponding terms $V_{CF}(r_i)$ in H_{CF} act. It is an irksome process because each time we have to go back to one-electron wavefunctions. We shall not go into details since it is outside the scope of this thesis. A full description is given by Bleaney and Stevens (1953 p.129). Instead we shall briefly describe Stevens's operator equivalents method.

This method relies largely on the result that within a manifold of states for which J is constant, there are simple relations between the MEs of potential operators and appropriate angular momentum operators. In order to proceed one replaces the "cartesian" Hamiltonian $H_{CF}(x_i, y_i, z_i) = \sum_i V_{CF}(x_i, y_i, z_i)$ by an equivalent operator as follows: x, y, z are replaced by J_x, J_y, J_z respectively, always allowing for the noncommutation of J_x, J_y and J_z . This is done by replacing products of x, y and z by an expression consisting of all possible different combinations of J_x, J_y and J_z , divided by the total number of combinations (e.g. zx should be replaced by

$\frac{1}{2}(J_z J_x + J_x J_z)$). In this way an operator is formed with the same transformation properties under rotation as the potential. This construction is not at all trivial when the noncommutation effects cannot be immediately taken into account (see Hutchings 1964 p.265). Some simple examples are

$$\sum_i (3z_i^2 - r_i^2) = \alpha_J \langle r^2 \rangle [3J_z^2 - J(J+1)] = \alpha_J \langle r^2 \rangle O_2^0 \quad (1.9a)$$

$$\sum_i (x_i^2 - y_i^2) = \alpha_J \langle r^2 \rangle [J_x^2 - J_y^2] = \alpha_J \langle r^2 \rangle O_2^2 \quad (1.9b)$$

where $\langle r^n \rangle = \int_0^\infty [R(r)]^2 r^n r^2 dr$ and $R(r)$ is the radial part of the one-electron wavefunction. Details

concerning the multiplication factor α_J will be given later. Fortunately, the most commonly occurring operator equivalents have been listed once and for all (for instance Hutchings 1964 Table VIII). Once these equivalences have been established, it is matter of simple inspection to find the equivalent operator of the cartesian Hamiltonian H_{CF} .

Finally, the CF Hamiltonian can be written (Hutchings 1964 p.255) in its most common form:

$$H_{CF} = \sum_{\lambda, \mu} A_{\lambda}^{\mu} \langle r^{\lambda} \rangle \alpha_{\lambda} O_{\lambda}^{\mu} \quad (1.10)$$

Some frequently encountered expressions of O_{λ}^{μ} have been given e.g. by Smith and Thornley (1966), Abragam and Bleaney (1970 p.863) (note the difference in normalisation). The multiplicative factors α_{λ} 's, have been listed for REs for instance by Abragam and Bleaney (1970 p.874) -the current practice is to write $\alpha_1, \beta_1, \gamma_1$ for $\alpha_2, \alpha_4, \alpha_6$. Relations between the K_{λ}^{μ} of equation (1.6) and the A_{λ}^{μ} of equation (1.10) have been also given by Abragam and Bleaney (1970 p.862) (within the PCM).

The quantities $A_{\lambda}^{\mu} \langle r^{\lambda} \rangle$ are known as *Crystal Field Parameters*. Since neither the coefficients A_{λ}^{μ} nor the radial parts of the atomic wavefunctions are known with accuracy, it is customary to regard these as *adjustable* parameters determined by the experiment. For completeness, we also give another notation frequently met in the literature:

$$H_{CF} = \sum_{\alpha, m} B_{\alpha}^m O_{\alpha}^m \quad (1.11)$$

where

$$B_{\alpha}^m = A_{\alpha}^m \langle r^m \rangle \alpha_m = C_{\alpha}^m \alpha_m \quad (1.12)$$

(Sometimes, if $m=0$, we drop the 0 from the notation e.g. instead of C_4^0 we write C_4). As an example, we now give the most general operator equivalent potential with cubic point symmetry, within a manifold of angular momentum L composed of f -electron wavefunctions where the z -axis of quantisation has been chosen along a four-fold axis:

$$\begin{aligned} H_{CF} &= B_4^0 (O_4^0 + 5O_4^4) + B_6^0 (O_6^0 - 21O_6^4) \\ &= C_4 B_4 (O_4^0 + 5O_4^4) + C_6 B_6 (O_6^0 - 21O_6^4) \end{aligned} \quad (1.13)$$

(Lea et al 1962). The eigenvalues and eigenfunctions of H_{CF} , as given by equation (1.13), have been tabulated by Lea et al (1962) for $J = \frac{5}{2}, 3, \dots, 8$. They did this by rewriting equation (1.13) in the form:

$$H_{CF} = W \left[\frac{\chi}{F(4)} (O_4^0 + 5O_4^4) + \frac{1-|\chi|}{F(6)} (O_6^0 - 21O_6^4) \right] \quad (1.14)$$

where $B_4^0 F(4) = W\chi$ and $B_6^0 F(6) = W(1-|\chi|)$ with $-1 < \chi < 1$ and listing the eigenvalues and eigenfunctions as function of χ . The factors $F(4)$ and $F(6)$ depend only on J and are also listed in Lea et al (1962).

We can now compare theoretical PCM results and experiment for some dilute REs in noble metals. Before this, we should make clear that the operator equivalent Hamiltonian given by (1.10), and its equivalent forms, can be derived, as we shall discuss later, by using a completely different approach to the above and without imposing any of the restrictions of the PCM. This new derivation has been given again by Stevens (1974, 1976, 1977).

In Table 1.2 we present susceptibility, inelastic neutron scattering, EPR measurements and theoretical PCM results on samples of RE ions in noble metals. It is clear that the PCM does not apply very well for dilute RE alloys.

Table 1.2: Comparison between experimental results obtained from EPR, inelastic neutron scattering and susceptibility measurements on samples of RE ions in Ag and Au and theoretical results obtained from a lattice-sum PC calculation. All measurements have been performed on dilute alloys except those of ref.[d] which refer to the intermetallic compound.

Sample	Source	Experimental C_4 cm^{-1}	results C_4 cm^{-1}	Source	Theoretical C_4 cm^{-1}	results C_4 cm^{-1}
TbAg	a	-48.65	9.04	b	10.43	1.11
DyAg	a	-48.65	9.04	b	9.73	1.11
	b	-9 ± 3	3.8 ± 0.2			
	c	-42.7	9.4			
HoAg	a	-48.65	9.04	b	9.04	0.97
ErAg	a	-48.65 ± 1.39	9.04 ± 0.14	b	8.3	0.83
	d	-51	-6.5			
TmAg	a	-20.85 to -27.5	3.79	b	7.65	0.765
ErAu	a	-22.24 ± 2.78	4.17 ± 0.35	b	8.3	0.83
TmAu	a	-12.86 ± 1.04	1.39	b	7.65	0.765
YbAu	a	-18.77 ± 2.1	3.13 ± 0.21	b	6.95	0.695

[a] Williams G and Hirst L L 1969, Phys Rev **185**, 407-15

[b] Kikkert P J W 1980, PhD thesis, "Crystal Fields of Dy in non-magnetic metals", University of Groningen, The Netherlands

[c] Oseroff S, Passeggi M, Wohlleben D and Schultz S 1977, Phys Rev B **15**, 1283-90

[d] Furrer A 1975, J Phys C:Solid State Phys **8**, 824-38

This is not surprising in view of the simplicity of the model used. Let us recall and discuss some of the assumptions made.

- [1] The charges giving rise to the V_{CF} are assumed to lie entirely outside the RE ion i.e. there is no overlap of the RE ion wavefunctions onto the ligands. A quick inspection of the ionic radii for the involved ions will show us that in most cases this assumption is not correct. Important 4f/ligand charge penetration effects, which involve a two-electron mechanism, should be taken into account by assuming that the crystal consists of extended charge

distributions (see Newman 1971, Garcis and Faucher 1984, Chapter 3).

- [2] The ions are considered static in the crystal i.e. electron-phonon interactions and their effect on the energy levels are neglected. This approximation turns out to be a reasonable one since we will not be considering problems that explicitly depend on the interaction of the phonons with the RE ions (Hüfner 1978 p.42).
- [3] There is no interaction between adjacent RE ions which seems a reasonable approximation in view of the electronic structure of the RE ions and the fact that we are mainly interested in dilute heavy RE alloys.
- [4] All electrons are equivalent and the contribution of each is independent of the states of the other electrons in the open shell i.e. correlation effects are neglected and H_{CF} is a one-electron operator. Discrepancies, that arise from the "equivalent" treatment of the 4f electrons, in fitting theory to experiment although not usually pronounced, have been sufficiently unambiguous to provoke inclusion of two or more electron operators into the H_{CF} Hamiltonian (Bishon and Newman 1970, Morrison et al 1970, Judd 1977). Correlation effects have been proved quite important especially for S-state ions (for instance Tuszyński et al 1984, 1986 Chapter 8).
- [5] It neglects the effects of screening of the 4f-electrons by the filled outer electron shells of the RE ion (Sternheimer et al 1968) and in the case of metallic substances it completely overlooks the complex effects of the presence of the conduction electrons as well (Duthie and Heine 1979, del Moral 1984, Chapter 4)

In conclusion we can say that since the symmetry of the problem is unchanged, although quantitative corrections are needed, the qualitative features of the problem should remain unaltered. For a quantitative improvement [1] above, at least, should be properly incorporated for any system and in the case of metallic systems [1] and [5]. For S-state ions we shall see that [4] is of particular importance.

1.4. Experimental Determination of Crystal Fields

For completeness, we summarise the most important experimental techniques used for the determination of CF splittings in the solid state.

Electron Paramagnetic Resonance (EPR): In principle this method allows the determination of CF splittings in most alloy systems. It is especially appropriate for the very small CF splittings of S-state ions (Baberschke 1982). In a paramagnetic resonance experiment one measures the splitting ΔE of the lowest CF level in an external magnetic field B by means of microwave transitions i.e. one determines the g -factor of the level ($g = \frac{\Delta E}{\mu_B B}$, μ_B is the Bohr magneton). This g -factor allows us to draw conclusions about the CF ground state. It has been extensively used in RE salts (Bleaney and Stevens 1953) and to a lesser extent in metallic systems (for instance Oseroff et al 1977)

Hyperfine methods, like Nuclear Magnetic Resonance (for instance Belorisky et al 1984), Mössbauer effect (for instance Kikkert 1980, Post and Niesen 1984). These are rather indirect methods and as a consequence do not give a unique set of CFPs.

Optical methods : They have been extensively used for insulators (Dicke 1968, Hüfner 1978). According to Fulde (1986) only one example is known for metallic systems i.e. CeB_6 which has been studied by Raman scattering (Zirngiebl et al 1984)

Specific heat : The different CF levels give rise to Schottky anomalies from which the positions and degeneracies of the levels can be determined. The method has been applied to concentrated systems as well as to dilute alloys (for instance Hoenig et al 1974, Heiniger et al 1974, Parker et al 1977). The accuracy of the method is often limited by spin-spin interactions at low temperatures and by spin-phonon interactions and exchange effects among the REs at higher temperatures which distort the Schottky contribution (Shenoy et al 1982). Usually, one finds several CFPs which fit equally well the specific heat.

Magnetic susceptibility : CF levels identified from a study of the temperature dependence of the Van Vleck susceptibility. At low temperatures the susceptibility becomes constant instead of exhibiting a Curie law. It is reasonably accurate if the concentration of the RE ions is

accurately known. Again this method gives a set of CFPs and is limited by exchange interactions between RE ions and impurities with Curie law behaviour (Williams and Hirst 1969, Touborg et al 1978, Dunlap et al 1984).

Inelastic neutron scattering : This is the only direct method for determining the energy level separations and hence CFP in metals. Slow neutrons scattered by a system of ions will induce transitions between CF levels. It has become the dominant method for studying CF in metals and intermetallics (see for instance Prick and Loewenhaupt 1986a,b, Fulde and Loewenhaupt 1986), the reason being that the relevant interaction energies (i.e. the CF splittings) are well within the energy range of inelastic neutron scattering experiments. The method often fails in the case of dilute RE alloys, because for these systems the levels are broad and the low concentration makes a determination of the levels inaccurate (see discussion by Kikkert 1980).

Other more or less related methods, which are only of minor practical importance, can be found in the proceedings of the series of International Conferences on CF effects which are listed in the "References" section.

CHAPTER 2

MORE SOPHISTICATED CRYSTAL FIELD MODELS FOR METALLIC SYSTEMS

2.1. Introduction

In section 1.3.1 of Chapter 1 we made clear the inadequacy of the PCM to explain the CFPs for dilute RE alloys. More importantly, Touborg (1979) demonstrated that any model in which only external charges are assumed to be responsible for the CF fails to explain the CFP in the RE metals and their alloys. In this introductory section we shall attempt to briefly describe the most important efforts to explain the CF in RE metals and their alloys. It will become apparent that an accurate and universal method of determining the CFP in those systems has still not been found. We shall also describe a new approach developed by Stevens (1976) for studying RE doped crystals and a recent first principles quantum mechanical model developed by Dixon and Wardlaw (1986a) to determine the CF in metallic systems. Within this latter framework various effects such as exchange, charge penetration, screening, conduction electron character etc are studied systematically and as a result we expect that a detailed study of metallic systems within this model will yield significant insights into the microscopic origin of the CF at least for REs in dilute non-magnetic alloys and in particular the $\text{Er}^{3+}:\text{Al}$ system which we are interested in this thesis.

2.2. Phenomenological Treatments of the Conduction Electrons

When studying RE ions in metallic hosts, one might naively think that the outer 5p and 5s electrons, together with the conduction electrons, would screen out the CF from the metal ligands. In fact, it is found experimentally (Table 1.2 and Touborg 1979) that the CFs are considerably enhanced over those which would arise solely from the metal ligands, assuming a PCM to calculate these. Since we are studying metallic systems one should anticipate that the conduction-4f electron interaction is responsible for this enhancement. Two different approaches have been presented to investigate this phenomenon. The first approach arose from the work of Williams and Hirst (1969). They measured the magnetic susceptibilities of dilute alloys of heavy REs in the fcc structure of Silver and Gold, and attributed the departure of the susceptibility from Curie-Weiss behaviour to the effect of CFs. They also found that their results could be fitted using conventional CF theory (Stevens 1952), with the appropriate symmetry, provided the C_4 CFP was negative and between five to six times larger than the positive C_4 CFP. A PCM calculation provided much smaller values than the experimental ones and, more seriously, an incorrect sign for the leading C_4 CFP. Coles and Orbach (ref. 15 in Williams and Hirst 1969) suggested the occurrence of a non-magnetic 5d virtual bound state (vbs) on the RE impurity, as a possible explanation for the observed C_4 CFP. They producing convincing arguments to support this suggestion on the formation of such a vbs:

The difference between the valences of the host (Silver and Gold containing monovalent ions) and the usually trivalent RE impurity ions leads to the attraction of conduction electrons in order to screen the superfluous charge of the RE impurity. These screening electrons must be in states orthogonal to both the partially filled 4f and core shells. Spectroscopic data on the pure REs (Wybourne 1965 p.3) suggest that such a low-lying state satisfying the orthogonality criterion could be 5d-like. For example, Gd^{2+} has a ground configuration $4f^7 5d$. It may be also argued from the Friedel point of view (see for instance Daniel and Friedel 1965) that the loss of three valence electrons, with reference to the free atom configuration, would result in an impurity potential capable of partially binding a screening electron in a broadened atomic state of d-

like symmetry. They emphasised also that experimental evidence gathered on the first row of 3d-transition metal impurities in noble metal hosts strongly supports their argument and moreover indicates that the number of electrons accommodated in a 3d-vbs is close to the number occupying these 3d states in the free atom. In addition the general trend towards non-magnetic vbs as one passes from the first row to the third row of transition metal impurities in a given host, leads to the conclusion that the 5d-vbs in question will be both non-magnetic (at least g-values of EPR show no indication of an extra contribution) and occupied by only one electron (the 5d-5d Coulomb repulsion will be strong enough to prevent a population of more than one 5d electron for any reasonable binding impurity potential).

Using the above argument and assuming that the 5d vbs degeneracy is lifted to produce $5d_{xy}$, $5d_{yz}$, $5d_{zx}$ and $5d_e$ ($e = x^2 - y^2, 3z^2 - r^2$) states with a preferential filling of the $5d_e$ states Williams and Hirst estimated that for Eu^{2+} : $4f^7 5d^1$, $C_4 = -113 \text{ cm}^{-1}$ (-158°K) a value, certainly of the right sign, but too large. For this calculation they made the assumption that the 4f-5d overlap is small and so they neglected the exchange term. But as Chow (1973) pointed out the exchange term is not at all small and cancels a large fraction ($\approx 85\%$) of the direct contribution so that the 5d-vbs hypothesis gives a value for C_4 of the right sign but not big enough to explain the experimental value. The situation is considerably improved, as we shall see later in Chapter 5, by considering the screening effects of the conduction electrons on the 4f-5d(vbs) interaction. We found that screening effects modify the exchange interaction much more than the direct component, with respect to free ion values, and as a result the strong compensation of the direct by the exchange contribution (in the case of no screening) is reduced, the precise reduction of the compensation depending on the host material. As a result agreement between theory and experiment improves considerably.

The second approach has been proposed by Dixon and Dupree (1971a,b 1973) and refined by Dixon (1973). Here we shall give the refined version of Dixon (1973).

In order to describe the part of the CF which arises from the conduction electrons they used

a modified orthogonalised plane wave (OPW) Φ_k as the conduction electron wavefunction. They assumed that the interaction between conduction electrons is weak and that they may be considered as independent from each other and that two 6s electrons and one 4f electron of the free RE atom, when in a metal, enter the conduction band. Φ_k was taken to be a single OPW orthogonalised to:

- (i) all the core orbitals of the host (they actually only included those of nearest neighbours).
- (ii) core orbitals of the RE, including 5s and 5p.
- (iii) occupied 4f orbitals.
- (iv) in addition they incorporated an admixture of 5d character which was controlled by an adjustable parameter ϵ_d .

Within this model they found that the CFP are given by:

$$A_n^m \langle r^n \rangle = \left\{ A_n^m \langle r^n \rangle \left(1 + \frac{\xi}{Z} \right) + (R_n^m)_{4f} + (R_n^m)_{5d} \right\} (1 - \sigma_n) \quad (2.1)$$

where :

A_n^m is the CF coefficient calculated from the lattice sum PCM (Kasuya 1966).

$\langle r^n \rangle$ are the average values of the powers of r for the 4f orbitals.

ξ represents an enhancement of the lattice sum CFPs when overlap with nearest neighbours is taken into account.

Z is the valence of the host.

σ_n are the Sternheimer shielding factors which are approximately zero unless $n = 2$ (see Ahmad 1981)

$(R_n^m)_{4f}$ is the 4f contribution to the CFPs and has been calculated absolutely (see Dixon 1973). In the earlier version of this model (Dixon and Dupree 1973) the admixture was controlled by an adjustable parameter ϵ_f .

$(R_n^m)_{5d}$ is the 5d contribution (Dixon 1973) to the CFPs and was controlled by a mixing coefficient ϵ_d .

This crude model has been used to calculate CFs (for instance Kikkert 1980), electric field gradients (Devine and Dixon 1973) and to interpret susceptibility data (Keller and Dixon 1976). Satisfactory agreement was obtained in virtually all cases (Dixon 1974) which emphasises the importance of the d and f character of the conduction electrons. In spite of the success of this model to explain experimental results several criticisms may be levelled at its assumptions and its parameters :

- (i) It includes either one (ϵ_d) or two (ϵ_f, ϵ_d), depending on the version of the model, *adjustable* parameters with no obvious physical interpretation.
- (ii) It does not incorporate electron-electron interactions in a consistent way since it is assumed that conduction electrons are non-interacting.
- (iii) The conduction electrons are described in an effective one-electron way and we know that in reality the nature of the problem is a many-body one. As soon as this approach (one-body like) is adopted one comes up with the problem of making the wavefunction of the one conduction electron, orthogonal to occupied states on the impurity and neighbouring ions. If shells are completely filled this presents no difficulty, but if the impurity has an incomplete shell, problems arise. Basically what one is trying to do is to use a one electron theory for the conduction electrons and orthogonalise to many-electron impurity states, a procedure which is bound to run into difficulties simply because of occupancy of the 4f shell and the inability to ascribe electrons to specific one-electron states.

However one is bound to ask why this model has been so successful. We believe that this success can be explained partly by the presence of adjustable parameters but also because we are now able to give a microscopic physical interpretation of the parameters which appear in this model using a first principles approach given by Dixon and Wardlaw (1986a). We shall discuss again the parameters involved in equation (2.1) and their physical interpretation in the Concluding Remarks of the thesis.

2.3. Free Electron Screening Model

In the last section we have seen that the influence of the conduction electrons was taken into account by either a 5d-vbs (Williams and Hirst 1969) or a modified OPW with added 5d and 4f character under the assumption of non-interacting conduction electrons (Dixon 1973).

Duthie and Heine (1979) and del Moral (1984) investigated the effects of electron screening, which is one of the simplest and most important manifestations of the effect of electron-electron interactions, on CFPs for metallic RE materials. They considered a lattice of ions represented by an ionic pseudopotential $V(\underline{r})$ or in the extreme case by a point-ion potential $V(r) = \frac{1}{r}$ screened by a free electron gas through a dielectric screening function. They used Thomas-Fermi and Hartree screening although del Moral also considered Hartree-Fock screening (Ashcroft and Mermin 1976 p.340-4). They also introduced, for reasons of convergence of the CFPs, some kind of internal structure on the ions. Duthie and Heine investigated isolated RE ions substitutionally dissolved in *Au* and *Al*, and *PrSe*. Their striking conclusion was that free electron screening, far from being a strong effect, might actually be negligible although it sometimes reverses the sign of the C_4 CFP (for the *Al* structure). This interesting suggestion for a possible reversal of the sign of the C_4 CFP is investigated, for $Er^{3+}Au$, in Chapter 4 within the DW. We found that such a possibility is very small.

del Moral concentrated his studies in $REAl_2$ intermetallics. In these compounds the *Al* ions form a 12-fold shell of neighbours, while the RE ions are slightly more distant forming a 4-fold shell. Within the above described free electron screening model he found that the fourth order CFP is opposite in sign in comparison with experiment but this becomes correct if the screening is removed, the point-ion limit taken and the *Al* charge made zero. In order to explain this situation he considered free electron screening for the *Al* ions and a different type of screening, due to the existence of electrons of d-character at the Fermi level, for the RE ions. He was then able to explain satisfactorily the C_4 CFP but the situation was less satisfactory for the C_6 CFP.

Since a RE compound or alloy is a far more complicated system than point-ions in a free electron gas the usefulness of their conclusions is confined to the clarification of some issues of

interatomic screening and the importance of the d-character (del Moral 1984) of the conduction electrons around the RE ions for $REAl_2$. The importance of the d-character for fcc structures has been pointed out in a previous section (2.2) of this thesis and is fully incorporated into the theory of Dixon and Wardlaw (1986a) which we have used for our investigations and present at a later stage.

2.4. The σ - and π -bonding Approach for RE Compounds

Zolnierrek (1984, 1985) proposed a simple semiempirical way to calculate the CFPs for quasi-ionic and intermetallic compounds. His initiative was not to discover the microscopic origin of the CFs for RE compounds but to provide a simple and easy to use model for determining CFP which in turn could be used as a initial trial value in fitting procedures used to fit experimental data to a parametrised Hamiltonian. The determination of such an initial set is important since it improves the convergence of the fitting procedure. We should point out that in such a fitting procedure not only the CFP but also parameters like Slater integrals and the spin-orbit coupling coefficient are varied (Dieke 1968). In the light of its simplicity and the success it has had in predicting CFPs for quasi-ionic compounds (Zolnierrek 1984) and both the sign and magnitude for many RE alloys (Zolnierrek 1985) we shall give a brief account of its characteristics and discuss the reasons for its success.

Zolnierrek in his early investigations (Zolnierrek 1984) concentrated on non-metallic RE compounds. He essentially modified the classical PCM without using extra adjustable parameters. Firstly, the point charges which in the PCM are strictly localised at the ligand centres are replaced by an effective charge q_{eff} attributed to the electron charge of the σ -type in RE-ligand bonding. Secondly, the geometrical RE-ligand distance which in the PCM is related to crystal structure details only, is replaced by R_{eff} , reflecting the position of the electron charge maximum with respect to the RE origin. A schematic explanation of those modifications imposed on the PCM is given in Figure 3:

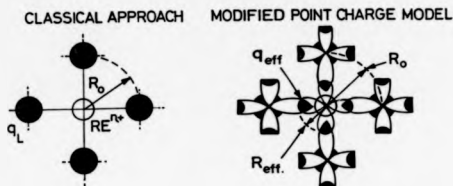


Figure 3: Schematic picture explaining the idea of the classical and modified PCM models. The black circles represent the charge of the ligands, open circles the positive charge of the RE ion (Zolnieriek 1984)

We can now easily see from Figure 3 that the essential differences between the classical PCM and its modified version concerns the position and magnitude of the charges generating the V_{CF} . They are supposed to be not at the ligand centres but somewhere on the straight line joining the RE and ligand ions, since the maximum of the electron charge for σ -type bonding is expected to lie between the outer shells of the RE ion and the ligand ions. Here we should point out that this σ -type modified PCM neglects all neighbours but the nearest ones and assumes that there is no interaction between the effective charges which produce the CF. For the determination of q_{eff} and R_{eff} in the σ -type bonding model he proposed the following two empirical formulas based on the concept of Pauli electronegativity (the ability of an atom to attract electrons, Atkins 1982 p.485) :

$$q_{eff}^{\sigma} = \frac{v_{RE}}{N_L} \left(\frac{\epsilon_L}{\epsilon_{RE}} - 1 \right) e \quad (2.2)$$

$$R_{eff}^{\sigma} = R_o \frac{\epsilon_L}{\epsilon_L + \epsilon_{RE}} \quad (2.3)$$

where q_{eff}^{σ} is the individual ligand charge per single bond, v_{RE} is the number of ionised electrons from the valence shell of the RE ion, e_L and e_{RE} are the ligand and RE electronegativities, N_L is the number of nearest ligand neighbours and finally R_0 is the metal-ligand distance taken from crystallographic data.

Using this modified version of the PCM he was able to predict, with fair accuracy for such a simple model, the CFP for many ion or quasi-ionic compounds with cubic point symmetry (Zolnieriek 1984). This σ -type version of the PCM failed to explain CFP for metallic systems and so he modified it to the so-called π -type. In other words he assumed that the maxima of the electron charge density responsible for the CF effects could be also localised off the RE-ligand straight lines (σ -bonding) which would formally correspond to the existence of the π or higher order chemical bonding. He treated the possibility of π -bonding only. In order to take into account the displacements of the electric charges whenever instead of the σ , the π bonding occurs, he introduced an extra parameter ξ . This ξ parameter is assumed to be given by:

$$\xi = \frac{e_L}{2 e_{RE}} \quad (2.4)$$

The effective distance between the RE ion and the π -charge is defined in the same manner as in the σ -bonding model:

$$R_{eff}^{\pi} = R_0 \frac{e_L}{e_L + e_{RE}} \quad (2.5)$$

whereas the effective charge is now defined by a different formula:

$$q_{eff}^{\pi} = \frac{v_{RE}}{N_L} \frac{e_L + e_{RE}}{e_{RE}} \epsilon \quad (2.6)$$

where N_L stands for the number of π -bonds, v_{RE} , e_L , e_{RE} , R_0 have the same meaning as in the σ -bonding model and ϵ is the elementary electron charge. In order to demonstrate that the π -bonding approach is working, he performed a set of calculations for selected RE metallic compounds of cubic symmetry. We present some of his results, in Table 2.1, to demonstrate the success or otherwise of the π -bonding model:

Table 2.1 : CFP (in cm^{-1}) calculated in the framework of the π model approach for the RE intermetallics with the CsCl structure. a_0 stands for a lattice constant of cubic unit cell. References in the last column concern only experimental data.

Sample	a_0	R_{Jf}^2	q_{Jf}^2	ξ	$A_0^0 \langle r^4 \rangle$		$A_0^0 \langle r^6 \rangle$		Ref
	A	A	e		model	exp	model	exp	
ErRh	3.361	1.940	0.375	1.000	-44.7	-85.8	-11.4	-13.1	a
ErPd	3.445	1.989	0.375	1.000	-39.5	-81.7	-9.6	-8.2	a
ErAg	3.574	1.960	0.341	0.863	-39.4	-50.0	-7.7	-6.5	a
HoCu	3.444	1.889	0.341	0.863	-49.7	-47.3	-12.0	-10.4	b
ErCu	3.430	1.881	0.341	0.863	-48.5	-58.4	-10.4	-10.5	a
TbZn	3.576	1.835	0.307	0.727	-25.6	-32.0	-12.8	-12.7	c
DyZn	3.563	1.828	0.307	0.727	-23.7	-31.3	-11.6	-13.9	c
ErZn	3.520	1.803	0.307	0.727	-20.8	-25.0	-9.9	-12.4	c
HoMg	3.761	1.699	0.261	0.545	+20.3	+29.0	-8.1	-9.0	b
ErMg	3.738	1.694	0.261	0.545	+19.8	-2.5	-7.0	-7.5	a

[a] Morin P, Pierre J, Schmitt D and Drexel W 1976, J Phys **37**, 611-6

[b] Schmitt D, Morin P and Pierre J 1977, Phys Rev B **15**, 1698-705

[c] Morin P, Rouchy J and du Tremolet de Lacheisserie E 1977, Phys Rev B **16**, 3182-93

As seen from Table 2.1 the agreement is quite satisfactory in some cases for the fourth order CFP and excellent for the sixth order CFP, at least excellent in comparison with the experimental results used by Zolnieriek. There are other measurements which give a similar fourth order CFP but positive sixth order CFP. For instance, for dilute $\text{Er}^{3+}:\text{Ag}$, $C_4 = -48.65 \pm 1.39 \text{ cm}^{-1}$ and $C_6 = +9.04 \pm 0.14 \text{ cm}^{-1}$ (Williams and Hirst 1969). Zolnieriek (1985) also performed theoretical calculations within the π -bonding approach for REM_2 intermetallics where $M = \text{Mg}, \text{Sn}, \text{Pb}$. He found again reasonable agreement with experiment.

From the above discussion we can say that at the present the π -bonding approach despite its simplicity seems to be a fairly accurate method for calculating a reasonable set of CFP for RE

intermetallics. It is certainly the simplest phenomenological method which predicts the right sign and magnitude for CFP of cubic structures. The most amazing fact is that the π -bonding model with the assumption of localised ligand charges works so well for the systems with de-localised conduction band electrons. This apparent inconsistency could be perhaps be understood in terms of the probability distributions of electronic charge along certain directions.

We recognise the usefulness of the π -bonding model for the RE intermetallics but we should also point out that it becomes more difficult to use for more complex structures. According to Zolnierak (1985) it is impossible to apply this method straightforwardly to intermetallics of lower than cubic symmetry. He also does not know how the model works for the actinide intermetallics. The assumption to consider only nearest neighbours can be perhaps understood if one thinks that the effect of neighbours further away from the RE are screened out because of conduction electrons.

2.5. Towards a Unified Treatment of Crystal Fields for Rare Earth Doped Compounds

2.5.1. Criticisms of Crystal Field Theory

So far, we discussed models based on semi-phenomenological effective Hamiltonians where a great deal of attention has been paid to the local symmetry by treating the 4f-electrons as localised about a particular site. However some crystals containing REs are periodic so it should be expected that the 4f-electrons would be in Bloch type orbitals which extend throughout the crystal rather than in localised orbitals. This criticism of CF theory was raised in the early fifties. These difficulties have been overcome by Stevens (1976) who proposed a new method of looking at "Crystal Fields" which is compatible with the above mentioned lattice periodicity. This was done in an article (1976) which was principally an investigation of the exchange interactions between RE ions in an insulating crystal. We shall explain his method in the subsequent sections 2.5.2, 2.5.3. In this section we concentrate on the criticisms levelled at CF theory.

The substance of the attack on CF theory is included in an earlier paper by Slater (1953). He had become convinced that the only way to understand ferromagnetism was through band theory

and that it was necessary to use determinantal wavefunctions based on Bloch functions. By implication he disliked the concept of localised moments, a basic concept of CF theory. He found it difficult to understand that on the one hand one is dealing with a periodic lattice and on the other electrons are treated as localised at individual sites. His point was that electrons are indistinguishable so it is unacceptable to treat some electrons as "captured" about specific sites and treat all "remaining" electrons in a rather cavalier fashion. To briefly illustrate this feature suppose that we are treating identical CF operators at sites A, B, ... each of which has local cubic symmetry. The CF operator of site A will contain a term of the form (for instance Hutchings 1964):

$$D \sum_i (35z^4 - 30r^2z^2 + 3r^4),$$

where the summation is only over the 4f-electrons associated with the RE ions at site A. Similarly, the CF of site B will contain a similar sum but this time only over the electrons associated with ion B and so on. So electrons have been distinguished.

2.5.2. The Perturbation Scheme of Stevens

In order to overcome these criticisms, Stevens went back to a basic general Hamiltonian H where electrons are not distinguished and by carefully defining an unperturbed Hamiltonian H_0 having all the symmetry properties of the actual Hamiltonian H he showed that CF theoretical ideas were essentially correct but for different reasons than those normally given. The main reason for seeking an unperturbed Hamiltonian H_0 with all symmetries of H build in, was to avoid the many difficulties (e.g. very slow convergence of the perturbation scheme) which arise if one tries to split H into an unperturbed Hamiltonian and a perturbation. It can happen, for example, if H_0 has less symmetry than H , that it is necessary to go to infinite order to restore symmetry. He required a scheme where good convergence is expected from low order perturbation theory so he proposed defining H_0 with all the symmetries of H .

Stevens (1976) began with the general Hamiltonian:

$$H = \sum_i \frac{p_i^2}{2m} - \sum_{M, L} \frac{\sum_{M'} Z_M e^2}{r_{M'L}} + \frac{1}{2} \sum_{i,j} \frac{e^2}{r_{ij}} + \dots \quad (2.7)$$

where the first term describes the kinetic energies of all electrons, the second term their electrostatic energies in the fields of the nuclei the third the mutual Coulomb repulsive energies and ... includes any other interactions. An exact solution was assumed to be out of the question so a particular form of perturbation theory was used, and the first step was to choose the unperturbed Hamiltonian. According to Stevens such an unperturbed Hamiltonian, H_0 , should have the following properties:

- [1] It should not distinguish between electrons i.e. it was to be invariant under the interchange of any two electrons.
- [2] It should have the space group symmetries of H , since then convergence in low order could be expected if the perturbation was small in some sense. As we have already mentioned earlier if it did not one might envisage going to infinite order to recover all the symmetries of H ; a very unsatisfactory situation.
- [3] Electrons creating "local" moments and conduction electrons should be treated on the same footing.
- [4] The perturbation $H - H_0$ should be small enough to give convergence in a reasonable order of the perturbation scheme.
- [5] The scheme should be tractable.

It is not obvious how all these requirements can be met in H by splitting it into two parts as had been done in the past by other workers and instead he defined H_0 on the basis of physical knowledge. He suggested that H_0 has as eigenstates states which we have reason to believe are close to being eigenstates of H . For instance, in many instances one is interested in the low-lying energy levels of a physical system so in a perturbation scheme, as the one proposed previously, one would be attempting to *modify the ground term*, and hence via coupling to higher levels to obtain a physical picture of the states of low energy.

H_0 should be Hermitian so the states which are chosen to be eigenstates of H_0 must be orthonormal. To construct such a set of antisymmetric and orthogonal wavefunctions for the systems under consideration (i.e. RE doped periodic insulating crystals) he used Wannier functions

(see Appendix A, Wannier 1937) but generalised Wannier functions can also be used in the same spirit for a non-periodic solid (Kohn and Onffroy 1973, Gay and Smith 1974). Dixon and Wardlaw (1986a) assumed such generalised Wannier wavefunctions for the localised electrons and Bloch wavefunctions for the conduction electrons of RE doped conductors. As is well known, the Wannier functions may be obtained from a Fourier transform of the Bloch functions. Let us denote by $W_n(\underline{r}-\underline{L})$ the Wannier function associated with the band index n and the lattice site \underline{L} and by B_λ Bloch functions where λ is a set of appropriate quantum numbers. He formed a Slater determinant, on site A, as:

$$\left\{ W_n^A, W_n^A, \dots, W_n^A, \dots \right\}$$

Similarly for site B:

$$\left\{ W_n^B, W_n^B, \dots, W_n^B, \dots \right\}$$

and so on. If the Slater determinant description of a state of the ion at site A is multiplied by a Slater determinant for the ion at site B the result is a product of determinants of the form:

$$\left\{ W_n^A, W_n^A, \dots, W_n^A, \dots \right\} \times \left\{ W_n^B, W_n^B, \dots, W_n^B, \dots \right\}$$

This state is antisymmetric with respect to interchange of electrons either at A or B, but is not antisymmetric with respect to interchange of electrons between A and B. To overcome this difficulty he formed the total Slater determinant:

$$\left\{ W_n^A, W_n^A, \dots, W_n^A, \dots, W_n^B, W_n^B, \dots, W_n^B, \dots \right\}$$

which is antisymmetric with respect to all interchanges of electrons. This procedure can be extended to any number of products. Since he used Wannier functions to describe the one-electron states, the antisymmetrised many-electron states will also be mutually orthogonal, if different. We could also include any conduction electron Bloch states $B_{\lambda_1}, B_{\lambda_2}, \dots$ to finally obtain:

$$|n\rangle = \left\{ W_n^A, W_n^A, \dots, W_n^B, W_n^B, \dots, W_{\lambda_1}^C, W_{\lambda_2}^C, \dots, B_{\lambda_1}, B_{\lambda_2}, \dots \right\}$$

Given any such state, $|n\rangle$, he formed its projection operator $P_n = |n\rangle \langle n|$ defined by:

$$P_n |k\rangle = \begin{cases} |n\rangle & \text{if } n=k \\ 0 & \text{otherwise} \end{cases}$$

Then any operator of the form $\sum_n \lambda_n P_n$, where λ_n are scalars, have the states $|n\rangle$ as eigenstates with eigenvalues λ_n . The λ_n can be chosen as convenient. In the initial version of his method, Stevens chose λ_n equal to the expectation value of H taken for the state $|n\rangle$. That is $\lambda_n = \langle n | H | n \rangle$, for if $|n\rangle$ approximates to an eigenstate of H , then $\langle n | H | n \rangle$ should approximate to an eigenvalue. Thus the unperturbed Hamiltonian was initially chosen as:

$$H_0 = \sum_n \langle n | H | n \rangle |n\rangle \langle n|$$

Stevens found that such an unperturbed Hamiltonian does not have the rotational symmetries of H , though it does have the translational and indistinguishability requirements. The difficulty stems from the fact that in defining the Slater determinants directions of quantisation for orbit and spin are introduced (for details see Stevens 1976 p.14-15). Another problem with the above choice is that there is a possibility some of the $|n\rangle$ may have almost the same energy and hence one would expect divergences in higher order (the reason being that higher order terms involve energy differences like $\langle n | H | n \rangle - \langle m | H | m \rangle$ as denominators).

The above problems have been circumvented by introducing *families* of $|n\rangle$ and taking the mean energies within a family instead of $\langle n | H | n \rangle$. Suppose now that we constructed, by using the above procedure, such a set of mutually orthogonal many-electron wavefunctions $|n\rangle$. One *family* can now be the states in which each RE site has an occupancy $(4f)^x$, with the conduction electrons in the lowest conduction band and all core electrons filled. Another could be that in which, say, three sites have $(4f)^{x-2}$, the rest have $(4f)^x$ and the displaced 4f-electrons are accommodated in the lowest conduction band with core orbitals given an occupancy so that the overall number of electrons is conserved. Obviously, the states in a given family have different energies (for a given $(4f)^x$ terms of different L, S differ in energy). For a given r -th family he defined its mean energy as:

$$E_r = \frac{\sum_n \langle n_r | H | n_r \rangle}{\sum_n \langle n_r | n_r \rangle} \quad (2.8)$$

where the projection operator for the r -th family is now defined by:

$$P_r = \sum_{n_r} |n_r\rangle \langle n_r| \quad (2.9)$$

and so the unperturbed Hamiltonian is given by:

$$H_0 = \sum_r E_r P_r \quad (2.10)$$

It has been found (Stevens 1976) that the H_0 given by (2.10) has all the required properties mentioned earlier in this section and any problems due to divergences in higher order are now resolved since the unperturbed energies are well separated. The perturbation will now be $H - H_0$. Having defined H_0 and $\epsilon V = H - H_0$ as the perturbation and specified that he is interested in the low-lying energy levels, degenerate perturbation theory in projection operator form, within the ground family (characterised by P_0) was performed. The details of such a perturbation scheme are given fully by Bates et al (1968). We only briefly describe the following steps. The eigenfunctions and eigenvalues of $H_0 + \epsilon V$ are known if it is possible to find a transformation $e^{i\epsilon X}$ such that:

$$e^{i\epsilon X} (H_0 + \epsilon V) e^{-i\epsilon X} \quad (2.11)$$

becomes diagonal. It is however, not usually easy to find such an X , and what is done is to try and choose it so that the MEs of the transformed Hamiltonian which couple the ground and excited families are as small as possible, at least to $O(\epsilon^2)$. It is found that the condition for this to be so is:

$$P_0 e^{i\epsilon X} (H_0 + \epsilon V) e^{-i\epsilon X} P_r = O(\epsilon^2), \quad r \neq 0 \quad (2.12)$$

which leads to:

$$P_0 X P_r = i \frac{P_0 V P_r}{E_r - E_0}, \quad r \neq 0 \quad (2.13)$$

The ground state energies are obtained from the effective operator:

$$P_0 e^{i\epsilon X} (H_0 + \epsilon V) e^{-i\epsilon X} P_0 \quad (2.14)$$

which to $O(\epsilon^2)$ simplifies to:

$$P_0 H_0 P_0 + \epsilon P_0 V P_0 - \epsilon^2 \sum_{r \neq 0} \frac{P_0 V P_r V P_0}{E_r - E_0} \quad (2.15)$$

This reduces to:

$$P_0 H P_0 = e^3 \sum_{r \neq 0} \frac{P_0 H P_r H P_0}{E_r - E_0} \quad (2.16)$$

since $P_0 H P_r = 0$ for $r \neq 0$ and $P_0 H P_0 + e P_0 V P_0 = P_0 H P_0$.

2.5.3. First Order Perturbation Theory - Example for non-S-state RE ions

To develop his perturbation scheme further Stevens used well established second quantisation techniques for electrons. The methods of second quantisation automatically take care of the required antisymmetry of the many-electron wavefunctions and are directly related to the Slater determinant representation. To simplify matters he transformed H in equation (2.16) into second quantised form using as a basis the complete set of one-electron orthonormal Wannier and Bloch functions. He noticed that if α' , α refer to an open shell at a particular site then pairs like $\alpha'_{m'} \alpha_{m\sigma}$ (where m, m' denote the components of orbital angular momentum and σ, σ' the spin components) have similar properties to combinations of raising and lowering angular momentum operators. He (Stevens 1974) established the following relationships:

$$\begin{aligned} \alpha'_{m'} \alpha_{m\sigma} &= \frac{1}{2} \sum_{s, j} \Delta_{ms's} O_{m'-m}^{(s)}(\mathcal{U}) (1 + 2s'_j) \\ \alpha'_{m'} \alpha_{m-\sigma} &= \frac{1}{2} \sum_{s, j} \Delta_{ms's} O_{m'-m}^{(s)}(\mathcal{U}) (1 - 2s'_j) \\ \alpha'_{m'} \alpha_{m-} &= \sum_{s, j} \Delta_{ms's} O_{m'-m}^{(s)}(\mathcal{U}) s'_j \\ \alpha'_{m'} \alpha_{m+} &= \sum_{s, j} \Delta_{ms's} O_{m'-m}^{(s)}(\mathcal{U}) s'_j \end{aligned} \quad (2.17)$$

Here $\sigma, \sigma' = +, -$ where we identify "+" as $m_s = \frac{1}{2}$ and "-" as $m_s = -\frac{1}{2}$. The sum is over electrons i and the rank n is that of the operators $O_{m'-m}^{(s)}(\mathcal{U})$ which have been defined and tabulated by Smith and Thornley (1966). $\Delta_{ms's}$ is given by:

$$\Delta_{ms's} = \frac{\langle m' | O_{m'-m}^{(s)} | m' \rangle}{N_2^2}$$

and the coefficients N_2^2 have been given by Stevens (1974). To understand relationships (2.17) note that the creator $\alpha'_{m'}$ transforms under rotations as a double tensor with orbital rank l and spin rank s . Similarly the annihilator $\alpha_{m\sigma}$, multiplied by a appropriate phase also transform like a double tensor (Judd 1967). The product operator of a creator and annihilator may therefore be

expanded in terms of appropriately coupled double tensors, the spin ranks of which will be zero or one. It is therefore not surprising to find that such a product operator can be written in terms of the orbital operators $O_p^{(k)}(U_i)$ and the components of spin operators s^i . It should be noted that the relationships (2.17) are equivalences since the left-hand sides are operators acting within a space whose basis is formed using occupation numbers for the one particle states labelled with quantum numbers n, l, m_l, m_s , whereas the right-hand side is a sum of operators acting on the m_l, m_s of the i -th electron. Hence the relationships (2.17) are really equivalences between operators of two types which give identical MEs when sandwiched between the same two determinantal states of f^N .

It is advisable to discuss the first order perturbation theory terms (i.e. $P_0 H P_0$) of equation (2.16) for the low-lying energy level problem for a specific case. The ground family, projected by P_0 , is defined to possess the characteristic feature that all its states have definite numbers of electrons in the various shells and conduction bands. So in first order one will finish up with expressions in annihilation and creation operators which conserve the numbers of electrons at particular sites. If equations (2.17) are used, these expressions, as we shall see later, reproduce the conventional CF theory.

Suppose an insulating crystal containing $N \text{ Er}^{3+}$ ions, the Ground Level of which, in the free ion is $4f^{11} : ^4f_{15/2}$. The $J = 15/2$ will usually be split in an insulating crystal. The ground family we assume to made up of electrons in filled shells but that 11 electrons per Er^{3+} site are in $4f^{11} : ^4f_{15/2}$. The ground family therefore contains 16^N states. The first step is to identify the second quantised operators which split $J = 15/2$ at site A. It is now convenient to denote by $a', a; b', b; \dots$ etc creation and annihilation operators of 4f-electrons at site A, B, \dots respectively and by f', f creation and annihilation operators of filled orbitals. One operator which can lead to a splitting of the $J = 15/2$ is of the form $a'a$. The one-electron (h) terms in H give such operators:

$$\sum_{\alpha\beta} \langle \alpha_\beta | h | \alpha_\alpha \rangle \alpha_\beta^\dagger \alpha_\alpha \quad (2.18)$$

Within the same family the only operators which can contribute to (2.18) (to first order) are those

which leave the number of electrons at a given site unaltered. The contributing $\alpha_p^+ \alpha_q$ pairs are of two kinds. They either refer to closed shells ($f_p^+ f_q$) or to open shells ($a_p^+ a_q$). In the former case f_q may annihilate an electron in a closed shell and f_p^+ must restore the electron to the same orbital (since it is the only one available), so $p=q$. $f_p^+ f_p$ is therefore equivalent to unity and the contribution from $\langle f_p | h | f_p \rangle f_p^+ f_p$ is just a contribution to the mean energy of the ground manifold given by $\langle f_p | h | f_p \rangle$. In the latter case a_q annihilates an electron in an open shell and a_p^+ restores the electron to the same shell but not necessarily to the same orbital in that shell. The contribution to $\langle 4f^{11}; 4f_{15/2} | H | 4f^{11}; 4f_{15/2} \rangle$ is $\langle a_p | h | a_q \rangle \langle 4f^{11}; 4f_{15/2} | a_p^+ a_q | 4f^{11}; 4f_{15/2} \rangle$. The physical interpretation of the above results can be understood as follows. Imagine that the electrons at site A described by $|n\rangle$. Then the $|n'\rangle$ is related with the state $|n\rangle$ of the whole crystal. $|n\rangle$ can be obtained by acting on $|n'\rangle$ with suitable creation operators, all of which act at sites other than A. That is:

$$|n\rangle = g_B^+ g_C^+ \cdots |n'\rangle \quad (2.19)$$

where g_B refers to site B etc. But

$$\langle n | \alpha_p^+ \alpha_q | n \rangle = \langle n' | \cdots g_B^+ g_C^+ \alpha_p^+ \alpha_q g_B^+ g_C^+ \cdots | n' \rangle = \langle n' | \alpha_p^+ \alpha_q | n' \rangle \quad (2.20)$$

if α_p and α_q are orbitals at A. It therefore follows that the contributions to MEs of the form $\langle n | H | n \rangle$ from orbitals associated with the site A are precisely those which would be found if all the electrons not at A were removed. The energy of what remains would be the one-electron part of the free-ion-like energy of the ion at A together with its energy in the CF of all the nuclei other than A, for the nuclei are not removed. i.e. from the one-electron terms the only contributions to the splittings come from the Coulomb interactions with adjacent nuclei. Each $\sum_{m=0}^{\infty} a_m$ is replaced with an angular momentum operator in L (see equivalences 2.17) which is subsequently replaced, by using the Wigner-Eckart theorem, by an operator in L ($L=6$) and then by an operator in J ($J=15/2$). The result is a typical crystal-field-like equivalent operator (see equation 1.13), and the local symmetry is fully reflected when all the various terms are collected together. Further crystal-field-like terms come from the two-electron operators of types $a' f f a$ and $a' f' a f$ for the $f f$ is equivalent to unity. In general the two-electron terms have the form:

$$\sum_{p \neq q} \langle \alpha_p \alpha_q | g | \alpha_p \alpha_q \rangle \alpha_p' \alpha_q' \alpha_p \alpha_q \quad (2.21)$$

There are three distinct possibilities for non-zero contributions to the MEs $\langle n | H | n \rangle$: (i) α_p and α_q remove closed shell electrons. (ii) α_p refers to an open shell at a specific site (say B), and α_q refers to a closed shell. (iii) both α_p and α_q annihilate open shell electrons.

In case (i) it can be seen that the resulting energy can be identified as the core-core two-electron energy but notice that it is not the one which would be deduced on simple electrostatic arguments since part of it is of exchange-like origin (Stevens 1976 p.27).

In case (ii) either $\alpha_p = \alpha_q$ and α_p and α_q belong to the same open shell at B, in which case they can denoted by b_p and b_q or $\alpha_p = \alpha_q$ and α_p and α_q belong to the same open shell at B and they be denoted by b_p and b_q . The former possibility contributes:

$$\langle b_p \alpha_q | g | b_p \alpha_q \rangle b_p' b_p \quad (2.22)$$

and the latter:

$$- \langle \alpha_p b_q | g | b_p \alpha_p \rangle b_p' b_q \quad (2.23)$$

Both possibilities have similar operators $b' b$ but the first is associated with a direct ME whereas the second has an exchange-like ME. In other words they contribute in a similar way to one-electron contributions but with different MEs. The MEs can be used to identify the origin of the terms. The $b' b$ shows that they are to be associated with open shell sites at B. If α_q is at site B as well then the direct term $\langle b_p \alpha_q | g | b_p \alpha_q \rangle$ is free-ion-like. If α_q is not at B then it is natural to identify $\langle b_p \alpha_q | g | b_p \alpha_q \rangle$ as part of the crystal-field at B due to electrons in closed shells on other ions. It is very interesting to identify the origin of term (2.23). If α_p is at site B then the term $-\langle \alpha_p b_q | g | b_p \alpha_p \rangle$ can be identified as a free-ion-like exchange contribution, but if α_p is not at site B it can be regarded as an additional contribution to the CF of entirely quantum origin.

The remaining *third possibility*, when all α 's refer to open shell electrons does not contribute crystal-field-like terms (Stevens 1976 p.29) and anyway it is not of interest to us since in this thesis we concentrate in dilute systems i.e. we consider systems with well separated RE magnetic ions so that there is no interaction between them.

In conclusion the first order theory for the ground manifold leads to a spin Hamiltonian of the form:

$$E_0 + \sum_A h_A(J_A) + \sum_{A \neq B} h_{AB}(J_A J_B) \quad (2.24)$$

where E_0 contains all contributions to the mean energy of the ground manifold, h_A contains crystal-field-like terms and h_{AB} exchange interactions between magnetic sites. In this thesis we shall only be interested in the crystal-field-like part of (2.24).

We postpone the discussion of the first order perturbation for S-state ions and of the second order contributions (notice that it is possible to have crystal-field-like contributions from second order) for the second part of this thesis since in the first part we concentrate our discussion of Er^{3+} :Au only on first order contributions. We hope that we have made sufficiently clear the Stevens treatment for the low-lying energy levels of a RE doped crystal. We summarise that the first order perturbation terms give large single-site terms which contribute to the mean energy of the ground manifold and reproduce CF theory. Corrections to this, appear mainly (Stevens 1976) in second order and they renormalise the crystal-field-like parameters which are already present in first order. A clear route has been provided by him whereby one can pass from a general Hamiltonian to a spin-Hamiltonian without distinguishing electrons.

2.6. The Determination of Crystal Fields Using a Recently Developed Unified Scheme

2.6.1. Introduction

In the previous section we have given a brief description of the treatment of Stevens for insulators doped with paramagnetic ions. As we have already mentioned in section 2.5 this treatment can be extended to conductors. This has been accomplished by Dixon and Wardlaw (1986a), (DW hereafter) in an attempt to study CFs in dilute RE alloys. Dilute alloy problems, although apparently simple, are very difficult to describe in a tractable way. The main reason for this is the presence of conduction electrons and their subsequent effects. For instance, screening effects arise because of them and if there is a difference in the valency of the impurity ion and the host metal ions, electrons from the conduction bands can become semi-localised. One expects

that any physically sensible model for conductors should incorporate such effects and especially the effects of screening in zeroth order. We shall briefly highlight the DW model and will present explicitly only terms of interest for the purposes of this thesis which appear in the first order perturbation scheme of DW. The full model is explained adequately in the original paper of DW.

2.6.2. Incorporation of Screening

As we have already pointed out any physically sensible model for metals should incorporate screening in zeroth order. DW concentrated their studies on a magnetic heavy RE ion, considered as a single impurity, substitutionally dissolved in a non-magnetic host and surrounded by a rigid regular array of ions in an otherwise perfectly periodic metallic host. Lattice vibrations and their interactions with the electrons are specifically excluded. To incorporate screening they performed a Bohm-Pines-like unitary transformation (Bohm and Pines 1953) on a general Hamiltonian of interacting electrons and nuclei. Their starting Hamiltonian was H_1 given below:

$$H_1 = \sum_i \frac{p_i^2}{2m} + \frac{1}{2} \sum_{i,j} \frac{e^2}{|r_i - r_j|} + \frac{1}{2} \sum_{n,m} \frac{Z_n Z_m e^2}{|R_n - R_m|} - \sum_n \frac{Z_n e^2}{|r_i - R_n|} + \sum_i \xi_i \hat{L}_i \hat{S}_i \quad (2.25)$$

where the summations are over all electrons (denoted by i and j) and nuclei (denoted by n and m). r_i 's and R_n 's denote position vectors for electrons and nuclei respectively and Z_n denotes the charge of the n -th nucleus. After following the above mentioned transformation applied to electrons and nuclei they finally obtained, within the Random Phase Approximation (RPA) the following Hamiltonian

$$H_2 = \sum_i \frac{p_i^2}{2m^*} + \frac{1}{2} \sum_{i,j} \frac{e^2}{|r_i - r_j|} F(k_i, |r_i - r_j|) + \frac{1}{2} \sum_{n,m} \frac{Z_n Z_m e^2}{|R_n - R_m|} F(k_n, |R_n - R_m|) - \sum_n \frac{Z_n e^2}{|r_i - R_n|} F(k_i, |r_i - R_n|) + \sum_i \xi_i \hat{L}_i \hat{S}_i \quad (2.26)$$

where m^* is an effective electronic mass given by $m/[1 - (\beta^2)]$ where β is related to the screening constant k_F (see section 2.6.3) by $\beta = \frac{k_F}{k_F}$, k_F being the Fermi wave vector. $F(k, r_{ij})$ is the screening function and is discussed in the section 2.6.3. In other words H_2 is obtained from the starting Hamiltonian H_1 by replacing m by m^* and the bare Coulomb interactions replaced by screened

ones. To obtain the result in equation (2.26) a series of exact unitary transformations were used and the RPA then only used to obtain the new form of kinetic energy (for details see DW). In DW other terms involving electron-plasmon and nuclei-plasmon interactions also arose as well as a modification of the spin-orbit coupling. These were shown at metallic densities to be at least of order α^2 times those retained where α is an order parameter whose size is $\approx 1/16$. Hence, for our purposes we neglect these terms. H_2 was taken by DW as the total Hamiltonian to perform degenerate perturbation theory following the scheme of Stevens (see section 2.5). In section 2.6.4 we will show how the method of Stevens is used on H_2 .

2.6.3. The screening constant k_e and the screening function $F(k_e r)$.

The function $F(k_e r)$ is defined (Raimes 1961 p.292-3) by:

$$F(k_e r) = 1 - \frac{2}{\pi} \int_0^{k_e r} \frac{\sin x}{x} dx \quad (2.27)$$

and it is an example of dynamic screening since it is due to the re-description of the motion of the electrons in terms of plasma oscillations plus short-range interactions among electrons (Raimes 1957). The graph of the screening function is shown in Figure 4, and the function $\exp(-k_e r)$ is also shown for comparison. We can see that for values of $k_e r$ less than 2, the functions are very similar, falling rapidly from unity at the origin to nearly zero. At larger values of $k_e r$ the function $F(k_e r)$ oscillates with slowly decreasing amplitude. In other words the effective range is about $2/k_e$. These oscillations become negligible when multiplied by $e^{-2/r}$ (see Figure 5).

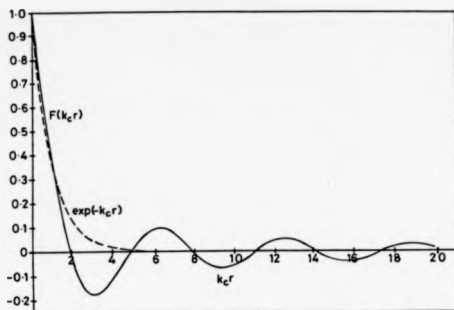


Figure 4: The full curve represents the function $F(k_e r)$ of equation (2.27) and the broken curve the function $\exp(-k_e r)$.

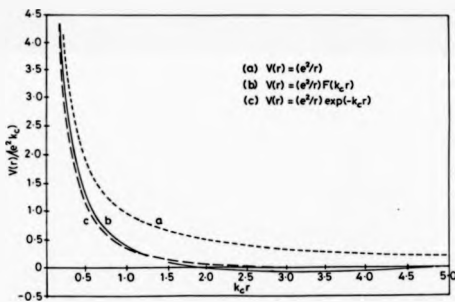


Figure 5: Comparison of the unscreened Coulomb interaction e^2/r with $(e^2/r)F(k_e r)$ and $(e^2/r)\exp(-k_e r)$.

It is enough, for the purpose of this thesis, to say that k_e is a *screening parameter*. Its physical

significance is more complicated but qualitatively it represents the magnitude of the maximum wave vector for which it is useful to introduce plasmons. Plasmon co-ordinates and momenta do not finally appear in H_2 although they do appear in intermediate steps for reasons given by DW. Theoretically and within the RPA the value of this critical wave vector is given by (Pines 1964 p.109-110):

$$k_c^{RPA} = \beta^{RPA} K_F \quad (2.28)$$

$$\beta^{RPA} = 0.47 \sqrt{r_s/a_0} \quad (2.29)$$

where r_s is defined (within the Independent Electron Approximation - IEA) as the radius of a sphere whose volume is equal to the volume per conduction electron and it is measured in units of the Bohr radius a_0 (see for instance Ashcroft and Mermin 1976 p.5). k_F is the Fermi wave vector (within the IEA) given by:

$$k_F = \frac{1.92}{r_s} \quad (2.30)$$

(Ashcroft and Mermin 1976 p.36). By combining equations (2.28), (2.29), (2.30) we finally obtain:

$$k_c^{RPA} = \frac{0.9024}{r_s^{3/2}} \quad (2.31)$$

For instance, for silver $r_s^{\text{Ag}} = 3.02 a_0$ and so $k_c^{RPA} = 0.52 a_0^{-1}$.

It is of outmost importance to point out that recent measurements (Eisenberger et al 1975, Zacharias 1975, Gibbons et al 1976, Batson et al 1976) in *Al*, *Li* and *Na* show that plasmons exist at values of the wave vector k beyond k_c^{RPA} given by (2.31). Such a conclusion has also been reached by the theoretical work of Pal et al (1980) and Pal and Tripathy (1985). They found that if one goes beyond the RPA plasmons exist far beyond the k_c^{RPA} . So we recognise that there is some doubt concerning the exact values of k_c . To give an idea of the magnitude of k_c we present the Table 2.2 below which contains values of β^{RPA} , β^P (P = Pal et al 1980) and β^{exp} for *Al*, *Li* and *Na*.

Table 2.2 : Values of β^{RPA} , β^F , β^{sw} for Al, Li and Na. r_s is in units of a_0 .

METAL	r_s	β^{RPA}	β^F	β^{sw}
Al	2.07	0.68	1.48	1.23 [a]
Li	3.22	0.84	1.83	1.40 [b]
Na	3.96	0.94	1.32	1.11 [c]

[a] Zacharias P 1975, J Phys F: Metal Physics **5**, 645-56

[b] Eisenberger P, Platzman P M and Schmidt P 1975, Phys Rev Lett **34**, 18-20

[c] Gibbons P C, Schnatterly S E, Ritsko J J and Fields J R 1976, Phys Rev B **13**, 2451-60

If we assume the relationship $\beta^{sw} = C \times \sqrt{r_s/a_0}$, where C is a numerical coefficient, we found, by using the data of Table 2.2 and a least squares fitting procedure, that $C = 0.705$ i.e.

$$\beta^{sw} = 0.705 \times \left(\frac{r_s}{a_0}\right)^{1/2}$$

Great insight should not be attached to such a relationship since we used data only for three elements for our fitting procedure but we did use it to give us a qualitative estimation of the order of magnitude of k_c . Now k_c for silver becomes 1.5 times larger than the RPA value i.e. $0.78a_0^{-1}$. We should treat the value of k_c with some caution and later we discuss our results for a range of values of k_c .

2.6.4. First Order of the DW Model

After establishing equation (2.26) as the Hamiltonian describing the RE doped dilute alloy, Dixon and Wardlaw rewrite (2.26) using powerful second quantisation techniques. Creators and annihilators a', a are used to create and annihilate one-electron orbitals in the 4f shell of the RE, and will have a suitable subscript to describe both the spin and orbital components. Similarly, c', c referred to band states b', b to the core states and d', d to the 5d-vbs (the existence of such a vbs has been extensively discussed in section 2.2).

To describe the majority conduction electron states, which were assumed *s-like*, they used the Fourier transform of generalised Wannier functions. The 4f, core (b) and 5d-electron states

were taken to be the actual generalised Wannier functions (Appendix A) $W_{\mathbf{k}}(\mathbf{r} - \mathbf{L})$ as they form a complete orthonormal set, with the transformed functions, and are localised functions about particular sites. It has been discussed earlier and in Appendix A that the functions $a'10>, b'10>, c'10>, d'10>$ therefore form an orthogonal set of basis functions orthogonal between different bands and between sites.

In the spirit of the treatment of Stevens they now define the ground family, projected out by P_0 as follows: the conduction electrons are in the lowest bands, the RE has an occupancy $4f^4$ consistent with a fixed L and S , the 5d state is occupied by one electron or none and all other localised orbitals are fully occupied with spins up and down. It was assumed that a state of the system, in which the 5d state is unoccupied but an extra electron occupies a neighbouring site, is also included in the ground family.

They made use of degenerate perturbation theory in projector form described by Bates et al (1968) and given earlier in section 2.5.2. The unperturbed Hamiltonian H_0 was defined following Stevens (see equation 2.10) and $H_2 - H_0$ was treated as a perturbation. H_2 has been conveniently divided up into two parts H_A and H_B so that within H_A each term conserves the number of a, b, c and d electrons separately, whereas H_B contains all operators which are interconfigurational e.g. $a'c$ which destroys a conduction electron and creates an additional electron in a 4f-orbital.

They now make the following assumptions:

- (i) Only one 5d-electron resides in the 5d-vbs, in agreement with our discussion in section 2.2, or none.
- (ii) Terms which involve core states only are dropped, since they will only give constant contributions in first order and cannot give terms in second order, because they do not couple families with different numbers of core electrons.
- (iii) They neglect interactions between core states on different sites since there will not be significant mixing because the electrons in them are so tightly bound to their nuclei.
- (iv) In H_B there are a number of terms which couple the c and d states with core states (b). They neglect most such terms, since the c and d one-particle states are much higher in

energy than the 4f states and hence the energy of the core states, with the exception of those parts of H_B of the form $a'ab'b$, $d'db'b$, $e'eb'b$ which will appear in first order. There are other contributions from the Coulombic parts of H_B which generate many electron states from the ground family at energies close or greater than those between core and d or e states e.g. $a'a'cc$ connects the ground family to a state \approx twice the energy difference between the 4f and band states. Similar arguments apply to terms like $a'a'cd$. These latter have also been neglected.

- (v) The on-site parts of some terms vanish identically from inversion arguments e.g. $a'b'bc$. As a is odd and the on-site part of c is even only odd angular momenta terms from the screened Coulomb interaction will produce non-vanishing terms. However, this means that one b is odd and the other even i.e. different, so when this term operates on the ground family we get zero.
- (vi) They drop all Coulomb and one-body MEs in second order where at least one of the one-electron functions is on a site other than the impurity site.
- (vii) They recognise the importance of terms which transfer electrons between the 5d-vbs and the s-conduction band. At the impurity site they assume an energy difference between these two states, but transferring a d-electron to any other site requires very much less energy, so little in fact that they include these latter states within the ground family.
- (viii) If H_B^{eod} denotes an electron-electron term in H_B , and H_B^{cf} describes a crystal-field-like term in H_B which arises from the fourth term in (2.25), then for a-electrons, at least, the $[MEs\ of\ H_B^{cf}] \ll [MEs\ of\ H_B^{eod}]$. They neglect terms in second order of the form $P_0 H_B^{eod} P_a H_B^{eod} P_0$ as it will only produce isotropic terms and they are interested in CFs which act on the a-part of the Hilbert space. They finally retain terms $P_0 H_B^{eod} P_a H_B^{cf} P_0 + h.c.$ as these will be much larger than $P_0 H_B^{cf} P_a H_B^{cf} P_0$ which are neglected.

To clarify the above we write schematically the resulting Hamiltonian, after performing the perturbation theory, as follows:

$$\begin{aligned}
 H_1 = & \text{(Coulomb among } a \text{'s + 2-nd order) +} \\
 & \text{(Coulomb among } a \text{'s and } d \text{'s + 2-nd order) +} \\
 & \text{(Coulomb between } a \text{'s and } b \text{'s) +} \\
 & \text{(Coulomb between } c \text{'s and } d \text{'s) +} \\
 & \text{(Coulomb between } a \text{'s and } c \text{'s) +} \\
 & a^\dagger a \text{ (KE + attraction + } V_I + V_{CF} + \text{s.o. + 2-nd order) +} \\
 & c^\dagger c \text{ (KE + attraction + } V_I + V_{CF} + \text{s.o.) +} \\
 & d^\dagger d \text{ (KE + attraction + } V_I + V_{CF} + \text{s.o.) +} \\
 & [c^\dagger d (V_I + V_{CF}) + \text{h.c.}]
 \end{aligned}$$

where $V_I = -Z^A (e^2/r) F(k_F r)$, Z^A is the magnitude of the additional positive charge at the impurity site when a host ion is replaced by the impurity. V_{CF} is the *classical* CF interaction:

$$V_{CF} = - \sum_{n \neq a} \frac{Z_n e^2}{|L - R_n|} F(k_F |L - R_n|)$$

where the sum over n being over neighbour sites to the impurity site when a host ion is replaced by the RE impurity. Z_n is the charge of the n -th neighbouring nucleus.

The same authors have shown (Dixon and Wardlaw 1986b) that an impurity carrying a net difference in charge from the host ion it substitutes for has the effect, if the interaction is strong enough, of splitting off a band state, which they denoted by $|c_0\rangle$, from the rest of the band containing states $|c_p\rangle$. $|c_0\rangle$ was A_1 -like under rotations and leaves behind other A_1 states in the band as well as states of other representations which $|c_0\rangle$ does not couple to. The zeroth order part of $|c_0\rangle$ is simply the s-like Wannier function which would be present at the impurity site in the perfectly periodic host with no impurity. This particular component is orthogonal to the rest of the host band Wannier functions by construction. The operators $\tilde{c}_{a_0}^\dagger$ and \tilde{c}_p^\dagger , which create other band states with A_1 symmetry and other representations respectively, principally create electrons at sites other than the impurity site.

They performed further unitary transformations to weaken the 4f-conduction band and 5d-conduction coupling before averaging over the conduction and the 5d states to obtain an effective 4f CF Hamiltonian. In first order they finally obtained:

$$\begin{aligned}
 H_{eff} = & \sum_{\substack{m, m', \sigma, \sigma' \\ \sigma, \sigma' \neq \sigma}} V_{m, m', \sigma, \sigma'}^{a, a, a, a} b_{m, \sigma}^{\dagger} b_{m', \sigma'}^{\dagger} b_{m, \sigma} b_{m', \sigma'} \\
 & + \sum_{\substack{m, m', \sigma, \sigma' \\ \sigma, \sigma' \neq \sigma}} V_{m, m', \sigma, \sigma'}^{a, a, a, a} b_{m, \sigma}^{\dagger} b_{m', \sigma'}^{\dagger} \tilde{c}_{m, \sigma}^{\dagger} \tilde{c}_{m', \sigma'} \\
 & + \sum_{\substack{m, m', \sigma, \sigma' \\ \sigma, \sigma' \neq \sigma}} \left\{ \langle \tilde{c}_{0, \sigma}^{\dagger} | V_{sc} | \tilde{c}_{0, \sigma} \rangle - \delta_{\sigma, \sigma'} \langle \tilde{c}_{0, \sigma}^{\dagger} | V_{sc} | \tilde{c}_{0, \sigma'} \rangle \right\} \tilde{c}_{0, \sigma}^{\dagger} b_{m, \sigma}^{\dagger} \tilde{c}_{0, \sigma} \\
 & + \sum_{m, \sigma} V_{m, \sigma} b_{m, \sigma}^{\dagger} b_{m, \sigma}
 \end{aligned} \quad (2.32)$$

where

$$\begin{aligned}
 V_{m, m', \sigma, \sigma'}^{a, a, a, a} = & \left\{ \langle \sigma_1, \sigma_2 | \frac{e^2}{r_{12}} F(k, r_{12}) | \sigma_3, \sigma_4 \rangle \right. \\
 & \left. - \langle \sigma_1, \sigma_2 | \frac{e^2}{r_{12}} F(k, r_{12}) | \sigma_4, \sigma_3 \rangle \right\}
 \end{aligned} \quad (2.33)$$

$$V_{m, \sigma} = \langle \sigma_1 | V_{CF} | \sigma_4 \rangle \quad (2.34)$$

V_{CF} has been defined above and V_{sc} represents the screened Coulomb interaction between 4f and conduction electrons.

In the second and third terms of (2.32) the \tilde{c}_0 and d operators may be replaced by their averages. In the first term of (2.32) the $b^{\dagger}b$ is equivalent to unity since they referred to filled cores (see discussion of this term in section 2.5.3). So effectively we obtain a one-electron-like Hamiltonian in $a^{\dagger}a$. To convert the pairs of creators and annihilators of 4f-electrons into orbital angular momenta and spin operators, the equivalences of Stevens (2.17) can be used. The details of how this can be done will be given in the subsequent sections where the first order terms are discussed in more detail. Finally, after using (2.17), H_{eff} can be equivalently written as:

$$\sum_{\sigma, \sigma'} A_{\sigma, \sigma'}^{(n)} O_{\sigma, \sigma'}^{(n)}(L) \quad (2.35)$$

where $A_{\sigma, \sigma'}^{(n)}$ are CFPs containing contributions from the four terms of (2.32). Notice that the above A 's are not the same as the usually considered CFP (denoted by C 's, see equation 1.13). In this thesis we shall use the C 's and the relationship of the C 's to the A 's will become apparent during the discussion of CFP in the subsequent sections.

Concluding we should say that the DW model can be considered as the most advanced quantum mechanical theoretical model for calculating CF for RE doped dilute alloys since: (i) it

incorporates dynamic screening (ii) does not distinguish electrons (iii) incorporates the many-electron nature of the problem since it uses second quantisation techniques and (iv) properly treats the 5d-vbs. By working consistently within this model much will be revealed as far as the origin of CFs is concerned. We notice, for future reference, that in this latter theory CF-like terms do not arise solely from electrostatic mechanisms but there are non-classical components (e.g. exchange contributions) as well as terms in second order which have nothing to do with interaction between charges at all e.g. $P_0 KE P$, $KE P_0$, which have already been investigated in the literature (Dixon et al 1982).

CHAPTER 3

CONTRIBUTIONS TO CRYSTAL FIELD PARAMETERS FOR $Er^{3+}:Au$ FROM LIGAND ELECTRONS AND NUCLEI

3.1. Introduction

In this chapter we discuss the first and fourth terms of H_{eff} given by equation (2.32) i.e. the interaction between the 4f-electrons of Er^{3+} and the ligand Gold ions, treated as ionic entities with extended charge distributions in space. We show that the 4f/ligand interaction can be described for $Er^{3+}:Au$ using a pseudo-PCM in which we use different effective charges for the fourth and sixth order components of the cubic CF.

The theory of DW described in section 2.6 presented first order operators using annihilators and creators which referred to a set of orthonormal wavefunctions, namely the generalised Wannier functions, on the RE site and about the ligand sites. Using the 5d radial wavefunction for neutral Gold from Herman and Skillman (1963) and the 4f wavefunction for Er^{3+} from Freeman and Watson (1962) - see also Appendix B - we can calculate approximately the radial extent of each. If we add these and compare the result with the nearest neighbour distance $R_{nn} = 5.452 \text{ a.u.}$ in the fcc structure of Gold we can see that the radial overlap is expected to be very small indeed. Thus we can take the free ion functions on the ligand sites (Herman and Skillman 1963)

and the 4f given of Freeman and Watson (1962) to represent the generalised Wannier functions to a very good degree of approximation. Of course such an approximation will begin to break down as the overlap of the 4f wavefunction on Er^{3+} with ligand orbitals increases. Even if the 4f radial density is expanded relative to the non-relativistic Hartree Fock results of Freeman and Watson (1962) due to an indirect relativistic effect arising from the relativistic contraction of the core electrons (see Freeman and Desclaux 1979), the 5d(Au)-4f(Er^{3+}) overlap will still be small enough to use the above approximation. As we shall see later, it is wrong to think that since the overlap is small the penetration effects will be small and so the conventional PCM would be a reasonably good approximation.

In the DW model each of the Coulomb interactions appearing, at the end of a sequence of unitary transformations, involved a screening function $F(k_e, r_{12})$ (see section 2.6.2). The incorporation of screening into the 4f/ligand penetration mechanism is not easy to compute, particularly if the full electronic screening interaction is used as in the DW. A simpler and more practical approach of estimating its effect is to first of all determine the effective pseudo-charges and then to write the screened interaction as $F(k_e, |L-R|) / |L-R|$. This will be done in Chapter 4. We shall see later in this chapter that the 4f/ligand penetration effects occur only with nearest neighbour ions. We have shown in Chapter 4 that for the system $Er^{3+}:Au$ at least and within the limitations of that approach (see discussion of the value of k_e in section 2.6.3 and Chapter 4), if the ligands can be described as effective point charges in some sense, then screening modifies the fourth order CFP of nearest neighbours by only about 7% whereas the sixth order CFP is virtually unchanged from the nearest neighbour unscreened pseudo-PCM value. Hence we shall study an unscreened 4f/ligand interaction (i.e. $k_e=0$ and hence $F(k_e, r_{12}) = 1$ in DW model) and later modify our results, if necessary. It is worthwhile to notice that, as far as CFs in $Er^{3+}:Au$ are concerned, although screening does not seem to have any significant effect on the inter-site 4f/ligand mechanism (Chapter 4 and this Chapter) it does have a very important effect on the intra-site-like 4f/5d-vbs mechanism (Chapter 5).

We earlier mentioned that the 4f electron wavefunction do have a small overlap with those of ligand electrons. This should not mislead us into thinking that the penetration effects are not

important. To demonstrate the importance of this particular penetration effect we consider that the CFP are made up of two separate contributions from the ligand nuclei and the extended electronic charge of ligand ions. Following DW this may be written as (first and fourth terms of H_{eff}):

$$H_{4f \text{ ligand}} = \sum_{m_1, m_2, \sigma_1, \sigma_2} V_{m_1, m_2, \sigma_1, \sigma_2}^{\sigma_1 \sigma_2 \sigma_1 \sigma_2} b_{m_1, \sigma_1}^\dagger b_{m_2, \sigma_2}^\dagger a_{m_1, \sigma_1} a_{m_2, \sigma_2} + \sum_{m, \sigma} V_{m, \sigma} a_{m, \sigma}^\dagger a_{m, \sigma} \quad (3.1)$$

In equation (3.1) the m 's and σ 's indicate the components of orbital and spin angular momentum respectively. $b_{m, \sigma}^\dagger$ creates a core spin-orbital of the ligand from the vacuum with component of orbital angular momentum m , and a spin component σ , which may be $m_z = \frac{1}{2}$ or $m_z = -\frac{1}{2}$. The a 's create 4f orbitals from the vacuum on the RE site and the subscripts are defined in the same way as for the b 's. MEs in the summations of equation (3.1) are defined by equations (2.33) and (2.34) but with $F(k, r_{12}) = 1$. In first order $b_1^\dagger b_1$ acts on the filled ligand core electronic ground state to produce unity (see discussion in section 2.5.3) so our effective Hamiltonian becomes:

$$H_{4f \text{ ligand}} = \sum_{m, \sigma} V_{m, \sigma} a_{m, \sigma}^\dagger a_{m, \sigma} + \sum_{m, \sigma} V_{m, \sigma} a_{m, \sigma}^\dagger a_{m, \sigma} \quad (3.2)$$

The Hamiltonian in equation (3.2) may now be re-expressed in terms of orbital and spin angular momentum operators using the set of Stevens's equivalences given by (2.17) to read as:

$$H_{4f \text{ ligand}} = \sum_{q, k} A_q^{(k)}(4f \text{ ligand}) O_q^{(k)}(L) \quad (3.3)$$

where the CFP $A_q^{(k)}(4f \text{ ligand})$ are found to be given by:

$$A_q^{(k)}(4f \text{ ligand}) = \sum_{m, \sigma} \frac{1}{2} \Delta_{m, m-q, \sigma, \sigma} (V_{m, m-q, \sigma, \sigma}^{\sigma, \sigma, \sigma, \sigma} + V_{m, m-q, \sigma, \sigma}^{\sigma, \sigma, \sigma, \sigma}) + \sum_{m, \sigma} V_{m, m-q, \sigma, \sigma} \Delta_{m, m-q, \sigma, \sigma} \quad (3.4)$$

3.2. Procedures to be Adopted for Calculations

In order to simplify our numerical calculations we shall assume that the axis of quantisation coincides with the internuclear axis connecting the Er^{3+} ion and one ligand ion. To make our procedure clear we concentrate on the interaction between the 4f-electrons of the Erbium and one ligand ion, considered to be a free ion with a point charge nucleus (of charge $Z_N \approx 1$) surrounded

by closed shells displaying an extended electronic charge distribution. No distortion of this distribution will be considered at this stage even though it is possible that the presence of a substitutional ion may bring about strains and deviations of this electronic charge from its free ion distribution. Axial symmetry then demands that $q=0$ and the position of the nucleus of the ligand will be $(R, \theta_1=0, \phi_1=0)$. Figure 6 shows the disposition of co-ordinate axes which we have used for the calculation of the direct contribution to the CFPs. Similarly, Figure 7 shows the co-ordinate axes used for the exchange case. The reasons for using two different co-ordinate arrangements will be discussed in sections 3.4 and 3.5.

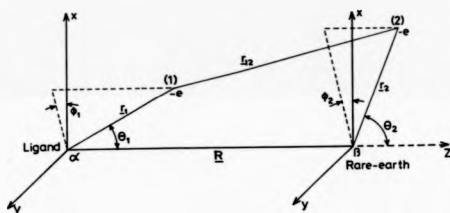


Figure 6: Interaction between a 4f(RE) and a ligand electron. Co-ordinate system used for the calculation of the direct part of $V_{4f,4f}^{(2)}(r_1, r_2, R, \theta_1, \theta_2, \phi_1, \phi_2)$ (see equation 2.33).

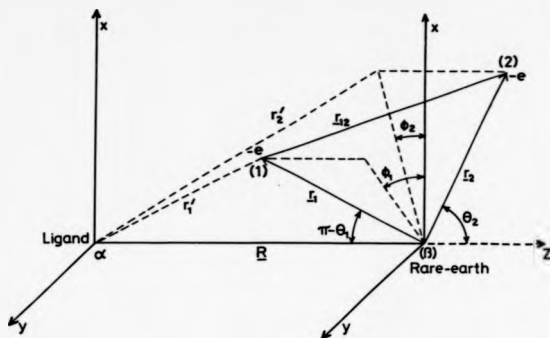


Figure 7: Interaction between a 4f(RE) and a ligand electron. Co-ordinate system used for the calculation of the exchange part of $V_{ee}^{4f, ligand}$ (see equation 2.33).

We were particularly interested in a Gold host which has a fcc structure. In a fcc-system the CF is described by two CFPs, the axial fourth and sixth order CFPs. We shall only discuss the penetration effects for these two CFPs but our analysis can be generalised to cover other cases.

In the next three sections we first present the wavefunctions we have used (section 3.3) and then examine the direct term of the Coulomb interaction (section 3.4). In section 3.5 we calculate exchange contributions to CFPs and finally in section 3.6 we discuss our results and the effects of screening on them.

3.3. Wavefunctions

In this section we present analytical forms of the wavefunctions we have used for Gold and for Er^{3+} . At a very early stage of our study we realised that, as far as we were aware and could ascertain, there were no reliable analytical wavefunctions for Gold. We decided to use the wavefunctions, given in numerical form, by Herman and Skillman. These are self-consistent solu-

tions of the non-relativistic Hartree-Fock-Slater equations for neutral ions. We have fitted these for Gold to linear combinations of Slater-like wavefunctions using the least-squares method and since they could be so useful the results are given in the Appendix B. If the Gold orbitals have a separable wavefunction of the form $R(r) Y_l^m(\theta, \phi)$ then $P(r) = rR(r)$ is actually tabulated where the normalisation condition is $\int_0^\infty R^2(r) r^2 dr = 1$ and r is in atomic units. We have also used the wavefunction for the 4f orbital of the Er^{3+} given by Freeman and Watson (1962), listed in Appendix B as well.

3.4. Contributions to the CFPs from the Direct Coulomb Term without Screening

To evaluate these contributions we inevitably have to calculate two-centre integrals and the most usual way of proceeding is to express all wavefunctions in the integrand in a common co-ordinate system. Another approach has recently been adopted in the work of Garcia and Faucher (1984) following much earlier developments by Buehler and Hirschfelder (1951, 1952), which we henceforth denote by BH1 and BH2. This method not only permits a simple evaluation of two-centre direct coulombic integrals but greatly reduces the time of computation. According to BH1 and BH2 the inverse distance between electrons (1) and (2) (see Figure 6), where the radius vector r_1 of electron (1) is relative to one site and the position vector r_2 of electron (2) is relative to the other site, is given by:

$$\frac{1}{r_{12}} = \sum_{\mu, \nu} b_{\mu, \nu}^{(1)}(r_1, r_2; R) Y_{\mu}^{\nu}(\theta_1, \phi_1) Y_{\nu}^{\mu}(\theta_2, \phi_2) \quad (3.5)$$

where $b_{\mu, \nu}^{(1)}$ is a function of r_1, r_2 and the distance between the sites R . This coefficient is related to that in BH1 and BH2 ($B_{\mu, \nu}^{(1)}(r_1, r_2; R)$) by :

$$b_{\mu, \nu}^{(1)}(r_1, r_2; R) = B_{\mu, \nu}^{(1)}(r_1, r_2; R) \times \left[\frac{(4\pi)^2}{[n_1, n_2]} \frac{(n_1 + |\mu|)!}{(n_1 - |\mu|)!} \frac{(n_2 + |\mu|)!}{(n_2 - |\mu|)!} \right]^{1/2} \quad (3.6)$$

where we have used the shorthand $[n_1, n_2] = (2n_1 + 1)(2n_2 + 1)$.

By using the properties of 3j-symbols (Rotenberg et al 1959), integrating over all angles and bearing in mind we are calculating a CFP from one nucleus of charge Zie_i at position $(0,0,R)$, we finally obtain:

$$A_0^{(n)} = 7 \times \left(\begin{smallmatrix} 3 & 0 & 0 \\ 0 & 0 & 0 \end{smallmatrix} \right) \times \frac{\langle 311 | O^{(n)} | 13 \rangle}{R_0^2} \times$$

$$\left\{ - \sum_{l,j} \frac{2[l]}{4\pi} \frac{1}{[n]^n} \int_0^{\overline{r}_1} \int_0^{\overline{r}_2} R_0^2(r_1) R_{4j}^2(r_2) b_{0,n}^0(r_1, r_2; R) r_1^2 r_2^2 dr_1 dr_2 \right.$$

$$\left. + \frac{Z}{[n]} \int_0^{\overline{r}_1} R_{4j}^2(r) \frac{r^2}{r_1^{n+1}} r^2 dr \right\} \quad (3.7)$$

where $r_< = \min(r, R)$ and $r_> = \max(r, R)$. The reduced MEs $\langle 311 | O^{(n)} | 13 \rangle$ can be found for instance in Smith and Thornley (1966). l is the principal quantum number of electrons on the ligand which have an orbital angular momentum l . The value of Z for Gold is +79. The expressions for $b_{0,n}^0$, as functions of r_1, r_2 and R , can be found for the three regimes defined below by combining equation (3.6), BH1 and BH2. They are given by:

Regime I, $R > r_1 + r_2$

$$b_{0,n}^0 = (-1)^n \frac{4\pi}{[n]^n} \frac{r_2^n}{R^{n+1}}$$

Regime III, $r_2 > R + r_1$

$$b_{0,n}^0 = (-1)^n \frac{4\pi}{[n]^n} \frac{R^n}{r_2^{n+1}}$$

Regime IV, $r_1 > R + r_2$

$$b_{0,n}^0 = 0, \quad \text{if } n > 0$$

$$= \frac{4\pi}{r_1}, \quad \text{if } n = 0$$

In what is termed Regime II where $|r_1 - r_2| \leq R \leq r_1 + r_2$ the appropriate expression for $b_{0,n}^0$ is far more complicated but can be found by using equation (3.6) and BH2. It is straightforward to obtain the CFPs produced by a no-longer axial ligand with coordinates (R, Θ, Φ) , with respect to the z-axis joining the RE and the ligand, by noting (see Garcia and Faucher 1984) that :

$$A_q^{(n)} = A_0^{(n)} C_q^n(\Theta, \Phi) \quad (3.9)$$

where the C_q^n denote normalised spherical harmonics (Silver 1976 p.71).

By taking proper account of appropriate radial integration limits and the fact that we shall only consider $n > 0$, the "extended charge" CFPs due to one ligand of Gold along the z-axis may be written as:

$$\begin{aligned}
 A_0^{(n)} &= 7 \times \left(\frac{3}{0} \frac{n}{0} \frac{3}{0} \right) \times \frac{\langle 311O^{(n)} | 13 \rangle}{N_z^2} \times \\
 &\left\{ - \sum_{l,j} \frac{2[l]}{[n]} \frac{(-1)^n}{R^{n+1}} \int_{r_1=0}^R \int_{r_2=0}^{R-r_1} R_{4f}^2(r_2) R_{4f}^2(r_1) r_1^2 r_2^{n+2} dr_1 dr_2 \right. \\
 &- \sum_{l,j} \frac{2[l]}{4n[n]^{1/2}} \int_{r_1=0}^R \int_{r_2=k-r_1}^{R-r_1} R_{4f}^2(r_2) R_{4f}^2(r_1) b_{0,n}^0(r_1, r_2, R) r_1^2 r_2^2 dr_1 dr_2 \\
 &- \sum_{l,j} \frac{2[l]}{[n]} (-1)^n \times R^n \int_{r_1=R}^{\infty} \int_{r_2=k-r_1}^{\infty} R_{4f}^2(r_2) R_{4f}^2(r_1) r_1^2 r_2^{n+1} dr_1 dr_2 \\
 &\left. + \frac{79}{[n]} \left[\frac{1}{R^{n+1}} \int_0^R R_{4f}^2(r) r^{n+2} dr + R^n \int_{r=R}^{\infty} R_{4f}^2(r) r^{1-n} dr \right] \right\} \quad (3.10)
 \end{aligned}$$

In order to discuss and clarify the differences between the extended charge treatment and the conventional PCM we introduce (following Garcia and Faucher 1984) the following variable:

$$p_n = \frac{A_0^{(n)}(\text{extended charge})}{A_0^{(n)}(\text{PCM})} \quad (3.11)$$

where:

$$A_0^{(n)}(\text{PCM}) = 7 \times \left(\frac{3}{0} \frac{n}{0} \frac{3}{0} \right) \times \frac{\langle 311O^{(n)} | 13 \rangle}{N_z^2} \times \frac{(Z - \sum_{l,j} 2[l])}{[n]} \times \frac{\langle r^n \rangle}{R^{n+1}} \quad (3.12)$$

where $\langle r^n \rangle = \int_0^R R_{4f}^2(r) r^{n+2} dr$ in the usual way. Note that the conventional PCM CF-Hamiltonian acting within the 4f configuration is determined from the interaction between completely localized effective charges $Z_{4f}^{N,l} |e|$ for each ligand ion N and the 4f RE electrons. $Z_{4f}^{N,l}$ is then determined as the difference between the net negative electronic charge of the ion and its nuclear charge i.e. in equation (3.12) $Z - \sum_{l,j} 2[l] = Z_{4f}^{N,l}$. If we had defined p_n for a no longer axial ligand because of equation (3.9), the angular orientation of the ligand, $Y_q^{(n)}(\Theta, \Phi)$, would cancel out so that the p-ratio remains a sensible comparison to make.

We have computed values of ρ_a for a limited number of distances for the case of $Er^{3+}.Au$. The results are summarised in Figure 8. Similar behaviour has been found for negatively charged ligands ($Cl^-O^{2-}F^-$) the REs being $Nd^{3+}, Eu^{3+}, Tm^{3+}$, in Garcia and Faucher (1984).

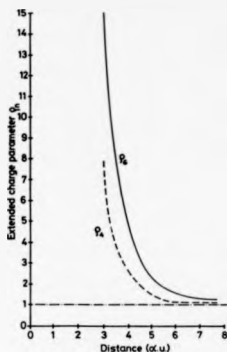


Figure 8: ρ_a parameter as a function of internuclear distance for $Er^{3+}.Au$. Contributions solely from the Direct Coulomb term have been considered.

The nearest neighbour distance (nnd) in the fcc structure of Gold, assuming that Erbium enters substitutionally is 3.542 a.u. (1 a.u. = 0.5292 Å). For this distance we found $\rho_a = 1.211$ and $\rho_s = 1.761$. We have also considered non-realistic distances $R = 3$ a.u. (where $\rho_a = 7.847$, $\rho_s = 14.473$) and $R = 3.75$ a.u. (where $\rho_a = 3.579$, $\rho_s = 7.941$) to give the qualitative Figure 8. One should note carefully that we have assumed orthogonality of the Er^{3+} and Gold wavefunctions throughout which for the nnd is a very good approximation. However for smaller distances this orthogonality will begin to break down for certain orbitals i.e. in principle we should take orthogonality corrections into account. We did not consider this worthwhile since the nnd for $Er^{3+}.Au$ is 3.542 a.u. and we only wished to give a qualitative feel for what one should expect if there was greater penetration between the RE ion and the ligand. From Figure 8 we see that for large values of R

the asymptotic value of ρ_n is unity for any value of n permitted for cubic symmetry. It is possibly worth noting that the $A_0^{(8)}$ extended charge values were very close to the PCM values. As we might expect the PCM is well justified for the second nearest neighbours (when $R = 7.71$ a.u.) and shells of neighbours even further out but the situation is quite different for the nearest neighbours. As the 4f electron penetrates the electronic charge distribution of the outer ligand orbitals of the nearest neighbour Gold ion it effectively experiences less of this latter charge and hence a more positive charge.

For each value of n separately we see that the ligand ion is effectively acting as a pseudo-point charge, "pseudo" since a different value of this effective charge is obtained for different values of n . Thus, for the $n=6$ CFP, which was small with respect to experimental values (Williams and Hirst 1969) when calculated within the PCM, is greatly improved when penetration effects are considered since the latter increase this particular PCM CFP by a factor of ≈ 1.8 . If we consider the $n=4$ CFP we can see that penetration will not explain the negative sign found by Williams and Hirst (1969). The PCM gives a value for the fourth order CFP which is opposite in sign to the experimental one, as is well known (see Table 1.2).

3.5. Contributions to the CFPs from the Exchange Term without Screening

In the previous section we have taken into account only the direct part of the Coulomb interaction of equation (2.33). We wish to determine whether the exchange contribution is quantitatively important for the determination of CFP for $Er^{3+}Au$. We find that it is not of any significance for the nearest neighbours and essentially zero for all other neighbours. Unfortunately, in this case, we have found that we cannot use the development of BH1, BH2 reliably and so we have resorted to the most common treatment whereby we transform the components of the integrand arising into a common co-ordinate system. Our new co-ordinate system has been already presented in Figure 7 of section 3.2. The inverse distance between electrons (1) and (2) (see Figure 7) may be expanded, in the usual way, as a series of products of spherical harmonics:

$$\frac{1}{r_{12}} = \sum_{\lambda=0}^{\infty} \sum_{\mu=-\lambda}^{\lambda} \frac{4\pi}{2\lambda+1} \frac{r_1^{\lambda}}{r_2^{\lambda+1}} Y_{\lambda}^{\mu*}(\theta_1, \phi_1) Y_{\lambda}^{\mu}(\theta_2, \phi_2) \quad (3.13)$$

To evaluate exchange MEs there are seemingly two different co-ordinate systems we could use. We may choose that with the origin at the RE ion (β in Figure 7) or at the ligand site (α in Figure 7). However, we found, in agreement with Gajek and Mulak (1985) that the second choice requires much longer computer time. The reason for this is that, if we expand the 4f wavefunctions, with $l=3$, over the ligand site, the alpha-expansion of Sharma (1976) becomes far more complicated than for d, p or s electrons i.e. the complexity of the alpha-expansion increases dramatically with increasing orbital angular momentum quantum number l .

We define g_{4f} as the 4f wavefunction of the RE ion and f_{4lm} as the wavefunctions of the ligand ion. As we must calculate a two-body ME with its radial and angular integrals we distinguish two different 4f and ligand orbitals by writing:

$$\begin{aligned} g_{4f}(r_1, \theta_1, \phi_1) &= R_{4f}(r_1) Y_{40}^m(\theta_1, \phi_1) \\ g_{4f}(r_2, \theta_2, \phi_2) &= R_{4f}(r_2) Y_{40}^m(\theta_2, \phi_2) \\ f_{4lm}(r_1, \theta_1, \phi_1) &= \sum_{j_1} A_j(k, j, m | R, j_1) Y_{4j_1}^m(\theta_1, \phi_1) \\ f_{4lm}(r_2, \theta_2, \phi_2) &= \sum_{j_2} A_j(k, j, m | R, j_2) Y_{4j_2}^m(\theta_2, \phi_2) \end{aligned} \quad (3.14)$$

where the $A_j(k, j, m | R, j)$ are defined appropriately (for example see equation 3.17) by using the alpha-expansion technique Sharma (1976). It is now straightforward to integrate the exchange contribution (including the angular parts of the operators from Stevens equivalences) over the angular variables by making use of the properties of 3j and 6j symbols (Rotenberg et al 1959). We obtain

$$\begin{aligned} &= \sum_{k,j,m} \sum_{l_1, l_2} \sum_{j_1, j_2} (2-5_{j_1 j_2}) \times (-1)^{j_1+m+l_1} \times 7 \times \frac{<3110^{(m)}13>}{N_4^2} \times \\ &\left(\begin{matrix} 3 & 0 & 0 \\ 0 & 0 & 0 \end{matrix} \right) \left(\begin{matrix} j_1 & j_2 & j \\ 0 & 0 & 0 \end{matrix} \right) \left(\begin{matrix} j_1 & j_2 & j \\ -m & m & 0 \end{matrix} \right) \left\{ \begin{matrix} j_1 & j_2 & j \\ 3 & 3 & \lambda \end{matrix} \right\} \times [1, j_1, j_2]^{1/2} \times f_k^{j_1 j_2}(4f, klm) \end{aligned} \quad (3.15)$$

where $f_k^{j_1 j_2}(4f, klm)$ are one-centre radial integrals given by:

$$f_k^{j_1 j_2}(4f, klm) = \int_0^\infty \int_0^\pi \int_0^{2\pi} A_j(k, j, m | R, j_1) R_{4f}(r_2) \frac{r_2^2}{r_2^{3+1}} R_{4f}(r_1) A_j(k, j, m | R, j_2)$$

$$r_1^2 r_2^2 dr_1 dr_2 \quad (3.16)$$

where $r_c = \min(r_1, r_2)$ and $r_s = \max(r_1, r_2)$. The reduced MEs $\langle 3110^{(1)} | 13 \rangle$ are the same as in equation (3.7). In equation (3.15), the procedure $\sum_{j_1, j_2} \sum_{j_1, j_2} (2 - \delta_{j_1 j_2})$ has been used instead of \sum_{j_1, j_2} to save computer time since the quantity, defined in (3.15), is independent of permutation of the j_1, j_2 indices (see properties of 3j and 6j symbols, Rotenberg et al 1959) and those of alpha-expansions (Sharma 1976).

Since the overlap between the 4f RE orbital and the outer 5d(on Au) is small we decided initially to estimate the contribution to the CFP from the 4f($E^{3/2}$)-5d(Au) exchange term and if this contribution was found important to incorporate other ligand orbitals as well. A full treatment would involve the following alpha-expansion for the 5d(Au) orbital (see the wavefunction of the 5d(Au) orbital in the Appendix B). That is:

$$A_j(k, l, m | R, r) = \frac{1}{r} \left[\sum_{A=1}^3 C_A \alpha_j(4Z_A, l, m | R, r) + \sum_{A=4}^5 C_A \alpha_j(3Z_A, l, m | R, r) \right] \quad (3.17)$$

The C_A in equation (3.17) have been given in the Appendix B and the α_j are the alpha-expansions appropriate to the Slater-like summands in the 5d orbital of Gold (Sharma 1976). The use of (3.17) is very time consuming to compute, the reason being that $l_{5d}=2$ and the alpha expansion is used ten times (see equation 3.16). To avoid this problem, and since we are initially interested in an estimation of the order of magnitude of the exchange contribution, we used the fact that in the region of interest (i.e. where significant overlap occurs - $R_{Au} = 5.452 \text{ a.u.}$ - so this corresponds to the region from the second node of the 5d-Au orbital and outwards) the contribution to the integrals of (3.16) will be due to the "tail" of the 5d radial wavefunction (see Figure 9).

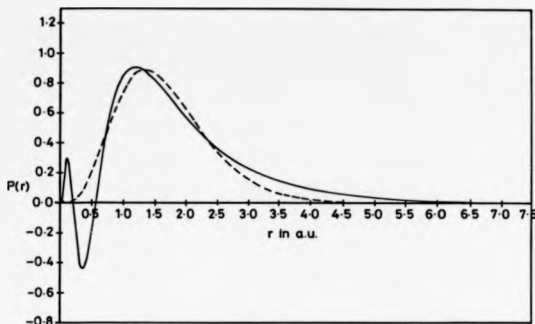


Figure 9: The Hermann-Skillman 5d radial wavefunction of Gold, $P_{5d}(r)$, given in the Appendix (full curve) and the approximation used, given by equation (3.18), for the estimation of the exchange contribution (dotted curve).

Explicitly we fitted that part of the 5d-Au radial orbital wavefunction, between $r_1 = 0.57361 \text{ a.u.}$ and $r_2 = \text{point where the wavefunction is essentially zero}$, to one Slater orbital of the form :

$$P_{5d} = r^4 \times 15.430971 \times e^{-1.0011742r} \quad (3.18)$$

Using (3.18) instead of (3.17) the use of the alpha expansion in (3.16) is reduced from ten to two times. The other approximation we have used is a practical approach to the convergence problem of the infinite series of equation (3.15) developed by Gajek and Mulak (1985). With these very reasonable approximations for the nnd we found that the contribution to the fourth and sixth order CFP are of the order $\approx +6.4 \times 10^{-3} \text{ cm}^{-1}$ and $\approx -1.2 \times 10^{-3} \text{ cm}^{-1}$ which in comparison with the corresponding direct values of -0.251 cm^{-1} and $+0.011 \text{ cm}^{-1}$ are negligible. Within the same approximations, exchange contributions were found practically zero for ligands further away than the nearest ones. We believe, therefore that we can neglect the exchange contributions for any distance $R \gg \text{nnd}$. If the two ions approach each other the approximation in Figure 9 will start to break down and so, in this case, we must use the exact alpha-expansion in equation (3.17). We decided not to perform such a calculation for two reasons. Firstly, the computation would become

excessively time consuming and secondly, in heavy RE noble metal complexes the relevant nnd and radial extents of outer orbitals are very similar to the case we have discussed, namely $Er^{3+}:Au$ and so exchange effects are expected negligibly small.

3.6. Conclusion and Discussion of Chapter 3

As we might expect ligands farther away than the nnd act, to a very good degree of approximation for a Gold host, as effective charges of +1 as far as the CF experienced by the 4f electrons on the Er^{3+} is concerned (we should make clear that in the presence of screening, ligands other than the nn will be completely screened out - see Chapter 4). Nearest neighbour ligands behave quite differently and their contribution to the CFPs differs considerably for the fourth and sixth CFP. Exchange contributions of the 4f/ligand penetration mechanism have been found to be quite negligible for $Er^{3+}:Au$. From equation (3.11) we see that if we multiply the point charge value of the net charge on such ligands by p_e , this will give effective charges or pseudo-Point Charges (pseudo-PCs) which will take account of the effect of extended charge on the ligand. As we have seen above $p_e=1.211$ whereas $p_a=1.761$ so the effect of the extended charge is very significant as regards the magnitude of CFPs. Furthermore these effective charges are unlike those appearing in the conventional PCM since they differ markedly with n even where, as in our compound $Er^{3+}:Au$, the overlaps between 4f and ligand orbitals are small.

For our system it is quite clear that even when extended charge distributions are used on the ligands this effect cannot explain the negative sign of the fourth order CFP in the literature. The extended electronic charge on the ligands has the largest effect on the sixth order CFP, and will multiply the unscreened PCM by 1.761, giving about 1.5 cm^{-1} (we are referring to CFP of the fcc system and not the axial one considered in this chapter) which improves considerably the agreement with the experimental value 4.17 cm^{-1} (Williams and Hirst 1969).

CHAPTER 4

SCREENING EFFECTS ON THE 4f/LIGAND MECHANISM FOR Er^{3+} :Au

4.1. Introduction

In Chapter 3 we have calculated contributions to CFPs from the unscreened interaction of ligand electrons and nuclei with the 4f-electrons of Er^{3+} when it is substitutionally dissolved in Gold. As we have already mentioned the incorporation of the full electronic screening of DW into the 4f/ligand penetration mechanism is difficult to compute. To estimate its effect we first determine the effective pseudo-PCs and the screened interaction is written as $F(k, |L - R|) / |L - R|$, where R represents the position vectors of neighbouring sites on which are the pseudo-PCs, and L the position vector of a 4f-electron with respect to the RE site. This approximation is justified in section 4.2. The most striking feature of our results is that if we use the DW model, screening tends to slightly increase the magnitude of the CFPs over their naive PCM value. This is contrary to what one might have expected and is brought about partly because a sizable contribution, of opposite sign, arises in a conventional lattice sum unscreened PCM, from next nearest neighbours, and, in the presence of screening, this component is screened out.

4.2. Justification of Approximation made in Section 4.1

To get a qualitative understanding of the above screening effects let us imagine the Er^{3+} :Am system when: (i) it is represented by extended electronic distributions for both Er^{3+} and Gold ions and (ii) when the electrons of Er^{3+} have extended distributions in space but the Gold ions are now considered as pseudo-PCs. In the former case one should expect that the screening will be less effective than in the latter. The reason being that in the first case less electronic charge will be present between the extended electronic charge distributions than in the latter where Gold-electrons and nuclei have been "absorbed" in a pseudo-PC. The above argument is useful if we find that by treating the system as in case (ii) screening effects are not important and so there is no need to consider the full DW screening of the more realistic case (i).

Of course a quantitative argument to support the approximative estimation of screening is desirable. The screened 4f/ligand-electrons interaction is written (first term of equation 2.32) as:

$$-\sum_{\substack{m_1, m_2 \\ \sigma_1, \sigma_2}} \langle \sigma_1, \sigma_2 | \frac{e^2}{r_{12}} F(k, r_{12}) | \frac{\sigma_1, \sigma_2}{m_1, m_2} b_{m_1, \sigma_1}^\dagger b_{m_2, \sigma_2} b_{m_2, \sigma_2} b_{m_1, \sigma_1} \rangle \quad (4.1)$$

where we omit the exchange part since it has been found, in section 3.5, negligible in comparison to the direct part. The m 's and σ 's have been defined previously (for instance in section 3.1). The orbitals in equation (4.1) on the Er^{3+} and Gold ions form part of a complete orthonormal set (section 3.1). It is matter of careful inspection of Figure 6 to be able to express the screened Coulomb interaction of equation (4.1) as:

$$\frac{e^2}{|L_1 + \bar{L} - L_2|} F(k, |L_1 + \bar{L} - L_2|) \quad (4.2)$$

which may be expanded as:

$$\sum_{L, M} g_L(r_1, |L_2 - \bar{L}|) Y_L^M(\theta_1, \phi_1) Y_L^M(\bar{\theta}, \bar{\phi}) \quad (4.3)$$

where (θ_1, ϕ_1) represent the orientation of L_1 (see Figure 6) and $\bar{\theta}, \bar{\phi}$ of $L_2 - \bar{L}$. As we have repeatedly mentioned earlier (for instance section 2.5.3) the operator $b^\dagger b$, corresponding to filled cores, is equivalent to unity. On summing over the core orbitals of a given angular momentum, an angular contribution of the form $\sum_M |Y_L^M|^2$ is produced from the core orbitals in equation (4.1) which

has no angular dependence. Hence in equation (4.3) $L = 0$, and only $g_0(r_1, |R - L_2|) \propto C$, where C is a constant, need be considered in calculating contributions of equation (4.1). g_0 may be found exactly in principle but a better approach suitable for making approximations is to write equation (4.3) as:

$$\frac{e^2 F [\mu(1 - h^2 - 2hx)]^{1/2}}{R'(1 - h^2 - 2hx)^{3/2}} \quad (4.4)$$

where $\mu = k_z R'$, $R' = |L_2 - R|$, $h = \frac{r_1}{R}$ and x is the cosine of the angle between $L_2 - R$ and L_1 . As L_2 refers to a 4f-electron, whose wavefunction is sharply peaked and close to the origin, $|R - L_2|$ is expected to be larger than r_1 in general (of course there is always some very small overlap of the "interacting" neighbouring wavefunctions). g_0 will now be the coefficient of the Legendre polynomial $P_0(x) \propto C'$, where C' is a new constant proportional to the above C , appearing in equation (4.2) when it is Taylor expanded in powers of h . An approximate expansion for g_0 may then be obtained by truncating this series at an appropriate power of h . This has been found (Dixon 1986, private communication) to be:

$$\frac{e^2}{|L_2 - R|} \left\{ F(k_z |L_2 - R|) - \frac{h^2}{3\pi} (\sin\mu + \mu \cos\mu) - \frac{2h^4}{4! \times 5\pi} [2(\sin\mu - \mu \cos\mu) - \mu^2(\sin\mu + \mu \cos\mu)] + \dots \right\} \quad (4.5)$$

Note that the leading term of $F(k_z, r_{12})$ is 1. For an estimation of the terms between the curly brackets of equation (4.5) we choose the "worst" possible values for the quantities involved. We have used $r_1 = 1.64a_0$, $R = 5.452a_0$, $R' = |L_2 - R| = 3.81a_0$, $\mu = k_z R' = 0.7a_0^{-1} \times 3.81a_0 = 2.67$ and used that $|\sin\mu \pm \mu \cos\mu| \leq |\sin\mu| + |\mu| |\cos\mu| \leq 1 + 2.67 = 3.67$, $h^2 = \frac{\langle r_1^2 \rangle}{R^2} = \frac{2.6394}{R^2} = 0.182$,

$h^4 = \frac{\langle r_1^4 \rangle}{R^4} = 0.0644$. By using these values we see that the term in h^2 is approximately one order of magnitude smaller than the first term and the term in h^4 is about two orders of magnitude smaller than the first term. We therefore expect a reasonably accurate estimation of the screening by neglecting all terms in h^2 and higher powers of h .

4.3. Calculation

The other part of the 4f/ligand interaction is the interaction of the 4f-electrons of Er^{3+} with the neighbouring Gold nuclei at R_n . This interaction is given by:

$$\sum_{m,m'} \langle \sigma_2 | V_{CF} | \sigma_4 \rangle \delta_{m,m'} \delta_{m,m'} \quad (4.6)$$

where V_{CF} has been defined in section 2.6.4. As we have already proved for the unscreened case, see Chapter 3, equations (4.1) and (4.6) combine to give an effective one-body operator which may clearly be written in the form of equation (4.6) but with the Z_n becoming the pseudo-PCs defined in Chapter 3. This situation is not quite as simple as the above might suggest since we have found in Chapter 3, that for different parts of the CF interaction different values of the magnitude of the effective PCs must be used.

By using these pseudo-PCs we calculate that the contributions to the C_4 and C_6 CFPs, for Er^{3+}, Au , defined by equation (1.13) have as follows:

$$C_4 = \left\{ -0.125 \left(\frac{4\pi}{5} \right)^{1/2} \sum_R Y_4^{00}(\theta_R, \phi_R) \langle a_4(r, R) \rangle \right\} \times Z_{n,A}^{eff} \times \frac{e^2}{a_0} \quad (4.7)$$

$$C_6 = \left\{ -0.0625 \left(\frac{4\pi}{13} \right)^{1/2} \sum_R Y_6^{00}(\theta_R, \phi_R) \langle a_6(r, R) \rangle \right\} \times Z_{n,B}^{eff} \times \frac{e^2}{a_0} \quad (4.8)$$

where :

$$Z_{n,A}^{eff} = \begin{cases} +1.211 & n = \text{nearest neighbours} \\ +1 & n = \text{all other neighbours} \end{cases}$$

$$Z_{n,B}^{eff} = \begin{cases} +1.761 & n = \text{nearest neighbours} \\ +1 & n = \text{all other neighbours} \end{cases}$$

The averages are defined by :

$$\langle a_n(r, R) \rangle = \int_0^\infty R_4^2(r) a_n(r, R) r^2 dr \quad (4.9)$$

where the function $a_n(r, R)$ is the coefficient appearing in the expansion of the function

$\frac{F(k_c | r - R |)}{1 - R}$ in Legendre polynomials. That is

$$\frac{F(k_c | r - R |)}{1 - R} = \sum_{n=0}^{\infty} a_n(r, R) P_n(\cos \gamma)$$

where γ is the angle between r and R and $a_n(r, R)$ is defined in Appendix C. When $k_c = 0$ (i.e. no screening) the average $\langle a_n(r, R) \rangle$ collapses to $\frac{\langle r^2 \rangle}{R^{n+1}}$.

Before discussing the quantitative effect of screening on the CFPs, given by equations (4.7), (4.8), we should determine the value of k_c to be used. Although in this chapter we consider only the effects of screening and do not consider in detail the contributions to CFPs from the 5d-vbs we shall see that whether the 5d-vbs is bound or not does, however, limit the effects which screening can have on the CFPs.

4.4. Approximate evaluation of the Screening Constant k_c .

To obtain k_c we have calculated the energy of the eleven 4f-electrons of the Er^{3+} ion, including a modified kinetic energy, the screened Coulomb attraction to the Er^{3+} nucleus and the screened Coulomb repulsion between 4f-electrons and those in core shells and other 4f orbits. We have used the 4f radial wavefunction of Freeman and Watson (1962). In a similar way to the method described in section 4.3 we have used an effective charge to combine the attraction of the Er^{3+} nucleus and repulsion by core electrons. We also did this when calculating the 4f and 5d energies denoting the effective charges by Z_{eff}^{4f} and Z_{eff}^{5d} . For the 4f energy we initially put $k_c = 0$ and derived an expression for the 4f energy as a function of Z_{eff}^{4f} . The resulting energy was equated to the 4f energy from empirical data (Dieke 1968) for the free Er^{3+} . This equation determined $Z_{eff}^{4f} = 18.94$. The 4f energy was then recalculated for $k_c \neq 0$, the kinetic energy now being $\frac{p^2}{2m} (1 - \frac{\beta^2}{6})$ where $\beta = 1.569 k_c a_0$ and m was the bare electron mass. Assuming that the 4f energy is not significantly modified (see our discussion in section 1.2 and Freeman and Watson 1962) in the presence of screening we obtain an equation for k_c , Z_{eff}^{4f} being already determined. This procedure gave $k_c = 0.713 a_0^{-1}$ (Christodoulos 1985).

The validity of this procedure is questionable since:

(i) we are using Freeman and Watson Hartree-Fock non-relativistic wavefunctions for a free Er^{3+} ion and

(ii) it seems as though the value of k_c is independent of the host which is certainly not the case.

On the other hand we believe that the magnitude of our value is a reasonable one since:

(i) according to our discussion of section 1.2 the energy of the 4f-electrons of Er^{3+} is not much modified when embedded in a host and

(ii) the value obtained is reasonably near to the one obtained by using the empirical relation determined in section 2.6.3 i.e. $0.78a_0^{-1}$.

However we need a starting point and so we shall discuss our estimations of the screening effects for $k_c = 0.713a_0^{-1}$. As we see later the exact value of k_c , provided that it is close to the above value, will not affect our conclusions.

To determine a form for the 5d-vbs we have made a linear interpolation between existing numerical data for the neutral Gd and Lu atoms (Herman and Skillman 1963) and made a least squares fit to the following parametrised wavefunction :

$$R_{5d}^{Er^{3+}}(r) = r^{2.5} \sum_{i=1}^2 C_i e^{-Z_i r} + r^2 \sum_{i=3}^5 C_i e^{-Z_i r} \quad (4.10)$$

We give the parameters of this fit in Table B.15 of Appendix B. For our calculations we used a 24-parameter 5d radial wavefunction (Christodoulos 1985) but here we present a more elegant form which gives the same results. Using the same method as for the 4f case we find $Z_{eff}^{5d} = 6.386$ (the 5d energy being obtained from empirical data of Dieke 1968). When screening is inserted with $k_c = 0.713a_0^{-1}$, the 5d energy becomes $1.54 \frac{e^2}{a_0}$, i.e. unbound, so is consistent with the assumptions used in the DW model. In view of the uncertainty in the value of k_c in Figure 10 we have computed the variation of the 5d energy (in $\frac{e^2}{a_0}$ units) against k_c (in a_0^{-1} units) and we note carefully that at approximately $k_c \approx 1.15a_0^{-1}$ the energy becomes negative and remains so for higher values of k_c . As there is no experimental evidence to suggest the 5d state is bound, in fact

there is much to the contrary, this feature suggest that we cannot have $k_c \geq 1.15a_0^{-1}$ for Er^{3+} .

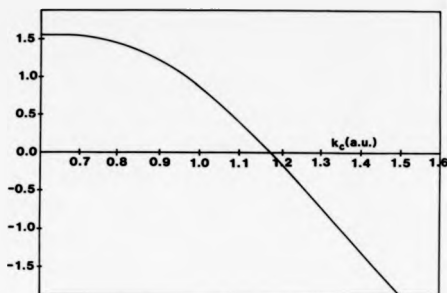


Figure 10: Variation of the 5d-vbs energy (in e^2/a_0) with the value of k_c (in a_0^{-1})

4.5. Results and Comparison with earlier work

In Table 4.1 we present our results for C_4 and C_6 in the sixth column. We compare them with the experimental values of Williams and Hirst (1969) (second column, $1K = 0.695 \text{ cm}^{-1}$), the lattice sum unscreened PCM with an effective charge of +1 on all neighbours (third column), the calculations of Duthie and Heine (1979) (fourth column) and a DW screened PCM with effective charges of +1 on all neighbours in order to distinguish the effect of screening from penetration effects (fifth column). Duthie and Heine used free electron screening in a conventional PCM with effective charges of +1 on all neighbours and found values for both C_4 and C_6 which are much smaller than the unscreened lattice-sum PCM values.

Table 4.1: Comparison between theory and experiment

CFPs	experiment	unscreened PCM all neigh ch=+1	Duthie-Heine Hartree screening	this work all neigh ch=+1	this work accurate eff ch
	cm^{-1}	cm^{-1}	cm^{-1}	cm^{-1}	cm^{-1}
C_4	-22.24 ± 2.78	8.3	1.33	10.42	12.62
C_6	4.17 ± 0.35	0.83	0.42	0.926	1.63

Our calculations use DW screening which has been introduced systematically via unitary transformations from a general Hamiltonian (see section 2.6) and gives, for $k_c = 0.713a_0^{-1}$, CFPs which are larger than the lattice-sum values. We expect our approach to be physically more reasonable since it is well known that free electron screening exaggerates the screening effect (Pines 1964, Raimis 1972, when combined with the work of Daniels et al 1970 and Raether 1980). The value of C_4 we calculate using a lattice-sum unscreened PCM with all neighbouring charges equal to +1 is mainly made up of contributions from nearest ($C_4^* = 11.2264\text{cm}^{-1}$) and next nearest neighbours ($C_4^{\text{nn}} = -3.969\text{cm}^{-1}$). When screening is introduced ($k_c = 0.713a_0^{-1}$) C_4^* is slightly reduced to $C_4^* = 10.42\text{cm}^{-1}$ whereas $C_4^{\text{nn}} = -0.39\text{cm}^{-1}$ (In Table 4.1 -fifth column- we present C_4 as the value of C_4^* only. This is so because we found that the contribution of all neighbours except the nearest is of the order of 2% of the C_4^*). Thus the effect of screening in the first order DW model is to effectively make C_4 more positive (relative to the net unscreened PCM value) since the negative component from next nearest neighbours is reduced by a factor of ten. By taking into account the accurate effective pseudo-PCs of Chapter 3 we finally obtain $C_4 = 12.62\text{cm}^{-1}$. Since there is considerable uncertainty in the value of k_c we have plotted C_4 against k_c in Figure 11 and we see that for $0 \leq k_c \leq 0.8 a_0^{-1}$ C_4 does not change appreciably (remember that the k_c obtained from the empirical formula defined in section 2.6.3 was $0.78a_0^{-1}$).

In the case of the C_6 CFP, in the unscreened model, the second nearest neighbours again give a negative contribution but only about 6% of the magnitude of that from nearest neighbours.

When screening is introduced C_6^{∞} becomes negligible and C_6 is principally determined by nearest neighbours.

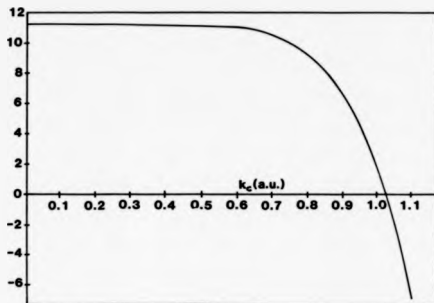


Figure 11 : Variation of C_4 (in cm^{-1}) with k_z (in a_0^{-1}). Only nearest neighbour contributions with charges of +1 have been taken into account.

After $k_z = 0.8a_0^{-1}$ there is a dramatic change and when $k_z > 1.04a_0^{-1}$ C_4 changes sign. The fact that the experimental value of C_4 is negative is very difficult to explain by choosing larger values of k_z because for (see Figure 10) a value of k_z appropriate to make C_4 agree with experiment would mean that the 5d state was bound. This would imply very different effective moment values from experiment and possible g-value changes in EPR. These are not observed which implies that the 5d state is not bound.

4.6. Conclusion for Chapter 4

Our calculations have shown that DW screening modifies the C_4 CFP of nearest neighbours by only about 7% whereas the corresponding C_6 CFP is virtually unchanged (see section 4.5). The contributions from second and higher order shells of neighbours have been found negligible. We

also show that DW screening affects the magnitude of CFPs, in comparison with unscreened PCM values, by up to 20% (see Table 4.1). The probability that screening is responsible for the reversal in sign of C_4 is small because the range of screening parameters required would create a bound 5d state in contradiction to experiment. The negative contribution to C_4 from next nearest neighbours is virtually screened out thereby effectively increasing the C_4 CFP. A similar result has been found for the C_4 CFP with a more pronounced enhancement due to penetration effects (see Chapter 3).

CHAPTER 5

CONTRIBUTIONS TO CRYSTAL FIELD PARAMETERS FOR Er^{3+} :Au FROM A 5d VIRTUAL BOUND STATE

5.1. Introduction

Some years ago it was proposed (section 2.2, Coles and Orbach in ref. 15 of Williams and Hirst 1969) that a non-magnetic 5d-vbs on the RE site, when interacting with the 4f electrons of the RE, could explain the magnitude of the C_4 CFP and more importantly its sign which is opposite to that which one might calculate using a naive PCM (Table 1.2). The creation of such a state could be understood by considering the difference between the valence of the host ions and the substitutional RE (section 2.2). The formation of such a non-magnetic state on a trivalent RE ion in a monovalent non-magnetic noble metal has been supported by several workers (e.g. Devine 1974, Lacueva et al 1982 and references therein). Chow (1973) estimated the 4f-5d(vbs) contribution to the C_4 CFP for Dy^{3+} , Er^{3+} and Yb^{3+} in Silver and Gold.

The aim of this Chapter is to examine in detail firstly the effects of conduction electron screening on the 4f-5d(vbs) interaction, where we assume that the 5d-vbs does not mix with orbitals on neighbouring sites, at least initially and secondly the penetration effects of the 5d-vbs with ligand orbitals. This latter effect has been studied by making the 5d-vbs orthogonal

to ligand states, and calculating their subsequent effects on the 4f ground state splitting. The mixing of the 5d-vbs with the conduction band states is assumed weak (DW).

We point out that considerably better agreement with experiment than Chow's calculations may be obtained by taking into account the screening of the 4f-5d(vbs) interaction by conduction electrons while the penetration effects have been proved not important (at least with the 5d-vbs radial wavefunction of equation (4.11) - obviously, the more extended the 5d-vbs radial wavefunction the more significant the penetration effects). We show that screening modifies the exchange part of this interaction considerably but only changes the direct component by a negligible amount compared with the exchange. Our study concentrates on the $Er^{3+}:Au$, but is trivially extended to the $Er^{3+}:Ag$ case and may readily be adapted for Dy^{3+} and Yb^{3+} in Silver and Gold, to compare with the work of Chow (1973).

5.2. Preliminaries

It is normally argued (section 2.2) that, in cubic symmetry, the 5d-vbs splits into the irreducible representations t_{2g} (xy, yz, zx) and e_g ($x^2-y^2, 3z^2-r^2$) which are defined as follows (note that we have dropped the common radial factor, Ballhausen 1962 p.64):

$$\begin{aligned} e_g^+ &= d_{x^2-y^2} = \frac{1}{2^{\frac{1}{2}}} (Y_2^2 + Y_2^{-2}) = \frac{1}{r^2} \left(\frac{5}{4\pi}\right)^{\frac{1}{2}} \frac{\sqrt{3}}{2} (x^2 - y^2) \\ e_g^+ &= d_{3z^2-r^2} = Y_2^0 = \frac{1}{r^2} \left(\frac{5}{4\pi}\right)^{\frac{1}{2}} \frac{1}{2} (3z^2 - r^2) \\ t_{2g}^0 &= d_{xy} = \frac{1}{i 2^{\frac{1}{2}}} (Y_2^2 - Y_2^{-2}) = \frac{1}{r^2} \left(\frac{5}{4\pi}\right)^{\frac{1}{2}} \sqrt{3} xy \\ t_{2g}^1 &= d_{yz} = -\frac{1}{2^{\frac{1}{2}}} (Y_2^1 - Y_2^{-1}) = \frac{1}{r^2} \left(\frac{5}{4\pi}\right)^{\frac{1}{2}} \sqrt{3} yz \\ t_{2g}^2 &= d_{zx} = -\frac{1}{i 2^{\frac{1}{2}}} (Y_2^1 + Y_2^{-1}) = \frac{1}{r^2} \left(\frac{5}{4\pi}\right)^{\frac{1}{2}} \sqrt{3} zx \end{aligned} \quad (5.1)$$

The three t_{2g} states, having angular dependence xy, yz and zx extend towards the positively charged nearest neighbours in the fcc lattice, while the two e_g , having angular dependence x^2-y^2 and $3z^2-r^2$, extend into regions midway between the fcc nearest neighbours. This geometry means that the t_{2g} will have lower energy than the e_g states. It is assumed therefore that the three t_{2g} states have an equal probability of containing at most one electron. The interaction between

these partially occupied states and the 4f electrons gives rise to a crystal-field-like splitting. According to the DW model the 4f-5d(vbs) interaction can be written in second quantised form as: (second term of equation 2.32)

$$H_{4f/5d} = \sum_{\substack{m,m',n,n',p,p_1,p_2 \\ \sigma,\sigma_1,\sigma_2}} V_{m,m',n,n',p,p_1,p_2}^{\sigma,\sigma_1,\sigma_2} a_{m,\sigma}^\dagger a_{m',\sigma_1}^\dagger a_{n,\sigma_2}^\dagger a_{n',\sigma}^\dagger a_{p,\sigma} a_{p_1,\sigma_1} a_{p_2,\sigma_2} \quad (5.2)$$

where the annihilators and creators destroy and create electrons in generalised Wannier states at the RE site and have been defined previously. The ME in equation (5.2) is defined by equation (2.33).

In section 5.3 we shall discuss the effects of conduction electron screening on the 4f-5d(vbs) interaction where, to represent generalised Wannier functions, we have used the 4f radial wavefunction of Freeman and Watson (1962) which is orthogonal to the 5d-vbs wavefunction we have used, given by equation (4.11). In other words we suppose both the 4f and 5d-vbs wavefunctions are orthogonal to all neighbouring orbitals. Although such an approximation is a sound one for the 4f wavefunction (see discussion in section 3.1) it is not clear at all for the 5d-vbs wavefunction because this latter wavefunction is much more extended than the 4f one and so one should calculate carefully the effect of overlap with neighbouring orbitals. In section 5.4 we make the 5d-vbs wavefunction of equation (4.11) orthogonal to neighbouring electronic orbitals and recalculate the 4f/5d(vbs) contribution to CFPs with the new 5d-vbs wavefunction. We find that the contribution to the C_4 CFP is not significantly altered. We also find that there is a contribution to the C_6 CFP, although it is not quantitatively important. This contribution is qualitatively interesting and comes about due to the mixing of the 5d-vbs with neighbouring electronic orbitals. It is worth noting that, so far, such a contribution was not attributed to the 5d-vbs (see our discussion in section 5.4).

5.3. Contributions of the 4f/5d(vbs) Mechanism to the CFPs when the 5d-vbs Free Ion Wavefunction of Equation (4.11) is Used

By using the equivalences of Stevens (equation 2.17) between pairs of second quantised operators and orbital and spin angular momentum operators we obtain the following expressions

for the direct and exchange contributions to C_4 CFP:

$$C_4(\text{direct}) = \frac{35}{9} \times \begin{pmatrix} 3 & 0 & 0 \\ 0 & 0 & 0 \end{pmatrix} \times \begin{pmatrix} 2 & 0 & 0 \\ 0 & 0 & 0 \end{pmatrix} \times \frac{\langle 3110^{(4)}113 \rangle}{N_4 \times 8 \times \kappa_{4f,A}} \times$$

$$F^4(4f, 5d) \times \sum_{m_1=-1,1,2} (-1)^{3+m_1} \begin{pmatrix} 2 & 4 & 2 \\ -m_1 & 0 & m_2 \end{pmatrix} \quad (5.3)$$

$$C_4(\text{exchange}) = -\frac{32}{3} \times \frac{\langle 3110^{(4)}113 \rangle}{N_4 \times 8 \times \kappa_{4f,A}} \times \sum_{m_1=-3}^3 \sum_{m_2=-1,1,2} \sum_{n=-1,1,3} G^*(4f, 5d) \begin{pmatrix} 2 & 0 & 3 \\ 0 & 0 & 0 \end{pmatrix}^2 \times$$

$$(-1)^{3-m_1} \begin{pmatrix} 3 & 4 & 3 \\ -m_1 & 0 & m_1 \end{pmatrix} \left[\frac{1}{2} \begin{pmatrix} 3 & n & 2 \\ -m_1 & m_1-m_2 & m_2 \end{pmatrix}^2 + \frac{1}{2} \begin{pmatrix} 3 & n & 2 \\ -m_1 & m_1+m_2 & -m_2 \end{pmatrix}^2 \right] \quad (5.4)$$

where for a single 4f electron $\kappa_{4f,A} = 2/(45 \times 11)$ (Stevens 1952). $\langle 3110^{(4)}113 \rangle = 279.217657$ (Smith and Thornley 1966), $N_4^2 = 8662.5$ (Stevens 1974) and the radial Slater integrals are defined as:

$$F^4(4f, 5d) = e^2 \int_0^\infty \int_0^\infty R_{4f}^2(r_1) R_{5d}^2(r_2) a_4(r_1, r_2) r_1^2 r_2^2 dr_1 dr_2 \quad (5.5)$$

$$G^*(4f, 5d) = e^2 \int_0^\infty \int_0^\infty R_{4f}(r_1) R_{5d}(r_1) a_n(r_1, r_2) R_{5d}(r_2) R_{4f}(r_2) r_1^2 r_2^2 dr_1 dr_2 \quad (5.6)$$

The function $a_n(r_1, r_2)$ arise from an expansion of the screened Coulomb repulsion in Legendre polynomials (see Appendix C).

The parameter k_c which we use here is defined in section 4.4. Due to the uncertainty in the determination of k_c (see discussion in sections 2.6.3 and 4.4) we provide in Table 5.1 the values of the above Slater integrals and compare them with the corresponding ones of Chow (1973) for different values of k_c . By using the values of 3j-symbols from Rotenberg et al (1959) and the Slater integrals in Table 5.1 we obtain $C_4(\text{direct})$ and $C_4(\text{exchange})$ displayed in Table 5.2.

Table 5.1 : Values of 4f-5d(vbs) Slater integrals for $Er^{3+}:Au$. k_z is in a_0^{-1} units and the Slater integrals in cm^{-1} .

	Chow (1973)	$k_z = 0.0$	$k_z = 0.713$	$k_z = 1.1$
$F^4(4f, 5d)$	11752.4	11522.61	11522.30	11509.43
$G^1(4f, 5d)$	10331.0	10407.44	9348.46	7518.93
$G^3(4f, 5d)$	8585.6	8526.16	8523.88	8479.40
$G^5(4f, 5d)$	6584.6	6513.16	6513.16	6513.16

Table 5.2 : Values of contributions to C_4 in cm^{-1} for $Er^{3+}:Au$ due to the direct and exchange terms of the 4f-5d(vbs) interaction. k_z is in units of a_0^{-1} .

	Chow (1973)	$k_z = 0.0$	$k_z = 0.713$	$k_z = 1.1$
$C_4(\text{direct})$	-163.23	-160.04	-160.03	-159.85
$C_4(\text{exchange})$	140.43	140.90	130.49	112.33
$ \frac{\text{exch.}}{\text{dir.}} $	86%	88%	82%	70%
$C_4(\text{dir.}) + C_4(\text{exch.})$	-22.8	-19.14	-29.54	-47.52

From experiment (Williams and Hirst 1969) the values of C_4 for $Er^{3+}:Ag$ and $Er^{3+}:Au$ are (note that the conversion factor, to obtain these results in cm^{-1} , is taken as $1K = 0.695 \text{ cm}^{-1}$):

$$C_4(Er^{3+}:Ag) \approx -48.65 \pm 1.39 \text{ cm}^{-1}$$

$$C_4(Er^{3+}:Au) \approx -22.24 \pm 2.78 \text{ cm}^{-1}$$

From Table 5.2 we see that the strong compensation of the total value of C_4 , made up of exchange and direct parts, measured by the ratio $| \frac{\text{exchange}}{\text{direct}} |$, in the case of no screening ($k_z = 0.0 a_0^{-1}$), wakens with increasing k_z and, as a result, an increasingly larger negative contribution is obtained for C_4 . A screened pseudo-PC contribution for $Er^{3+}:Au$ is about 12.62 cm^{-1} (see Table 4.1). We now see that for $k_z = 0.713 a_0^{-1}$ the sum of the 4f-5d(vbs) and the screened

pseudo-PC contributions give a total value of $\approx -17 \text{ cm}^{-1}$, in satisfactory agreement with experiment for $\text{Er}^{3+}:\text{Au}$. The dependence of the 4f-5d(vbs) mechanism on the host is through the k_z and interpenetration effects of the 4f electrons and of the 5d-vbs with the ligand electrons. Since $k_z^{\text{Au}} = (\frac{3.01}{3.02})^{1/2} k_z^{\text{Ag}}$ (DW) we see that the contribution from the 4f-5d(vbs) mechanism, in the $\text{Er}^{3+}:\text{Ag}$ alloy, remains virtually the same. A screened PC contribution, for $k_z = 0.712 a_0^{-1}$, for $\text{Er}^{3+}:\text{Ag}$ gives $C_4 = +10.23 \text{ cm}^{-1}$. In Chapter 3 we found that the penetration of the 4f with ligand electrons can be effectively considered by assuming, for the C_4 case, a net pseudo-PC of 1.211 on the ligands for $\text{Er}^{3+}:\text{Au}$. It is known that the metallic radius of Gold is virtually the same as for Silver (Samsonov 1968 p.102,p.106). This suggests that the pseudo-PCs for Silver should have a similar value to those in Gold since the nearest neighbour distances for Gold and Silver are approximately the same. Of course, there will be some differences, but these changes will certainly not explain the large difference in magnitude between C_4 for Gold and C_4 for Silver. As far as the penetration effects of the 5d-vbs with ligand electrons and their subsequent effect on the 4f splitting, these have been estimated (by making the 5d-vbs orthogonal to ligand electrons) for $\text{Er}^{3+}:\text{Au}$ (see section 5.4) and found to be of no significant importance. We expect, by using similar arguments as in the 4f/ligand penetration mechanism above, that the 5d-vbs/ligand contribution is not important for $\text{Er}^{3+}:\text{Ag}$ as well. Within the first order of DW and the approximations of our calculations we cannot explain the difference in the C_4 CFP of Silver and Gold although later we put forward a possible mechanism whereby agreement might be obtained using information which is available from band structure calculations (see Chapter 9).

5.4. Corrections to the Contributions Obtained in Section 5.3 Due to Orthogonalisation of the Free 5d-vbs to Neighbouring Sites

The calculation in section 5.3 has been performed using a free ion 5d-vbs wavefunction whereas the DW model employs an orthonormal basis set. To obtain an orthogonal 5d-vbs wavefunction we have used the method of Löwdin (1950). If the original free ion orbitals are denoted by $|\phi_p\rangle$ and the new combinations by $|\lambda_p\rangle$ then :

$$|h_n\rangle = \sum_p (\tilde{I} + S)_{np}^{-1} |\phi_p\rangle \quad (5.7)$$

where the overlap matrix \tilde{S} is so defined that :

$$S_{np} = \begin{cases} \langle \phi_p | \phi_n \rangle & , \text{ if } n \neq p \\ 0 & , \text{ if } n = p \end{cases} \quad (5.8)$$

Finally:

$$|h_n\rangle = |\phi_n\rangle - \frac{1}{2} \sum_p S_{np} |\phi_p\rangle + \frac{3}{8} \sum_p S_{np} S_{pp} |\phi_p\rangle + \dots \quad (5.9)$$

We decided initially to estimate the contribution to the CFPs assuming that the 5d-vbs overlaps only with the outermost 5d orbital of Gold and if this contribution was found important to incorporate other ligand orbitals as well. Thus, we describe the 5d-vbs by $15d-\text{vbs}; \Gamma, 0\rangle$ where Γ means that the orbital transforms like the irreducible representation Γ of the cubic point group under rotations about its own site and "0" denotes that the orbital is localised about the impurity site which has been taken as the center of the coordination system (see Figure 12):

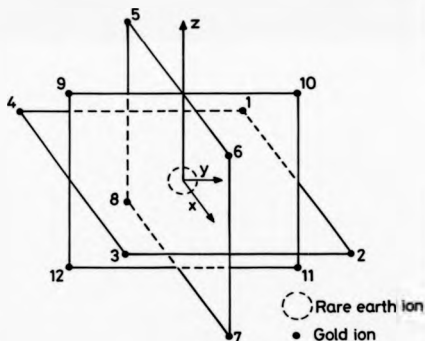


Figure 12: The twelve nearest neighbours (labelled as 1, 2, ..., 12) of the fcc structure of $Er^{3+}:Au$. The impurity site is labelled as 0.

The position of the twelve nearest neighbours of the RE site is given, in polar coordinates, in Table 5.3.

Table 5.3: Polar coordinates of the twelve nearest neighbours of the RE site.

Site	Position	Site	Position	Site	Position
1	$\theta = \frac{\pi}{2}, \phi = \frac{3\pi}{4}$	5	$\theta = \frac{\pi}{4}, \phi = \pi$	9	$\theta = \frac{\pi}{4}, \phi = \frac{3\pi}{2}$
2	$\theta = \frac{\pi}{2}, \phi = \frac{\pi}{4}$	6	$\theta = \frac{\pi}{4}, \phi = 0$	10	$\theta = \frac{\pi}{4}, \phi = \frac{\pi}{2}$
3	$\theta = \frac{\pi}{2}, \phi = \frac{7\pi}{4}$	7	$\theta = \frac{3\pi}{4}, \phi = 0$	11	$\theta = \frac{3\pi}{4}, \phi = \frac{\pi}{2}$
4	$\theta = \frac{\pi}{2}, \phi = \frac{5\pi}{4}$	8	$\theta = \frac{3\pi}{4}, \phi = \pi$	12	$\theta = \frac{3\pi}{4}, \phi = \frac{3\pi}{2}$

The new 5d-vbs wavefunction is given by:

$$|5d-vbs; \Gamma, new\rangle = |5d-vbs; \Gamma, 0\rangle - \frac{1}{2} \sum_{R \neq R'} S_{RR'} |5d-Au; \Gamma' R' (label \text{ of site })\rangle \quad (5.10)$$

where we have retained only the terms linear in overlaps and the irreducible representation in the left-hand side denotes the generic irreducible representation of the particular state. Note that the summation in equation (5.10) contains 5d orbitals of Gold *centred on neighbouring sites*. There are 25 possible overlaps between *d*-orbitals of the central and a neighbouring site (see states of equation 5.1). Since there are 12 nearest neighbours one should expect $25 \times 12 = 300$ overlaps in principle at any rate. Fortunately, this number is reduced considerably due to symmetry arguments. Since such a calculation is a very complicated one and liable to possible errors due to the many factors involved (e.g. five *d*-orbitals on each nearest neighbouring site, 12 nearest neighbours etc) we actually calculated numerically all possibilities and compared with symmetry arguments. We obtained full agreement, as expected, so our cross-check was satisfactory, confirming the results previously obtained. To calculate the overlaps we developed a method for the expansion of an off-site function about the site of interest which is described in full in Appendix D.

After an intricate calculation we finally found that the five new orthogonalised 5d-vbs states are given by:

$$\begin{aligned}
 |5d-vbs; e_g^*, 0\rangle = & |5d-vbs; e_g^*, 0\rangle - \frac{1}{2} \left\{ \delta_{13} [|e_g^*, 1\rangle + |e_g^*, 2\rangle + |e_g^*, 3\rangle + |e_g^*, 4\rangle \right. \\
 & + \delta_{11} [|e_g^*, 5\rangle + |e_g^*, 6\rangle + |e_g^*, 7\rangle + |e_g^*, 8\rangle + |e_g^*, 9\rangle + |e_g^*, 10\rangle + |e_g^*, 11\rangle + |e_g^*, 12\rangle] \\
 & + \delta_3 [|e_g^*, 5\rangle + |e_g^*, 6\rangle + |e_g^*, 7\rangle + |e_g^*, 8\rangle - |e_g^*, 9\rangle - |e_g^*, 10\rangle - |e_g^*, 11\rangle - |e_g^*, 12\rangle] \\
 & \left. - \delta_{15} [|t_{2g}^*, 5\rangle - |t_{2g}^*, 6\rangle + |t_{2g}^*, 7\rangle - |t_{2g}^*, 8\rangle \right. \\
 & \left. - |t_{2g}^*, 9\rangle + |t_{2g}^*, 10\rangle - |t_{2g}^*, 11\rangle + |t_{2g}^*, 12\rangle] \right\} \quad (5.10a)
 \end{aligned}$$

$$\begin{aligned}
 |5d-vbs; e_g^*, 0\rangle = & |5d-vbs; e_g^*, 0\rangle - \frac{1}{2} \left\{ \delta_2 [|e_g^*, 1\rangle + |e_g^*, 2\rangle + |e_g^*, 3\rangle + |e_g^*, 4\rangle \right. \\
 & + \delta_{11} [|e_g^*, 5\rangle + |e_g^*, 6\rangle + |e_g^*, 7\rangle + |e_g^*, 8\rangle - |e_g^*, 9\rangle - |e_g^*, 10\rangle - |e_g^*, 11\rangle - |e_g^*, 12\rangle] \\
 & + \delta_1 [|e_g^*, 5\rangle + |e_g^*, 6\rangle + |e_g^*, 7\rangle + |e_g^*, 8\rangle + |e_g^*, 9\rangle + |e_g^*, 10\rangle + |e_g^*, 11\rangle + |e_g^*, 12\rangle] \\
 & \left. - \delta_7 [2 |t_{2g}^*, 1\rangle - 2 |t_{2g}^*, 2\rangle + 2 |t_{2g}^*, 3\rangle - 2 |t_{2g}^*, 4\rangle + |t_{2g}^*, 5\rangle - |t_{2g}^*, 6\rangle + |t_{2g}^*, 7\rangle - |t_{2g}^*, 8\rangle \right. \\
 & \left. + |t_{2g}^*, 9\rangle - |t_{2g}^*, 10\rangle + |t_{2g}^*, 11\rangle - |t_{2g}^*, 12\rangle] \right\} \quad (5.10b)
 \end{aligned}$$

$$\begin{aligned}
 |5d-vbs; t_{2g}^*, 0\rangle = & |5d-vbs; t_{2g}^*, 0\rangle - \frac{1}{2} \left\{ 2\delta_7 [|e_g^*, 1\rangle - |e_g^*, 2\rangle + |e_g^*, 3\rangle - |e_g^*, 4\rangle \right. \\
 & - \delta_{23} [|t_{2g}^*, 5\rangle - |t_{2g}^*, 6\rangle + |t_{2g}^*, 7\rangle - |t_{2g}^*, 8\rangle + |t_{2g}^*, 9\rangle - |t_{2g}^*, 10\rangle + |t_{2g}^*, 11\rangle - |t_{2g}^*, 12\rangle] \\
 & + \delta_{22} [|t_{2g}^*, 5\rangle + |t_{2g}^*, 6\rangle + |t_{2g}^*, 7\rangle + |t_{2g}^*, 8\rangle + |t_{2g}^*, 9\rangle + |t_{2g}^*, 10\rangle + |t_{2g}^*, 11\rangle + |t_{2g}^*, 12\rangle] \\
 & \left. + \delta_{21} [|t_{2g}^*, 1\rangle + |t_{2g}^*, 2\rangle + |t_{2g}^*, 3\rangle + |t_{2g}^*, 4\rangle] \right\} \quad (5.10c)
 \end{aligned}$$

$$\begin{aligned}
 |5d-vbs; t_{2g}^*, 0\rangle = & |5d-vbs; t_{2g}^*, 0\rangle - \frac{1}{2} \left\{ \delta_{23} [|t_{2g}^*, 5\rangle + |t_{2g}^*, 6\rangle + |t_{2g}^*, 7\rangle + |t_{2g}^*, 8\rangle \right. \\
 & - \delta_{22} [|t_{2g}^*, 1\rangle - |t_{2g}^*, 2\rangle + |t_{2g}^*, 3\rangle - |t_{2g}^*, 4\rangle + |t_{2g}^*, 9\rangle - |t_{2g}^*, 10\rangle + |t_{2g}^*, 11\rangle - |t_{2g}^*, 12\rangle] \\
 & + \delta_{21} [|t_{2g}^*, 1\rangle + |t_{2g}^*, 2\rangle + |t_{2g}^*, 3\rangle + |t_{2g}^*, 4\rangle + |t_{2g}^*, 9\rangle + |t_{2g}^*, 10\rangle + |t_{2g}^*, 11\rangle + |t_{2g}^*, 12\rangle] \\
 & \left. - \delta_7 [\sqrt{3} (|e_g^*, 5\rangle - |e_g^*, 6\rangle + |e_g^*, 7\rangle - |e_g^*, 8\rangle) \right. \\
 & \left. + |e_g^*, 5\rangle - |e_g^*, 6\rangle + |e_g^*, 7\rangle - |e_g^*, 8\rangle] \right\} \quad (5.10d)
 \end{aligned}$$

$$\begin{aligned}
 |5d-vbs; i_{2d}, new \rangle = & |5d-vbs; i_{2d}, 0 \rangle - \frac{1}{2} \left\{ \delta_{21} [|i_{2d}, 9 \rangle + |i_{2d}, 10 \rangle + |i_{2d}, 11 \rangle + |i_{2d}, 12 \rangle] \right. \\
 & + \delta_{22} [|i_{2d}, 1 \rangle + |i_{2d}, 2 \rangle + |i_{2d}, 3 \rangle + |i_{2d}, 4 \rangle + |i_{2d}, 5 \rangle + |i_{2d}, 6 \rangle + |i_{2d}, 7 \rangle + |i_{2d}, 8 \rangle] \\
 & + \delta_5 [\sqrt{3} (|e_g, 9 \rangle - |e_g, 10 \rangle + |e_g, 11 \rangle - |e_g, 12 \rangle) - |e_g, 9 \rangle + |e_g, 10 \rangle - |e_g, 11 \rangle + |e_g, 12 \rangle] \\
 & \left. - \delta_{25} [|i_{2d}, 1 \rangle - |i_{2d}, 2 \rangle + |i_{2d}, 3 \rangle - |i_{2d}, 4 \rangle \right. \\
 & \left. + |i_{2d}, 5 \rangle - |i_{2d}, 6 \rangle + |i_{2d}, 7 \rangle + |i_{2d}, 8 \rangle] \right\} \quad (5.10e)
 \end{aligned}$$

where we have used the notation $|i_{2d}, \text{label of site} \rangle$ instead of the full $|5d-Au; i_{2d}, \text{label of site} \rangle$ for simplicity. The δ 's represent overlaps the origin of which can be easily understood by careful inspection of the d -states multiplied by these δ 's and equation (5.10) e.g. δ_{25} in equation (5.10e) is related to the overlap $\langle i_{2d}, 1 | i_{2d}, 0 \rangle$ which has the same magnitude as $\langle i_{2d}, 2 | i_{2d}, 0 \rangle$ and so on. These δ 's have been found to have the following numerical values:

$$\begin{aligned}
 \delta_1 &= -0.04501 \\
 \delta_2 &= +0.03220 \\
 \delta_3 &= +0.04458 \\
 \delta_7 &= +0.01057 \\
 \delta_{11} &= +0.006465 \\
 \delta_{12} &= -0.07075 \\
 \delta_{13} &= +0.01831 \\
 \delta_{22} &= -0.02538 \\
 \delta_{23} &= +0.05661 \\
 \delta_{25} &= -0.04537
 \end{aligned} \quad (5.11)$$

The subscripts of the δ 's have no obvious significance to the reader but we wish to keep this notation since it has been used throughout our lengthy calculation, to avoid confusion.

Once the orthogonalised $5d-vbs$ states were determined the corresponding MEs V of equation (5.2) become (initially we concentrated only on the direct part and if this contribution was found to be important we intended to incorporate the exchange term as well):

$$\begin{aligned}
 &\langle 4f m_1, 5d-vbs; \Gamma_1, new \mid V_{SC} \mid 4f m_3, 5d-vbs; \Gamma_2, new \rangle = \\
 &\langle 4f m_1, 5d-vbs; \Gamma_1, 0 \rangle - \frac{1}{2} \sum_{R_1, R_2, \Gamma_1} S_{R_1, R_2, \Gamma_1} \langle 5d-Au; \Gamma_1', R_1(\text{label of site}) \rangle \mid V_{SC} \mid \\
 &4f m_3, 5d-vbs; \Gamma_2, 0 \rangle - \frac{1}{2} \sum_{R_1, R_2, \Gamma_2} S_{R_1, R_2, \Gamma_2} \langle 5d-Au; \Gamma_2', R_2(\text{label of site}) \rangle = \\
 &\langle 4f m_1, (5d-vbs; \Gamma_1, 0) \mid V_{SC} \mid 4f m_3, (5d-vbs; \Gamma_2, 0) \rangle \\
 &- \frac{1}{2} \sum_{R_1, R_2, \Gamma_1} S_{R_1, R_2, \Gamma_1} \langle 4f m_1, (5d-vbs; \Gamma_1, 0) \mid V_{SC} \mid 4f m_3, (5d-Au; \Gamma_2', R_2(\text{label})) \rangle \\
 &- \frac{1}{2} \sum_{R_1, R_2, \Gamma_1} S_{R_1, R_2, \Gamma_1} \langle 4f m_1, (\Gamma_1', R_1(\text{label})) \mid V_{SC} \mid 4f m_3, (5d-vbs; \Gamma_2, 0) \rangle \\
 &+ \frac{1}{4} \sum_{R_1, R_2, \Gamma_1} \sum_{R_3, R_4, \Gamma_2} S_{R_1, R_2, \Gamma_1} S_{R_3, R_4, \Gamma_2} \langle 4f m_1, (5d-Au; \Gamma_1', R_1(\text{label})) \mid V_{SC} \mid \\
 &4f m_3, (5d-Au; \Gamma_2', R_2(\text{label})) \rangle \quad (5.12)
 \end{aligned}$$

where V_{SC} denotes the screened Coulomb interaction. It is trivial exercise to show that the second and third terms of the right-hand side of equation (5.12) are equal. Notice that they involve one off-site orbital and one overlap. The fourth term involves the square of an overlap and two off-site orbitals which indicates that we expect it to be at least an order of magnitude smaller than the second and third terms, if not orders of magnitude. We concentrate on the second term of equation (5.12). In order to calculate this ME we suppose that r_1 and r_2 refer to the RE site and so expand the off-site 5d-Au orbital with respect to the RE site (see Appendix D). We have used, as before, the 4f radial wavefunction of Freeman and Watson (1962) in the form $R_{4f}(r)Y_3(\theta, \phi)$ and for the 5d-states we incorporated the new t_{2g} -like states defined by equations (5.1) and (5.10) where a general off-site d -state has the form :

$$f(lz-\frac{1}{2}) \left[b_1 Y_2^{m_1} + b_2 Y_2^{-m_1} \right]$$

If the off-site state transforms like the e_g^* irreducible representation then $b_1 = b_2 = 1/(2^{1/2})$. If it transforms like the e_g^* then $b_1 = 1, b_2 = 0$. If it transforms like the t_{2g}^0 then $b_1 = -b_2 = 1/(i 2^{1/2})$. Finally, if it transforms like the t_{2g}^1 $b_1 = -b_2 = -1/(2^{1/2})$ and for the t_{2g}^2 representation $b_1 = b_2 = -1/(i 2^{1/2})$. Similarly the on-site 5d-vbs is represented by:

$$R_{5d}^{E_{2n}}(r) [a_1 Y_2^{m_1} + a_2 Y_2^{-m_1}]$$

The values of the coefficients a_1, a_2 are defined similarly as the above b 's.

We found, using the expansion of the screened Coulomb interaction given in Appendix C and equations (1.19), (1.43) of Rotenberg et al (1959), that the contributions to the C_4 and C_6 CFPs were as follows:

$$\begin{aligned} & \frac{153.6987447}{2} \times \sum_{\lambda=0}^{\infty} \sum_{\mu=-\lambda}^{\lambda} \sum_{L_1=0}^{\infty} \sum_{L_2=0}^{\infty} (-1)^{2\lambda+L_1+L_2} F_{\lambda}^{L_1 L_2} (4f, 5d^{E_{2n}}, 5d^{A_6}) \\ & \left(\frac{4!}{(2\lambda)! (4-2\lambda)!} \right)^{1/2} R^{\lambda} (2L_1+1) \sqrt{2L_2+1} \\ & \begin{pmatrix} 0 & 0 & 0 \\ 0 & 0 & 0 \end{pmatrix} \begin{pmatrix} 0 & 0 & 0 \\ 0 & 0 & 0 \end{pmatrix} \begin{pmatrix} 0 & 0 & 0 \\ 0 & 0 & 0 \end{pmatrix} \begin{pmatrix} 0 & 0 & 0 \\ 0 & 0 & 0 \end{pmatrix} \begin{pmatrix} 0 & 0 & 0 \\ 0 & 0 & 0 \end{pmatrix} \begin{pmatrix} 0 & 0 & 0 \\ 0 & 0 & 0 \end{pmatrix} \begin{pmatrix} 0 & 0 & 0 \\ 0 & 0 & 0 \end{pmatrix} \begin{pmatrix} 0 & 0 & 0 \\ 0 & 0 & 0 \end{pmatrix} \\ & \left[a_1^* b_1 \begin{pmatrix} 2-\lambda & \lambda & 2 \\ m_6-\mu & \mu & -m_6 \end{pmatrix} \begin{pmatrix} 2 & L_1 & 2-\lambda \\ -m_6-\mu & \mu & m_6 \end{pmatrix} + a_1^* b_2 \begin{pmatrix} 2-\lambda & \lambda & 2 \\ -m_6-\mu & \mu & m_6 \end{pmatrix} \begin{pmatrix} 2 & L_1 & 2-\lambda \\ -m_6-\mu & \mu & m_6 \end{pmatrix} \right. \\ & \left. + a_2^* b_1 \begin{pmatrix} 2-\lambda & \lambda & 2 \\ m_6-\mu & \mu & -m_6 \end{pmatrix} \begin{pmatrix} 2 & L_1 & 2-\lambda \\ m_6-\mu & \mu & -m_6 \end{pmatrix} + a_2^* b_2 \begin{pmatrix} 2-\lambda & \lambda & 2 \\ -m_6-\mu & \mu & m_6 \end{pmatrix} \begin{pmatrix} 2 & L_1 & 2-\lambda \\ m_6-\mu & \mu & -m_6 \end{pmatrix} \right] \end{aligned} \quad (5.13)$$

where

$$F_{\lambda}^{L_1 L_2} (4f, 5d^{E_{2n}}, 5d^{A_6}) = e^2 \int_0^{\infty} \int_0^{\infty} R_{4f}(r_1) R_{5d}^{E_{2n}}(r_2) a_d(r_1, r_2) R_{4f}(r_1) \Lambda_6^{A_6}(r_2, R) \frac{r_1^{2-\lambda} r_2^{4-\lambda}}{r_1^2 r_2^2} dr_1 dr_2 \quad (5.14)$$

and $\Lambda_6^{A_6}(r_2, R)$ represents the radial part of the 5d-Au orbital after its expansion with respect to the RE site (see Appendix D). The values of m_2 and m_6 are fixed. From the selection rules of the 3j-symbols (Rotenberg et al 1959) and properties of the factorial we obtain that: $\lambda = 0, 1, 2$; $\mu = -\lambda, \dots, \lambda$; $L_1 = 0, 1, 2, 3, 4$; $\bar{m} = 0, 1, 2, \dots, 8$; $\bar{m} = -\bar{m}, \dots, \bar{m}$; $L_2 = 0, 1, 2, \dots, 10$; $M_2 = m_2 - m_6$ if we calculate the first term between the curly brackets, $M_2 = m_2 + m_6$ for the second, $M_2 = -m_2 - m_6$ for the third and $M_2 = -m_2 + m_6$ for the fourth term. We have retained many decimal places for numbers which we know exactly e.g. 3j-symbols and reduced MEs, to retain as accurate a picture as possible because, for instance, we cannot estimate the errors in the radial integrals because of uncertainties in the wavefunctions.

To obtain the contribution to the C_6 CFP we perform the following simple substitutions in equations (5.13) and (5.14):

(i) replace 153.6987447 by 234.9399044

(ii) replace 4's by 6's

and use $\langle 3110^{(6)} | 13 \rangle = 1232.991788$ (Smith and Thornley 1966), $N_2^2 = 116943.75$ (Stevens 1974). m_2 and m_6 are fixed again. Similarly $\lambda = 0, 1, 2$; $\mu = -\lambda, \dots, \lambda$; $L_1 = 0, 1, 2, 3, 4$; $\bar{m} = 2, 3, \dots, 10$; $\bar{m} = -\bar{m}, \dots, \bar{m}$; $L_2 = 0, 1, 2, \dots, 10, 11, 12$; M_2 is determined as previously. The values of the $F_{\lambda}^{A_6}(Af, 5d^{Er3+}, 5d^{Au})$ and $F_{\lambda}^{A_2}(Af, 5d^{Er3+}, 5d^{Au})$ radial integrals are given in Appendix E.

The contribution of relation (5.13) to the C_4 CFP, in the limit of no screening, has been found to be $+0.525 \text{ cm}^{-1}$ and so the contribution of both second and third terms of the right-hand side of equation (5.12) will be: $+1.05 \text{ cm}^{-1}$ i.e. 5.5% of the unscreened contribution of the first term (which is -19.14 cm^{-1}) of the right-hand side of equation (5.12) and of opposite sign. We can easily see from Appendix E that screening ($k_e = 0.713a_0^{-1}$) will reduce the above contribution of $+0.525 \text{ cm}^{-1}$ by up to about 3.8% i.e. the screened contribution of both second and third terms of the right-hand side of equation (5.12) will be about $+1.01 \text{ cm}^{-1}$, 3.4% of the first's term corresponding screened contribution of equation (5.12) which is -29.54 cm^{-1} (see Table 5.2). Clearly, it is not worthwhile to calculate the exchange contribution since even the direct part of the above mechanism is not important.

Similar conclusions have been reached for the C_6 CFP. We found that the contribution to the C_6 CFP due to the second and third terms of the right-hand side of equation (5.13), after the appropriate substitutions, is $+4.94 \times 10^{-3} \text{ cm}^{-1}$, which is negligible with respect to the pseudo-PC value of $+1.63 \text{ cm}^{-1}$ (see Table 4.1). Again we did not feel justified in calculating the screened direct and exchange contributions for the C_6 CFP. It is interesting to note that the first term of the right-hand side of equation (5.12) does not contribute to C_6 . The reason being that for $n=6$ the $(\begin{smallmatrix} 2 & 0 & 0 \\ 0 & 0 & 0 \end{smallmatrix})$ and $(\begin{smallmatrix} 2 & 0 & 0 \\ 0 & 0 & 0 \end{smallmatrix})$, which appear in equations (5.2) and (5.3) but with $n=4$, are equal to zero due to the relevant triangle condition (Rotenberg et al 1959).

5.5. Conclusion and Discussion of Chapter 5

We have shown that for a non-zero value of k_c , indicating the presence of screening in the 4f-5d(vbs) interaction, good agreement with experiment for $Er^{3+}:Au$ may be obtained. The value of k_c used is $\approx 0.713 \text{ a.u.}^{-1}$ (although this value has been questioned in Chapter 4). Fert and Levy (1977) studied magnetotransport properties of noble metals containing RE impurities and found that, in order to explain experimental results, it was necessary to reduce their 4f-5d(vbs) exchange integrals but not the corresponding direct ones relative to their values using atomic wavefunctions. This strongly supports our calculation above where screening has a marked effect on exchange integrals but leaves virtually unchanged the direct one.

It is important to point out some of the uncertainties in our calculations. Firstly the value of k_c is not known accurately but there is a lot of evidence (see section 2.6.3) to show that the value we have taken is close to that suggested by other workers i.e. \approx twice the RPA value. Our conclusions will not therefore be affected by slightly different values of k_c . Another particular source of error is the wavefunctions we have used. The 4f wavefunction was non-relativistic Hartree-Fock for trivalent ions whereas those for the 5d-vbs, where uncertainties are probably greater, were obtained from an interpolation procedure from Herman and Skillman (1963), (see section 4.4). Quite apart from the fact that these states have a finite lifetime, and hence width, which we have not incorporated, the numerical values between which we interpolated are for neutral ions and are non-relativistic (see section 4.4). The line widths given by Lacueva et al (1982) i.e. $\Delta_{4f} = 0.45 \text{ eV}$ and $\Delta_{5d} = 0.6 \text{ eV}$ suggest that for Gold vbs lifetimes are shorter than for Silver so we might expect a larger 5d-vbs contribution to the C_4 CFP in the Silver case.

CHAPTER 6

A QUALITATIVE ESTIMATION OF CONTRIBUTIONS TO CFPs FOR $Er^{3+}:Au$ AND $Er^{3+}:Ag$ FROM A SPLIT OFF STATE FROM THE CONDUCTION BAND

6.1. Introduction

It is well known (Economidou 1979 p.109) that when a single impurity at a substitutional site is present in an otherwise perfectly periodic host lattice, its effect is to produce at least one discrete energy level outside the host band. Since in the system under consideration, $Er^{3+}:Au$, the RE impurity carries a net difference in charge from the host ion it substitutes for we expect such an effect. Dixon and Wardlaw (1986b) provided an analytical description for the state split off from the host majority conduction band, which is assumed s-like, from such an impurity potential. They denoted the split off discrete state by $|c_0\rangle$ and found that it has A_1 -like symmetry i.e. invariant under all the operations of the cubic group but not rotationally invariant. According to the DW model and Dixon and Wardlaw (1986b) the $|c_0\rangle$, in a zeroth order of approximation, is the 6s-like Wannier function for $Er^{3+}:Au$ (or 5s-like for $Er^{3+}:Ag$) which would be present at the RE site in the perfect host and it is orthogonal to the rest of the band states by construction. It was found to have the form

$$|c_0\rangle = |c_0\rangle - \sum_k \frac{\langle A_k | V_1^{00} + H_{band} | c_0 \rangle \langle A_k |}{E_A - E_{c_k}} + \dots \quad (6.1)$$

where $|A_i\rangle$ are majority band functions which have A_1 - symmetry, V_1^{ab} is the additional potential arising from the presence of the RE impurity and H_{band} is the Hamiltonian for an electron in a perfectly periodic lattice. E_A is the energy of the corresponding band state and E_c is defined by:

$$E_c = \langle E_A \rangle + \langle c_0 | V_1^{ab} | c_0 \rangle \quad (6.2)$$

where $\langle E_A \rangle$ is the average energy of the original majority band before $|c_0\rangle$ split off. E_c is well separated by about half of the band width from the bottom of the band (Dixon and Wardlaw 1986b). To zero order in overlaps $|c_0\rangle$ will simply be the 6s state (or 5s for Er^{3+} ; Ag), $|c_0\rangle$, of the host but at the RE site. The interaction between the 4f(RE)-electrons and the $|c_0\rangle$ is given by (third term of equation 2.32):

$$\sum_{m_1 m_3} \left\{ \langle \tilde{c}_{0,\sigma} \sigma' | V_{sc} | \tilde{c}_{0,\sigma} \sigma' \rangle - \delta_{\sigma,\sigma'} \langle \tilde{c}_{0,\sigma} \sigma' | V_{sc} | \tilde{c}_{0,\sigma} \sigma' \rangle \right\} \tilde{c}_{0,\sigma} \sigma' \tilde{c}_{0,\sigma} \sigma' \quad (6.3)$$

where the second quantised operators have their usual meaning. To estimate the magnitude only of contributions to CFPs from equation (6.3) we made the following approximations:

- (i) We assume $\langle \tilde{c}_{0,\sigma} \sigma' \tilde{c}_{0,\sigma} \sigma' \rangle = \frac{1}{2}$ for both $\sigma = 1/2$ or $-1/2$ since it has to be occupied for there to be an interaction.
- (ii) The 6s-state of Gold (5s for Silver) couples only to the 6s-states (respectively 5s) of the nearest neighbours. $|c_0\rangle$, being a generalised Wannier function, must be orthogonal to core orbitals of the RE, the rest of the band states and orbitals on neighbouring ligands. Thus $|c_0\rangle$ will be the on-site 6s-state plus admixtures from neighbouring ligands which we have calculated using Löwdin's orthogonalisation technique and admixtures from the rest of the majority band states. We have retained only the 6s ligand contributions although 5d, 5p and 5s ligand states may be present. However the overlap with these latter 5d, 5p, 5s states is smaller than with the 6s ligand state since all these are fully occupied with a smaller radial extent.
- (iii) As far as the 6s(5s) radial wavefunction is concerned we are using the Herman and Skillman (1963) numerical data for neutral Au-atoms (respectively for Ag) to determine analytical expressions given by equations (6.4), (6.5) and Tables 6.1 and 6.2.

- (iv) Lowdin's method has been used to find the new "6s" state which may be written as in equation (6.6).
- (v) Terms incorporating majority band states $|A_i\rangle$ have been dropped at this stage because, for Gold, we expected their effect to be relatively small (see Chapter 9).

$$P_{6s}^{A_1}(r) = r^3(C_1 e^{-Z_1 r} + C_2 e^{-Z_2 r}) + r^3(C_3 e^{-Z_3 r} + C_4 e^{-Z_4 r}) + r^4(C_5 e^{-Z_5 r} + C_6 e^{-Z_6 r}) \quad (6.4)$$

$$P_{5d}^{A_2}(r) = r C_1 e^{-Z_1 r} + r^2(C_2 e^{-Z_2 r} + C_3 e^{-Z_3 r}) + r^3 C_4 e^{-Z_4 r} + r^4 C_5 e^{-Z_5 r} \quad (6.5)$$

where the normalisation condition is $\int P^2(r) dr = 1$ and r is in atomic units.

Table 6.1 : The parameters C_i and Z_i which define the 6s radial wavefunction of Gold given by equation (6.4).

i	C_i	Z_i
1	-0.42106137	0.721365
2	455.38158	20.219927
3	-28191.421	39.885772
4	-119.1105	6.8980116
5	-0.2780246	1.6866939
6	128.63094	5.4153185

Table 6.2: The parameters C_i and Z_i which define the $5s$ radial wavefunction of Silver given by equation (6.5).

i	C_i	Z_i
1	8.3102878	1.3811292
2	-21.15583	2.4085704
3	-332.24003	16.669123
4	-64.692329	5.2747694
5	0.089199946	1.052574

$$|6s; new\rangle = |6s; Au, on\rangle - \frac{1}{2} \sum_i S_{6s; Au-6s} |6s; Au, off\rangle \quad (6.6)$$

and similarly for the $5s$ -orbital of Silver, where $S_{6s; Au-6s}$ denotes the overlap defined in equation (6.7) and we have included only terms linear in overlap.

To calculate the overlaps involved in this calculation we used our development for expanding an off-site function about the site of interest (Appendix D). We find:

$$\begin{aligned} S_{6s; Au-6s} &= \langle 6s; Au, off | 6s; Au, on \rangle = 0.4123 \\ S_{5s; Ag-5s} &= \langle 5s; Ag, off | 5s; Ag, on \rangle = 0.4093 \end{aligned} \quad (6.7)$$

where we used the following nearest neighbour distances: $R_{Au}^{Au} = 5.451853 a_0$ and $R_{Ag}^{Ag} = 5.470783 a_0$. To test our numerical calculations for the overlap values we found that for $R_{nn} \rightarrow 0$ both overlaps tend to 1. All calculations were performed using neutral Herman and Skillman (1963) data fitted atomic wavefunctions. According to Samsonov (1968 p.102, p.106) Silver and Gold atoms have the same metallic radius. This suggests that in the metallic phase similar values for the overlaps are expected, the nearest neighbour distance being virtually the same for both fcc structures. There are no reliable estimations for the atomic radii of the neutral Gold and Silver atoms (Lucken 1961) so although we have some evidence that our calculations will give similar magnitudes for both the Gold and Silver metals we cannot estimate the changes in

magnitudes.

6.2. Direct Contributions

Once the wavefunctions to be used are determined, the direct MEs of equation (6.3) will become:

$$\begin{aligned}
 & \langle (6s; new), 4f_{m, \sigma'} | V_{SC} | (6s; new), 4f_{m, \sigma'} \rangle = \\
 & \langle (16s; Au, on) > - \frac{1}{2} \sum_{\vec{k}_1} S_{\vec{k}_1, Au}^{on} \langle 16s; Au, off \rangle, 4f_{m, \sigma'} | V_{SC} | \\
 & \quad (16s; Au, on) > - \frac{1}{2} \sum_{\vec{k}_1} S_{\vec{k}_1, Au}^{on} \langle 16s; Au, off \rangle, 4f_{m, \sigma'} \rangle = \\
 & \langle (6s; Au, on), 4f_{m, \sigma'} | V_{SC} | (6s; Au, on), 4f_{m, \sigma'} \rangle \\
 & - \frac{1}{2} \sum_{\vec{k}_1} S_{\vec{k}_1, Au}^{on} \langle (6s; Au, on), 4f_{m, \sigma'} | V_{SC} | (6s; Au, off), 4f_{m, \sigma'} \rangle \\
 & - \frac{1}{2} \sum_{\vec{k}_1} S_{\vec{k}_1, Au}^{on} \langle (6s; Au, off), 4f_{m, \sigma'} | V_{SC} | (6s; Au, on), 4f_{m, \sigma'} \rangle \\
 & + \frac{1}{4} \sum_{\vec{k}_1, \vec{k}_2} S_{\vec{k}_1, Au}^{on} S_{\vec{k}_2, Au}^{on} \langle (6s; Au, off), 4f_{m, \sigma'} | V_{SC} | (6s; Au, off), 4f_{m, \sigma'} \rangle \quad (6.8)
 \end{aligned}$$

where V_{SC} is the screened Coulomb interaction. The first term on the right-hand-side (RHS) of equation (6.8) leads to a rotationally invariant operator and so does not contribute to the C_4 and C_6 CFPs. The second and third terms are equal and do contribute to the C_4 and C_6 CFPs. As far as the last term of the RHS of equation (6.8) is concerned we expect it to be much smaller than the second and third ones and so it is neglected. The reason being that the fourth term involves the square of the overlap and two off-site states in comparison with only one overlap and one off-site state of the second and third terms. Straightforward algebra yields the following analytical expressions (within the above discussed approximations) for the contributions of the second and third terms of the RHS of equation (6.8) to the C_4 and C_6 CFPs:

$$C_4^{direct}(4f/c_0) = -S_{Au, Au} = 0.147704487 \sum_k Y_4^{0*}(\theta_k, \phi_k) F^{4A}(6s^{on}, 6s^{off}, 4f) \quad (6.9)$$

$$C_6^{direct}(4f/c_0) = -S_{Au, Au} = 0.061448781 \sum_k Y_6^{0*}(\theta_k, \phi_k) F^{6A}(6s^{on}, 6s^{off}, 4f) \quad (6.10)$$

where we take into account only nearest neighbours (since, for instance, all subsequent shells of neighbours are screened out by the screening action of the conduction electrons, see Chapter 4 or alternatively because the overlap between the 6s on the RE site and 6s on the second, third and higher order shells of neighbours is, to all intents and purposes, zero). The radial integrals are defined as:

$$F^{nA}(6s^{off}, 6s^{on}, 4f) = e^2 \int_0^{\infty} \int_0^{\infty} R_{Au}(r_1) R_{4f}(r_2) a_n(r_1, r_2) \Lambda_n^{Au}(r_1, R) R_{4f}(r_2) r_1^2 r_2^2 dr_1 dr_2 \quad (6.11)$$

with

$$\sum_{k=0}^{\infty} Y_4^{0*}(\theta_k, \phi_k) = -\frac{14}{5} \left[\frac{9}{4\pi} \right]^{1/2}, \quad \sum_{k=0}^{\infty} Y_6^{0*}(\theta_k, \phi_k) = -\frac{39}{16} \left[\frac{13}{4\pi} \right]^{1/2} \quad (6.12)$$

the function $a_n(r_1, r_2)$ arises from an expansion of the screened Coulomb repulsion in Legendre polynomials and has been considered in detail in Appendix C. $\Lambda_n^{Au}(r_1, R)$ represents the radial part of the 6s-Au orbital on the ligand after expanding it with respect to the RE site (Appendix D).

Obviously, these results can be easily extended for the case of Silver by substituting the 5s-Ag wavefunction for the 6s-Au wavefunction. We present the results of this calculation in Tables 6.3 and 6.4. To test the validity of our programmes in the Gold case for the calculation of the F direct radial integrals we have put $a_n(r_1, r_2) = 1$, $\bar{n} = 0$ and obtained the value of the $\langle 6s_{Au, off} | 6s_{Au, on} \rangle$ overlap as was expected. Similar tests were performed for Silver. At this point we should point out the difficulties faced in the numerical calculations of the F^{6A} radial integrals. The problem appeared near the lower limits of integration (i.e. near the origin). In view of the expected insignificance, at least for $Er^{3+}Au$, of the F^{6A} integrals, we decided not to perform the extremely time consuming exact calculations but instead to give estimations of their magnitude.

Table 6.3 : Values of the F direct radial integrals defined in equation (6.11), in $e^2 a_0$.

	$k_c = 0.0 a_0^{-1}$	$k_c = 0.713 a_0^{-1}$
$Au: F^{4A}(6s^{2m}, 6s^{2f}, Af)$	1.694×10^{-4}	1.685×10^{-4}
$Au: F^{6A}(6s^{2m}, 6s^{2f}, Af)$	2.2×10^{-5}	2.2×10^{-5}
$Ag: F^{4A}(5s^{2m}, 5s^{2f}, Af)$	1.951×10^{-4}	1.926×10^{-4}
$Ag: F^{6A}(5s^{2m}, 5s^{2f}, Af)$	2.5×10^{-5}	2.5×10^{-5}

Table 6.4 : CFPs derived from the direct $4f/c_0$ interaction for $Er^{3+}Au$ and $Er^{3+}Ag$ in cm^{-1} .

	$k_c = 0.0 a_0^{-1}$	$k_c = 0.713 a_0^{-1}$
$Au: C_4^{direct}$	+ 3.354	+ 3.336
$Au: C_6^{direct}$	+ 0.3	+ 0.3
$Ag: C_4^{direct}$	+ 3.835	+ 3.786
$Ag: C_6^{direct}$	+ 0.34	+ 0.34

6.3. Exchange Contributions

Since the overlap between the 6s-orbital on the RE site and the 6s-orbital on the nearest Au-neighbours (similarly for the Silver case) is significant we expect important "exchange" contributions. The "exchange" MEs of equation (6.3) are given by:

$$\begin{aligned}
 & -\frac{1}{2} \langle (6s; new), 4f_{m, \sigma'} | V_{SC} | 4f_{m, \sigma'}, (6s; new) \rangle = \\
 & -\frac{1}{2} \langle (16s; Au, on) - \frac{1}{2} \sum_{\ell} S_{\ell, Au} w_{\ell, Au} (6s; Au, off), 4f_{m, \sigma'} | V_{SC} | \\
 & \quad 4f_{m, \sigma'}, (16s; Au, on) - \frac{1}{2} \sum_{\ell} S_{\ell, Au} w_{\ell, Au} (6s; Au, off) \rangle = \\
 & -\frac{1}{2} \langle (6s; Au, on), 4f_{m, \sigma'} | V_{SC} | 4f_{m, \sigma'}, (6s; Au, on) \rangle \\
 & + \frac{1}{4} \sum_{\ell} S_{\ell, Au} w_{\ell, Au} \langle (6s; Au, on), 4f_{m, \sigma'} | V_{SC} | 4f_{m, \sigma'}, (6s; Au, off) \rangle \\
 & + \frac{1}{4} \sum_{\ell} S_{\ell, Au} w_{\ell, Au} \langle (6s; Au, off), 4f_{m, \sigma'} | V_{SC} | 4f_{m, \sigma'}, (6s; Au, on) \rangle \\
 & - \frac{1}{8} \sum_{\ell} S_{\ell, Au} w_{\ell, Au} S_{\ell, Au} w_{\ell, Au} \langle (6s; Au, off), 4f_{m, \sigma'} | V_{SC} | 4f_{m, \sigma'}, (6s; Au, off) \rangle \quad (6.13)
 \end{aligned}$$

In a similar way to the direct case (see equation 6.8) the first term of the RHS does not contribute to the C_4 and C_6 CFPs. The reason for this is that it can contribute only to third order CFPs and these will not appear in cubic symmetry. Arguing similarly to the direct case we neglect the fourth term of the RHS of equation (6.13) and evaluate contributions only from the second and third ones. After some algebraic manipulation we finally obtain:

$$C_4^{aux}(4f|c_0) = + S_{6s} w_{6s} \frac{9}{7 \times 2} 0.147704487 \sum_{\ell} Y_{\ell}^{00}(\theta_R, \phi_R) G^{3A}(6s^{aux}, 6s^{off}, 4f) \quad (6.14)$$

$$C_6^{aux}(4f|c_0) = + S_{6s} w_{6s} \frac{13}{7 \times 2} 0.061448781 \sum_{\ell} Y_{\ell}^{00}(\theta_R, \phi_R) G^{3A}(6s^{aux}, 6s^{off}, 4f) \quad (6.15)$$

where

$$G^{3R}(6s^{off}, 6s^{aux}, 4f) = e^2 \int_0^{\infty} \int_0^{\infty} R_{6s}(r_1) R_{4f}(r_2) a_3(r_1, r_2) R_{4f}(r_1) A_6^{Au}(r_2, R) r_1^2 dr_1 dr_2 \quad (6.16)$$

$a_3(r_1, r_2)$ and $A_6^{Au}(r_2, R)$ are defined in the same way as in the direct case (see Appendixes C and D). We faced, similar to the direct case, difficulties in the numerical calculation of the G^{3A} radial integrals so we only provide an estimation of their magnitude. We summarise our results in Tables 6.5 and 6.6.

Table 6.5: Values of the G exchange radial integrals defined in equation (6.16), in $e^2 a_0$

	$k_c = 0.0 \text{ } a_0^{-1}$	$k_c = 0.713 \text{ } a_0^{-1}$
$Au: G^{3A}(6s^{m-}, 6s^{n/1}, Af)$	5.18×10^{-5}	5.15×10^{-5}
$Au: G^{3B}(6s^{m-}, 6s^{n/1}, Af)$	6.6×10^{-6}	6.6×10^{-6}
$Ag: G^{3A}(5s^{m-}, 5s^{n/1}, Af)$	6.06×10^{-5}	6.02×10^{-5}
$Ag: G^{3B}(5s^{m-}, 5s^{n/1}, Af)$	7.7×10^{-6}	7.7×10^{-6}

Table 6.6: CFPs derived from the exchange $4f/c_0$ interaction for $Er^{3+}:Au$ and $Er^{3+}:Ag$ in cm^{-1} .

	$k_c = 0.0 \text{ } a_0^{-1}$	$k_c = 0.713 \text{ } a_0^{-1}$
$Au: C_6^{mch}$	-0.66	-0.656
$Au: C_6^{nch}$	-0.09	-0.09
$Ag: C_6^{mch}$	-0.77	-0.76
$Ag: C_6^{nch}$	-0.1	-0.1

6.4. Conclusion and Discussion of Chapter 6

In this chapter we attempted to estimate the contribution of the $|c_0\rangle$ generalised Wannier function to the CFPs of $Er^{3+}:Au$ and $Er^{3+}:Ag$.

In practice such a state should be the 6s (or 5s for Silver) generalised Wannier function of the host but at the RE site. This was mimicked by the free atom 6s-state plus a linear combination of admixtures of neighbouring orbitals which ensure the orthogonality property of the generalised Wannier functions, plus a mixture of majority A_1 -like band states (Dixon and Wardlaw 1986b). In this chapter we have made the approximation that only terms linear in the overlap to

6s(Au) orbitals of nearest neighbours is retained. We expect that this will be the dominant contribution, at least for $Er^{3+}:Au$, but actually we should consider smaller terms linear to 5d, 5p, 5s-Au orbitals (at least) and mixing to other conduction band states before we can fully assess the magnitude of the $|c_0\rangle$ contributions to the CFPs (see discussion in Chapter 9). From the above calculations we can say that the $|c_0\rangle$ does provide a contribution which will not significantly modify the value obtained for the C_4 CFP from the mechanisms considered in Chapters 3, 4, and 5, for $Er^{3+}:Au$ i.e. in total will get $\approx -14.3cm^{-1}$. We can also say that this mechanism tends to improve agreement with experiment for the C_6 CFP. In view of the involved uncertainties we do not feel justified in making a full numerical comparison with the results obtained in previous chapters.

The theory of DW, in first order, is therefore quite capable of explaining the size and sign of the C_4 and C_6 CFPs of $Er^{3+}:Au$ although it cannot explain why the CFPs are twice as big for the $Er^{3+}:Ag$ case as the $Er^{3+}:Au$ dilute alloy (at least within the approximations made in our calculation above). We postpone the discussion of this question until the Concluding Remarks section of the thesis.

CHAPTER 7

ZERO-FIELD SPLITTINGS FOR S-STATE IONS

7.1. Introduction - First Order Perturbation Theory for S-state Ions: $P_0 H P_0$

From Chapter 3 to Chapter 6 we were mainly concerned with an investigation of the CFs of the dilute RE-alloy $Er^{3+}:Au$. At a later stage, in Chapters 5 and 6 we made a comparison with $Er^{3+}:Ag$ and tried to elucidate why the experimental value of the C_4 CFP for these two alloys differ by a factor of two. All these latter calculations were performed within the particular first order treatment of the DW model. One of the reasons for doing this is that one expects sizable contributions to CFPs in first order for non-S-state ions and reasonably close agreement with experiment (Stevens 1976, DW). When we examine S-state ions the situation is quite different since they possess zero total orbital angular momentum in their ground levels (at least within the RS-coupling).

As an example suppose we consider an insulating crystal with N Gd^{3+} impurities. The Ground Level (see Chapter 1) of the free Gd^{3+} within the RS-coupling, according to Hund's rules (Chapter 1) is: $4f^7, 8S_{7/2}$. We can therefore think of the ground family (section 2.5.2) as being made up of electrons in closed shells, except for seven 4f-electrons at each of the N Gd^{3+} ions. In the absence of any interaction lifting the eightfold degeneracy the 4f electrons can be in any of

the eight M_S states of the Ground Level $4f^3, {}^4S_{3/2}$. In a similar way to the non-S-state case (see section 2.5.3) we define creation and annihilation operators as follows: a'_a, b'_b, \dots for 4f-electrons related to the sites A, B, \dots and f', f referring to filled orbitals which are not necessary on the RE sites. To obtain a splitting of the $J = S = 7/2$ one would expect that orbital operators of the form a'_a should appear.

Our Hamiltonian H involves in general one-electron spin-independent and spin-dependent operators (which we denote by h, h_s respectively) as well as two-electron spin-independent or dependent ones g, g_s . The main contributions to H are those of the kinetic energy, the Coulomb attraction between electrons and nuclei (these latter two being h -like), the Coulomb repulsion between electrons (g -like) and the spin-orbit coupling (h_s -like). These are the only terms we retain. We therefore drop all other spin dependent contributions like spin-spin, spin-other-orbit components and possible Zeeman terms which would otherwise arise (such terms are very much smaller than those we retain).

Let us now examine each of the contributions in turn when written in second quantised form in the spirit of the analysis of Stevens (section 2.5.2).

One-electron spin-independent terms in H within RS-states

Such operators as a'_a can be readily obtained, for instance from the h -like terms in H :

$$\sum_{a,n} \langle a_{n0} | h | a_{n0} \rangle a'_{n0} a_{n0} = \sum_n \langle a_n | h | a_n \rangle \sum_{\sigma} a'_{n\sigma} a_{n\sigma}$$

This type of operator would describe the crystal-field-like part of Coulomb attraction contributions which involve nuclei not at the site of the RE. By using the equivalences of Stevens (equation 2.17) $\sum_{\sigma} a'_{n\sigma} a_{n\sigma}$ becomes $\sum_{\sigma} \delta_{n\sigma} O_{n-\sigma}^{(0)}(U)$ where $\delta_{n\sigma}$ and the O operators have been already defined in section 2.5.3. Within any orbital singlet ($L=0$) each $\sum_{\sigma} O_{n-\sigma}^{(0)}(U)$ can be replaced by a constant i.e. *the one-electron spin-independent terms do not split the RS ground manifold.*

One-electron spin-dependent terms in H within RS-states

The most important A_2 -like term in H is the spin-orbit interaction. This usually appear in the form $\sum_i \xi(r_i) \underline{L} \cdot \underline{S}$ where \underline{L} is an orbital operator for the i -th electron whose components transform like those of a vector (i.e. according to the irreducible representation $D^{(1)}$ of the full rotation group). If we now replace the spin-orbit interaction by second quantised operators and then by angular momentum operators, the resulting expression will also transform like $D^{(1)}$. But no such operator can have MEs within an orbital singlet ($L=0$). To understand this we can simply apply the *Fundamental ME Theorem* (Heine 1964 p.103), which states that non-zero MEs are only possible if the product of the irreducible representations of the states between which an operator is sandwiched contains the representation according to which the operator transforms. In this case $D^{(0)} \otimes D^{(0)} = D^{(0)}$ and of course $D^{(1)}$ is not contained in $D^{(0)}$.

Two-electron spin-independent terms in H within RS-states

These are of several kinds. Those of type $a'f'fa$ and $a'f'af$ result in purely orbital terms for the $f'f$ may be commuted through to the right and replaced by unity (section 2.5.3). We can also have operators of the type $a'a'aa$ but these arise from the Coulomb repulsion of electrons on the same site, and, as this is rotationally invariant, it cannot lift the spin degeneracy of $S = J = 7/2$. The remaining possibilities are of type $a'b'ba$ and $a'b'ab$ but we are not interested in these mechanisms since later in our study we consider a single Gd^{3+} ion doped in lanthanum ethylsulphate.

Two-electron spin-dependent terms in H within RS-states

All these have invariably been omitted in phenomenological spin-Hamiltonians since they are expected to give very much smaller MEs (Stevens 1976 p.34).

In conclusion we can say that, within the Ground Level determined by RS-coupling, the first order perturbation theory of Stevens will contribute nothing to the splitting of the Gd^{3+} Ground Level. Such a splitting is well established for a variety of hosts (Abragam and Bleaney 1970 p.335) and although small, is not negligible. In this thesis we concentrate our S-state ion studies on Gd^{3+} -doped lanthanum ethylsulphate ($La(C_2H_5SO_4)_3 \cdot 9H_2O$). For this specific case it

has been found (for instance Dagg et al 1969) that there is a ZFS between the $M_J = \pm 7/2$ and $M_J = \pm 1/2$ doublets given by:

$$E(M_J = \pm 7/2) - E(M_J = \pm 1/2) = + 0.236 \text{ cm}^{-1}$$

To obtain these well determined small splittings from a theoretical model it is clearly necessary to go to higher order in perturbation theory and consider interactions with excited Levels. This was attempted by various researchers (see section 7.2) without any success. In fact, they found that either the suggested mechanisms produced a negligible contribution to the ZFS or they produced a ZFS of the wrong sign.

In view of the fact that the spin-orbit interaction significantly mixes the ground RS-Level $^4S_{7/2}$ into the first excited $^6P_{7/2}$ (and indeed others) we follow, for instance, Tuszyński et al (1984) in the literature and take the unperturbed manifold projected out by P_0 to be the *intermediate coupling ground state of Gd^{3+}* (often referred to as simply the spin-orbit mixed ground state) and all projectors for excited eigenstates of H_0 refer to intermediate coupling states. This has been defined already in section 1.1 as:

$$|^4S_{7/2}\rangle = 0.987 |^4S_{7/2}\rangle + 0.162 |^6P_{7/2}\rangle + \text{smaller admixtures}$$

where $|\dots\rangle$ implies intermediate coupling and $|\dots\rangle$ RS-coupling. These spin-orbit mixed states are obviously diagonal with a Hamiltonian which involves only on-site operators. It is clear that:

$$\begin{aligned} \langle ^4S_{7/2} | H | ^4S_{7/2} \rangle &= 0.987 \times 0.987 \langle ^4S_{7/2} | H | ^4S_{7/2} \rangle \\ &+ 0.987 \times 0.162 \langle ^4S_{7/2} | H | ^6P_{7/2} \rangle \\ &+ 0.162 \times 0.987 \langle ^6P_{7/2} | H | ^4S_{7/2} \rangle \\ &+ 0.162 \times 0.162 \langle ^6P_{7/2} | H | ^6P_{7/2} \rangle + \text{smaller admixtures} \end{aligned} \quad (7.2)$$

The first term on the RHS of equation (7.2) is proportional to that which has already been discussed above. As far as the second term is concerned, one-electron spin-independent terms cannot contribute since the interacting RS-states have different spin components and are therefore orthogonal. The only A_2 -like term of any significance in H is the spin-orbit interaction (V_{so}). The ME $\langle ^4S_{7/2} | V_{so} | ^6P_{7/2} \rangle$ does exist (Chatterjee et al 1976) but it has been found (see section 7.2) that it cannot explain the observed ZFS by performing standard perturbation theory using RS-

states as a basis. Two electron spin-independent components cannot contribute either, because of the orthogonality of the spin states and finally all two-body spin-dependent terms are insignificant and have been neglected in H (Stevens 1976 p.34). Similar arguments hold for the third term of the RHS of equation (7.2). The fourth term of the RHS of (7.2) should be examined more carefully. The main k -like terms in H are the kinetic energy and the Coulomb attraction between electrons and nuclei. The kinetic energy is isotropic so although it will contribute to the main energy of the ground state of Gd^{3+} it will not split its degeneracy. Part of the Coulomb attraction, the attraction of the 4f-electrons to their own nucleus, is also isotropic and so cannot raise the degeneracy either. The remaining part of the Coulomb attraction is the attraction of the 4f-electrons to neighbouring nuclei i.e. a crystal-field-like term. Although this is anisotropic, the related ME between the $^6P_{7/2}$ vanishes (Tuszyski 1983). It is a remarkable characteristic of ions with a half-filled open shell that all diagonal MEs within the free ion RS-coupling of the form $\langle ^{2S+1}L_J | V_{CF} | ^{2S+1}L_J \rangle$ are equal to zero. This is due to the charge conjugation symmetry of the free ion states (Newman 1970, Tuszyski 1983). Similar conclusions are obtained for the g -like Coulomb repulsion between electrons which can be divided into an isotropic part (if electrons are on one site) and a crystal-field-like one (if the electrons are on different sites one of which is the RE site). Finally it has been found that the spin-orbit interaction vanishes between the $^6P_{7/2}$ RS Levels (Chatterjee et al 1976). Again we face the problem of going to higher order perturbation mechanisms in order to explain the observed ZFS.

The above gives some indication at least of the difficulties encountered in trying to theoretically account for the ZFS for Gd^{3+} in lanthanum ethylsulphate. In section 7.2 we shall give a brief review of the main theoretical attempts where it will become clear that there was no satisfactory explanation until the recent work of Tuszyski, Dixon and Chatterjee (1984-hereafter TDC1, 1986-hereafter TDC2). The work of TDC1 and TDC2 invoked *intra-site* excitation mechanisms (e.g. where an electron is excited to another configuration but always remains on the Gd^{3+} site) which gave rise to a ZFS of the correct sign to agree with that obtained from experiment but approximately two times too large. Later in Chapter 8 we present an *inter-site* excitation mechanism which compensates the ZFS from TDC1 and TDC2 to produce a ZFS in good agreement with

experiment.

7.2. Review of Intra-Site Mechanisms Resulting in the ZFS of Gd^{3+}

Many attempts have been made in the literature to account theoretically for the ZFS, particularly to obtain a sign that agrees with that which is found from experiment. The situation has been reviewed by Wybourne (1966), Buckmaster et al (1972) and Smith et al (1977) but no satisfactory explanation had been found until recently. In this section we shall briefly review all mechanisms proposed up to 1984. The CF of the Gd^{3+} in C_{3h} symmetry, which is the appropriate point symmetry for the Gd^{3+} -doped lanthanum ethylsulphate (Fitzwater and Rundle 1959), has a potential energy V_{CF} which is written customarily as a sum of one-electron operators of the type $B_q^k C_q^{(k)}(j)$ (see Buckmaster et al 1972):

$$V_{CF} = B_0^2 C_0^{(2)} + B_0^4 C_0^{(4)} + B_0^6 C_0^{(6)} + B_6^6 [C_6^{(6)} + C_{-6}^{(6)}] \quad (7.2)$$

where B_q^k are CFPs and $C_q^{(k)}$ is a tensor operator which has the same rotational transformation properties as the spherical harmonic Y_k^q :

$$C_q^{(k)} = \left(\frac{4\pi}{2k+1} \right)^{1/2} Y_k^q \quad (7.3)$$

7.2.1. Hutchison, Judd and Pope Mechanism

Experimental results (for instance Dagg et al 1969) indicate that the second order axial CFP is much larger than the other CFPs so it is reasonable to try, initially, to find mechanisms which contribute mainly to the B_0^2 CFP. Hutchison et al (1957) noticed that the $\langle 4f^7, {}^4D_{7/2} | V_{CF} | 4f^7, {}^6P_{7/2} \rangle$ ME vanishes for the fourth and sixth order CF, but does not vanish for the second order axial CF potential $B_0^2 C_0^{(2)}$. They proposed the following schematic fourth-order mechanism:

$$\langle {}^4S_{7/2} | V_{so} | {}^6P_{7/2} \rangle \langle {}^6P_{7/2} | V_{so} | {}^4D_{7/2} \rangle \langle {}^4D_{7/2} | B_0^2 C_0^{(2)} | {}^6P_{7/2} \rangle \langle {}^6P_{7/2} | V_{so} | {}^4S_{7/2} \rangle$$

where V_{so} represents the spin-orbit interaction. The contribution to the ZFS produced by this mechanism has been found (Buckmaster et al 1972): -0.228 cm^{-1} . This mechanism provides one of the most important contributions to the ZFS but predicts the $\pm 7/2$ Kramers pair as lowest in

energy in contrast to experiment (Dagg et al 1969).

7.2.2. Judd Mechanism

Judd (1955) showed that the CF perturbation together with the spin-orbit interaction results in a splitting of the ground state through a fourth-order mechanism which may be represented as follows:

$$\sum_j [\langle {}^4S_{3/2} | V_{CF} | {}^6P_{7/2} \rangle \langle {}^6P_{7/2} | V_{CF} | {}^4L_J \rangle \langle {}^4L_J | V_{CF} | {}^6P_{7/2} \rangle \langle {}^6P_{7/2} | V_{SO} | {}^4S_{3/2} \rangle]$$

where 4L_J is an intermediate state in the $4f^7$ configuration. The contribution to the ZFS produced by this mechanism is very small and of the right sign (Buckmaster et al 1972): $+ 0.023 \text{ cm}^{-1}$.

7.2.3. Third-order Spin-Spin Interaction Mechanism

This third-order spin-spin mechanism first applied in the case of the Gd^{3+} in lanthanum ethylsulphate by Wybourne (1966). Schematically is represented as:

$$\langle {}^4S_{3/2} | V_{SO} | {}^6D_{7/2} \rangle \langle {}^6D_{7/2} | V_{CF} | {}^6P_{7/2} \rangle \langle {}^6P_{7/2} | V_{SS} | {}^4S_{3/2} \rangle$$

Wybourne found that this mechanism contributes to the ground state splitting a contribution of the right sign but only about $+ 0.001 \text{ cm}^{-1}$.

7.2.4. Second-order Spin-Spin Interaction Mechanism

Pryce (1950) has proposed a second order mechanism involving interaction with the $4f^6 6p$ configuration:

$$\langle {}^4f^7; {}^4S_{3/2} M_J | V_{SO} | 4f^6 6p; {}^6D_{7/2} M_J \rangle \langle 4f^6 6p; {}^6D_{7/2} M_J | V_{CF} | 4f^7; {}^4S_{3/2} M_J \rangle$$

This mechanism has been estimated by Wybourne (1966) as negligible.

7.2.5. Second-order Relativistic Mechanism

Since the CF is represented as a spin-independent operator, ME between states of different spin vanish in the non-relativistic limit e.g. the ME coupling the ${}^4S_{3/2}$ state to the ${}^6P_{7/2}$ state of the $4f^7$ configuration vanishes (section 7.1). Wybourne (1965b) pointed out that if relativistic effects are taken into account this ME is not zero. This mechanism is schematically presented as:

$$\langle {}^4S_{7/2} | V_{ee} | {}^6P_{7/2} \rangle = \langle {}^6P_{7/2} | V_{CF}^{(6)} | {}^4S_{7/2} \rangle$$

It has been found that this mechanism results in a larger contribution to the observed splitting but of the opposite sign (Wybourne 1966): -0.312 cm^{-1} .

7.2.6. Crystal Field Configuration Mixing Mechanism

The CF operators $C_q^{(k)}$ of equation (7.2) are one-electron operators and hence they can only couple the $4f^7$ configuration to others differing by at most one electron. Wybourne (1966) considered a second-order mechanism of the form:

$$= \sum_X \frac{\langle 4f^7; {}^4S_{7/2} | V_{CF} | X \rangle \langle X | V_{CF} | 4f^7; {}^6S_{7/2} \rangle}{\Delta E_X}$$

where X is a state belonging to an excited configuration and ΔE_X is the positive excitation energy. He found that we may regard these contributions as already incorporated in the mechanisms discussed in sections 7.2.1 and 7.2.2.

7.2.7. Electrostatically Correlated Crystal Fields

Rajnak and Wybourne (1964) proposed the following mechanism:

$$\langle {}^4S_{7/2} | V_{ee} | {}^6P_{7/2} \rangle = \langle {}^6P_{7/2} | V_{ECCF} | {}^6P_{7/2} \rangle = \langle {}^6P_{7/2} | V_{ee} | {}^4S_{7/2} \rangle$$

where

$$V_{ECCF} = - \frac{2}{\Delta E_{4f}} \sum_X \langle n l^N \psi | V_{CF} | X \rangle \langle X | V_C | n l^N \psi \rangle$$

V_C is the Coulomb potential, X is an excited state and ΔE_{4f} is the positive average energy of the excitation. The ECCF mechanism produces a negligible splitting (Wybourne 1966).

7.2.8. Fifth-order Configuration Interaction Mechanism

Wybourne (1966) noticed that the $4f^7({}^4S_{7/2})$ RS ground state of Gd^{3+} is perturbed by electrostatic interaction with the two ${}^4S_{7/2}$ levels of the $4f^5d^2$ configuration. He finally found that the so induced mechanism produces a negligible splitting to the Gd^{3+} ion.

7.2.9. Sixth-order Mechanisms

Buckmaster et al (1972) produced sixth-order mechanisms which contribute to the ZFS but they found that these mechanisms are negligible as far as the ZFS of Gd^{3+} in lanthanum ethylsulphate is concerned.

7.2.10. Lulek's Mechanism

Lulek (1969) suggested that a second-order perturbation mechanism involving an appropriately induced anisotropic spin-orbit interaction could perhaps explain the ZFS of the Gd^{3+} ion in an axial field. Buckmaster et al (1972) have shown that this mechanism produces a value of: -0.007 cm^{-1} .

From the above brief review we conclude that all mechanisms either yield negligible contributions or contributions of right magnitude but of wrong sign. The "most" important contributions to the ZFS of Gd^{3+} are summarised in Table 7.1.

Table 7.1 :
Calculated values (by using non-relativistic wavefunctions) for the contributions of various ground-state splitting mechanisms for $E(\pm 7/2) \leftarrow \rightarrow E(\pm 1/2)$ transitions (Buckmaster et al 1972, Wybourne 1966).

Mechanism	Contribution in cm^{-1}
Wybourne Relativistic	- 0.312
Hutchison-Judd-Pope	- 0.228
ECCF	+ 0.050
Judd	+ 0.023
Lulek	- 0.007
Third-order Spin-Spin Interaction	+ 0.001
Total	- 0.473
Experiment	+ 0.236

Clearly the theoretically predicted value of the splitting is too large and more seriously, of the wrong sign. It must be pointed out that for the above calculations Wybourne (1966) and Buckmaster et al (1972) used non-relativistic wavefunctions. Smith et al (1977) recalculated in the relativistic scheme of Sandars and Beck (1965) all the above mechanisms and found that although calculations of ZFS converged more rapidly, when using relativistic wavefunctions, the discrepancy between experiment (+ 0.236 cm^{-1}) and theory (which now gives a ZFS of - 0.432 cm^{-1}) still remains unexplained.

Newman (1970) provided a step forward for a qualitative understanding of the ZFS of Gd^{3+} in lanthanum ethylsulphate. He proposed the so-called Spin Correlated Crystal Field (SCCF).

7.2.11. Spin Correlated Crystal Fields

Newman's qualitative argument for the creation of the SCCF was that the strong attractive exchange forces between 4f electrons whose spins are similarly directed leads to a less extended

radial wavefunction and hence smaller B_q^k CFPs (Newman 1970). It has been found in the literature (for instance TDC1 and TDC2) and in Chapter 8 of this thesis that you do not need to consider 4f-electrons with relatively different radial wavefunctions in order to obtain a SCCF operator. A SCCF can arise from a second order perturbation mechanism. Such a mechanism will be discussed later in Chapter 8. Judd (1977) substantiated the idea of Newman by replacing every $C_q^{(k)}(i)$ in V_{CF} by:

$$C_q^{(k)}(i) + c_k (\mathfrak{S} \cdot \mathfrak{S}_i) C_q^{(k)}(i) \quad (7.4)$$

where \mathfrak{S}_i is the spin of electron i , and \mathfrak{S} is the total spin. The c_k are parameters, related to a particular rank (k), which according to Newman (1970) and Judd (1977) must necessarily be negative if the contraction of the radial function is to correspond to similarly directed spins. Notice that \mathfrak{S} includes \mathfrak{S}_i ($j \neq i$) i.e. the substitution (7.4) introduces a two-electron operator. Judd (1977) pointed out that the effect of this mechanism can be appreciable throughout the entire RE series and not only for the ground state splitting of Gd^{3+} in crystals.

Following the *schematic* approach of Judd (1977) TDC1 and TDC2 generated effective operators of the SCCF by using a number of second-order perturbation mechanisms and the method of Stevens, discussed earlier in the thesis in section 2.5.2, which combine the CF with one and two-electron operators in H . All the mechanisms invoked were *intra-site*. They found (for Gd^{3+} in lanthanum ethylsulphate by using relativistic wavefunctions) a value of $+0.853 \text{ cm}^{-1}$ which with all other mechanisms (-0.432 cm^{-1} , see relativistic calculation of Smith et al 1977) finally gives a new total splitting of $+0.421 \text{ cm}^{-1}$. This agrees in sign with the experimental value of $+0.236 \text{ cm}^{-1}$ but it is a factor of *two too large*. So although the mystery of the sign appears to be resolved, more research was needed to understand the size of the ground state splitting of Gd^{3+} in lanthanum ethylsulphate.

7.3. Conclusion and Discussion of Chapter 7

In this chapter we have attempted to show why a theoretical explanation of ZFSs in S-state ions and in particular Gd^{3+} -doped lanthanum ethylsulphate is such a difficult problem. A brief

review of the most important mechanisms which contribute to the ZFS of Gd^{3+} was given.

We should point out that all the mechanisms considered up to this point treat the host crystal in a rather cavalier way (for instance Wybourne 1966) i.e. they are *intra-site* mechanisms. Since there are hosts in which Gd^{3+} has a relative ZFS that is opposite in sign even though the hosts have the same point symmetry and similar structure (Newman and Urban 1972) we expect that the host in which the paramagnetic ion is present to provide an important contribution to the ZFS. It is the aim of Chapter 8 to present a simple model of *inter-site* contributions to the ZFS of Gd^{3+} in lanthanum ethylsulphate. We have found that these inter-site contributions are opposite in sign to the intra-site ones of TDC2. We show that the total ZFS which is calculated by incorporating the results of TDC2 combined with all theoretical mechanisms calculated so far (Smith et al 1977) as well as the contributions we investigate in Chapter 8 agrees well with experiment.

CHAPTER 8

INTER-SITE CONTRIBUTIONS TO SCCF AND ZFS FOR Gd^{3+} IN LANTHANUM ETHYLSULPHATE

In this chapter we seek to find a SCCF operator of the form

$$\mu O_0^{(2)} L_i L_j \quad , \quad i \neq j$$

where μ is a constant. We attempt to find the value of μ and hence, by using the work of TDC2 we find a contribution to the ZFS of Gd^{3+} in lanthanum ethylsulphate.

8.1. The Crystal Structure of Lanthanum Ethylsulphate

The crystal structure of the lanthanide ethylsulphates was first determined, using X-ray diffraction techniques, by Ketelaar (1937). This structure was further refined by Fitzwater and Rundle (1959). It was found that the unit cell consists of two molecules and that the RE ions occupy magnetically equivalent sites with C_{2v} symmetry. The point group symmetry is principally determined by the nine waters of crystallisation which cluster about the lanthanide ion at the vertices of three planar equilateral triangles shown in Figure 13.

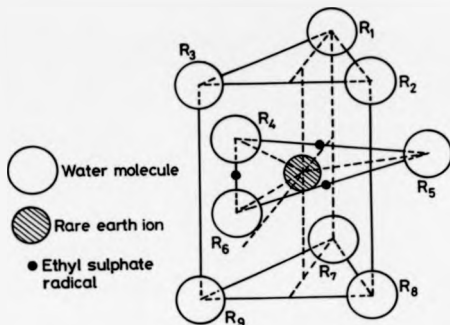


Figure 13: Diagram showing the geometrical configuration (not to scale) of the nearest neighbours surrounding a RE ion in an ethylsulphate crystal. R_1 to R_9 label Oxygen sites.

In the case of Gd^{3+} -doped lanthanum ethylsulphate, the Gadolinium ions enter substitutionally at the lanthanide sites. Three of the water molecules are coplanar with the Gadolinium ion itself and the corresponding Oxygen ions, which we have labelled R_4 , R_5 and R_6 , are located at the points $(4.7619a_0, \pi/2, (2n+1)\pi/3)$, in spherical polar coordinates, where $n = 0, 1, 2$. Another equilateral triangle of water molecules has Oxygen ions above the central plane containing Gd^{3+} at the points $(4.4785a_0, \theta, 2n\pi/3)$ - labelled R_1 , R_2 and R_3 . The angle θ is approximately 40° . The other triangle is below the central plane with Oxygen ions at $(4.4785a_0, \pi - \theta, 2n\pi/3)$ - labelled R_7 , R_8 and R_9 .

8.2. Preliminaries, Perturbation Theory and Empty States

The Hamiltonian from which we derive our mechanism we take to be

$$H = H_1 + H_2 + H_3 \quad (8.1)$$

where H_1 is the operator representing the kinetic energy of all the electrons in the Gd^{3+} -doped lanthanum ethylsulphate. The lattice of nuclei we assume rigid so the kinetic energy of the nuclei is not present. We also omit from consideration any repulsive energy associated with pairs of nuclei since this would appear in equation (8.1) merely as a constant energy and would ultimately

vanish in our second order mechanism as we see later. Thus we may write :

$$H_1 = \sum_i \frac{p_i^2}{2m} \quad (8.2)$$

H_2 describes the attraction of all electrons to the nucleus of the Gd^{3+} , which we suppose has a charge $Z|e|$ at the origin $\mathbf{R}_0 = 0$, as well as attractions to all other nuclei (with charge $Z_n|e|$) of the host lattice at positions \mathbf{R}_n . Hence :

$$H_2 = - \sum_i \frac{Ze^2}{r_i} - \sum_{n \neq 0} \frac{Z_n e^2}{|\mathbf{L} - \mathbf{R}_n|} \quad (8.3)$$

The Coulomb repulsion between pairs of electrons may be written :

$$H_3 = \frac{1}{2} \sum_{i,j} \frac{e^2}{|\mathbf{L}_i - \mathbf{L}_j|} \quad (8.4)$$

Apart from Coulomb repulsions between the 4f-electrons of the Gd^{3+} ion, equation (8.4) may bring about excitations which involve the filled core states of the Gd^{3+} ion itself or the filled core states of neighbouring ions. We shall be specifically interested only in those excitations of 4f-electrons to empty states on neighbouring ions such that at the end of such a transition filled core states remain filled. To obtain the operator corresponding to Newman's SCCF we used Stevens method discussed earlier in section 2.5.2. We represent a filled core state of the Gd^{3+} ion by $f'10\rangle$, where $10\rangle$ is the vacuum state, and suppose a 4f orbital can be written as $a'10\rangle$ (both f and a will also have appropriate subscripts denoting spin and orbital angular momentum). When H_3 is second quantised, there will be some terms of the form $f'_a f'_b$ or its Hermitian conjugate where $b'10\rangle$ is an empty orbital on a neighbouring ion. If this type of term is used to create an excitation of the type we are specially interested in, then we must have $i=j$, $f'_a f'_b$, giving unity between the initial and final state (section 2.5.3). Such a term may also arise if the f'_a refer to filled core orbitals on neighbouring ions so the effect, for our purposes at least, is to generate an effective one-body like operator $a'b$ (or its Hermitian conjugate). For simplicity we can absorb such terms into an effective charge, Z_{eff} , which replaces the bare magnitude of the nuclear charge Z . We can think of this effective charge as arising because the filled-core electrons repel the 4f-electrons thus reducing the attraction to the Gd^{3+} nucleus. Its introduction is strictly not necessary but it

simplifies considerably the presentation of our mechanism. A similar argument enables us to replace the bare neighbour nuclear charges by Z_a^{eff} . Thus H_2 and H_3 become replaced, for our purposes, by :

$$H'_2 = - \sum_i \frac{Z_{eff} e^2}{r_i} - \sum_{a \neq b} \frac{Z_a^{eff} e^2}{|D - R_a|} \quad (8.5)$$

$$H'_3 = \frac{1}{2} \sum_{i,j} \frac{e^2}{|D - L_j|}$$

The dash on the summation in H'_3 is to indicate that only MEs within the 4f orbitals alone or between the 4f orbitals and an empty state on a neighbouring ion are to be allowed. If we take into account the number of the core electrons of Gd^{3+} , which is 54 (including the $5s^2 5p^6$), then, as the atomic number of Gd^{3+} is $Z=64$, an approximate classical estimation for the value of Z_{eff} is 10. Later in this chapter we consider MEs between the ground state and one in which a 4f electron is excited to an empty 3s orbital on an Oxygen neighbour. That part of H'_3 which involves repulsions between the 4f electrons alone will clearly not contribute to such MEs. The second term of H'_2 is principally made up of two components. The first a large spherical component, evaluated by putting $L=0$ and a very much smaller crystal-field-like part (one could visualise this as a Taylor expansion in the small ratio r_i/R_a). The first component is essentially a constant potential energy, at the origin due to nine effective charges Z_a^{eff} so, as this appears between orthogonal many electron states when we use the projector form of perturbation theory, section 2.5.2, (i.e. the first involving the ground state and the second a state in which a 4f Wannier function is replaced by a 3s Wannier function on an Oxygen), it will vanish. The crystal-field part of H'_2 (from the second term) will be so small compared with the first term of H'_2 that we neglect it. We retain the first term of H'_2 and so H'_2 becomes :

$$H'_2 = - \sum_i \frac{Z_{eff} e^2}{r_i} \quad (8.6)$$

To obtain the SCCF operator from inter-site processes we use a particular form of degenerate perturbation theory using projection operators P , (section 2.5.2) for the degenerate states of the unperturbed Hamiltonian H_0 . Following the method of Stevens (see section 2.5.2), H_0 is

defined by :

$$H_0 = \sum_r E_r P_r \quad (8.7)$$

where E_r is given by :

$$E_r = \frac{\sum_{n \gg} \langle n_r | H | n_r \rangle}{\sum_{n \gg} \langle n_r | n_r \rangle} \quad (8.8)$$

In equation (8.8), $|n \gg$ denotes a particular intermediate coupling many-electron state (section 1.1) which arises from a given Term with a fixed orbital angular momentum L and spin S , and H is the actual Hamiltonian of the system. We write $| \cdots \gg$ for an intermediate coupling state to distinguish it from pure LS states $| \cdots \rangle$ (RS-coupling). The eigenvectors of the intermediate coupling states should not, strictly speaking, be designated by an RS-coupling symbol, as L and S have no definite values for these states. Nevertheless, it has been convenient to use such symbols (Dieke 1968 p.74-5). By setting up H_0 as in equation (8.7) we ensure that all those intermediate coupling states from a given term $2S+1L$ will be degenerate since they will belong to one *family* in the Stevens sense. For the ground state of Gd^{3+} these latter states will be degenerate anyway because the 6S Term will result in only one J Level as a result of spin-orbit coupling. However, excited Terms could give rise to more than one total angular momentum J when spin-orbit coupling is included.

The projectors appearing in equation (8.7) are now given by (see equation 2.9):

$$P_r = \sum_{n_r \in (L, S, J, M_r)} |n_r \gg \langle n_r | \quad (8.9)$$

where the sum is over all intermediate coupling states from a particular Term $2S+1L$ (the label r is shorthand for the term (L, S, J, M_r)).

Having defined H_0 we use degenerate perturbation theory in projector form (Bates et al 1968) with $H - H_0 = eV$ as the perturbation (see section 2.5.2). Finally the second order terms are given by:

$$= \sum_{r \neq 0} \frac{P_0 H P_r H P_0}{E_0 - E_r} \quad (8.10)$$

We shall write $H = H_1 + H_2^- + H_3^+$ and examine those parts of H which promote one electron to an empty state on an Oxygen ion neighbouring the Gd^{3+} ion.

In order to consider excitations of electrons to states on neighbouring Oxygen sites we must have wavefunctions for these states. We have assumed that they are 3s-like about the Oxygen ions. We have chosen 3s-states for simplicity because 3s would be the next s-state to be filled on the Oxygen ion. To make this as realistic and at the same as simple as possible we have chosen the form of the 3s wavefunction so that it will have two nodes and will be of the hydrogenic form

$$\phi_{3s}^R = A (4A)^{1/4} [1 - 2A\bar{r} + \frac{2}{3}A^2\bar{r}^2] e^{-A\bar{r}} Y_0^0(\bar{\theta}, \bar{\phi}) \quad (8.11)$$

In equation (8.11) A is a parameter, of dimension a_0^{-1} , to be adjusted later and for all $A \neq 0$, ϕ_{3s}^R is normalised. In this equation \bar{r} denotes $|\underline{r} - \underline{R}|$, \underline{R} being the position vector of the Oxygen site to which the 3s-state given by equation (8.11) is about and $(\bar{\theta}, \bar{\phi})$ are angles defining the orientation of the vector difference $\underline{r} - \underline{R}$. We have included the spherical harmonic Y_0^0 in the definition of ϕ_{3s}^R so that no confusion arises as to whether it has been incorporated or not. To find the parameter A , or at least a range of suitable values of A , we have minimised the sum of squares of the overlaps with the 1s and 2s states of neutral Oxygen (i.e. an Oxygen atom whose overall charge is zero, when one electron occupies the 3s-state of equation (8.11)) and demanded that the 3s-state should be an unbound state and be the s-state which has the lowest energy consistent with the orthogonality properties. As electrons on the Oxygen ions are shared with the hydrogen ions a neutral Oxygen ion seemed the most appropriate to use (although modification of the valency of Oxygen does not significantly affect our results, see our discussion in section 8.8). To build in orthogonality of the 3s wavefunction in (8.11) with 1s and 2s states of Oxygen we have used the wavefunctions of Clementi and Roetti (1974) which take the following form:

$$\begin{aligned} |\phi_{1s}^R\rangle &= \sum_{i=1}^3 C_i N_i e^{-Z_i r} + \sum_{i=1}^6 C_i N_i \bar{r} e^{-Z_i r} \\ |\phi_{2s}^R\rangle &= \sum_{i=1}^3 A_i N_i e^{-Z_i r} + \sum_{i=1}^6 A_i N_i \bar{r} e^{-Z_i r} \end{aligned} \quad (8.12)$$

The parameters in equation (8.12) are displayed in Table 8.1. The normalisation factors N_1, N_2 have dimension $a_0^{-3/2}$ and the N_3, N_4, N_5, N_6 $a_0^{-5/2}$ respectively. C_i and A_i , for $i=1$ to $i=6$, are dimensionless constants.

Table 8.1: Parameters for the 1s and 2s Oxygen wavefunctions

i	C_i	N_i	Z_i in a_0^{-1}	A_i
1	0.94516	42.02042	7.61413	-0.22157
2	0.03391	102.05506	13.75740	-0.00476
3	-0.00034	4.33977	1.69824	0.34844
4	0.00241	11.18652	2.48022	0.60807
5	-0.00486	44.58165	4.31196	0.25365
6	0.03681	96.23147	5.86596	-0.19183

Thus we have, numerically, evaluated

$$S = |\langle \phi_{1s}^R | \phi_{2s}^R \rangle|^2 + |\langle \phi_{2s}^R | \phi_{3s}^R \rangle|^2$$

as a function of A . The minimum of S , constrained by the demand that the 3s-state must be of the lowest unbound energy consistent with the orthogonality properties, occurs when A ranges approximately between $A = 1.4$ and $A = 2.0$. To ensure $|\phi_{1s}^R\rangle$ is as close as possible to the condition of being orthogonal to $|\phi_{1s}^R\rangle$ and $|\phi_{2s}^R\rangle$ with the lowest unbound energy, A must be chosen in this range.

In Table 8.2 we present the results of our calculations for a range of values of A from $A = 1.0$ to $A = 2.0$ units. For completeness we have also listed, in Table 8.3,

$$E_{3s} = \langle \phi_{3s}^R | \frac{p^2}{2m} - \frac{e^2}{r} - \frac{Z_{eff}^{3s} e^2}{R_{ev}} | \phi_{3s}^R \rangle = \frac{A^2 \hbar^2}{2m} - \frac{A e^2}{3} - \frac{Z_{eff}^{3s} e^2}{R_{ev}}$$

in units of (e^2/a_0) , where we have assumed that the electron occupying ϕ_{3s}^R "sees" an effective Oxygen charge of $+1$. The term $-Z_{eff}^{3s}(e^2/R_{ev})$ represents the attraction of the 3s-electron by the

Gd^{3+} ion. R_m is the average distance of the Oxygen ions from the Gd^{3+} impurity (i.e. $4.6202a_0$).

Z_{eff}^{3i} is the magnitude of an effective positive charge which should not be confused with Z_{eff} or Z_{eff}^{II} of equation (8.3). If Z_{eff}^{3i} were due to Gd^{3+} alone and there was no overlap between the 3s-orbital on the Oxygen site and the outer orbitals of the Gd^{3+} ion then we might expect $Z_{eff}^{3i} = +3.0$. Such an overlap is expected small and so we should expect a Z_{eff}^{3i} not much larger than +3. Since the uncertainty of the value of Z_{eff}^{3i} we calculated the 3s-energy for a range of values of it (Table 8.3).

Table 8.2 : *Overlaps and sum of squares of overlaps S.*

A in a_0^{-1}	$\langle \phi_{1s}^R \phi_{2s}^R \rangle$	$\langle \phi_{2s}^R \phi_{3s}^R \rangle$	S
1.0	0.1069	0.1976	0.050473
1.1	0.1067	0.1887	0.046993
1.2	0.1047	0.1690	0.039523
1.3	0.1012	0.1405	0.029982
1.4	0.0963	0.1049	0.020279
1.5	0.0902	0.0641	0.012245
1.6	0.0832	0.0194	0.007299
1.7	0.0754	0.0278	0.006459
1.8	0.0670	0.0765	0.010341
1.9	0.0581	0.1258	0.019201
2.0	0.0458	0.1750	0.033002

Table 8.3 : Energy of $1\phi_{1/2}^2$, in e^2/a_0 , for a range of values of Z_{eff} and A .

A	$Z_{eff}=0.0$	$Z_{eff}=3.0$	$Z_{eff}=3.5$	$Z_{eff}=4.0$	$Z_{eff}=4.5$
1.0	0.1667	-0.4826	-0.3908	-0.6991	-0.8073
1.1	0.2383	-0.4110	-0.5192	-0.6275	-0.7357
1.2	0.3200	-0.3293	-0.4375	-0.5458	-0.6540
1.3	0.4117	-0.2376	-0.3458	-0.4541	-0.5623
1.4	0.5133	-0.1360	-0.2442	-0.3525	-0.4607
1.5	0.6250	-0.0243	-0.1325	-0.2408	-0.3490
1.6	0.7467	0.0974	-0.0108	-0.1191	-0.2273
1.7	0.8783	0.2290	0.1208	0.0125	-0.0957
1.8	1.0200	0.3707	0.2625	0.1542	0.0460
1.9	1.1717	0.5224	0.4142	0.3059	0.1977
2.0	1.3333	0.6840	0.5758	0.4675	0.3593

8.3. Categorising of Excitations

To systematise the different types of excitation via terms of equation (8.10), we write each in the form $B_1 : B_2$ where this is understood to be shorthand for :

$$- \sum_{\alpha} \frac{P_0 B_1 P_{\alpha} B_2 P_0}{E_{\alpha} - E_0} \quad (8.13)$$

H_1, H_2^{\pm} clearly correspond to one-body operators whereas H_3^{\pm} corresponds to a two-body operator. H_1 and H_2^{\pm} are combined to define an operator

$$X = \frac{p^2}{2m} - Z_{eff} \frac{e^2}{r} \quad (8.14)$$

On the other hand, H_3^{\pm} is a two-body operator for which we write

$$U = \frac{e^2}{2|E_1 - E_2|} \quad (8.15)$$

H_1 and H_2^+ , when second quantised take the form (for instance see section 2.5.3)

$$\sum_{i,j} \langle s | X | t \rangle \alpha_i^\dagger \alpha_j \quad (8.16)$$

where the states $|s\rangle$ and $|t\rangle$ are part of an orthonormal set in the usual way (section 2.5.2). H_2^+ may be written (see equation (2.21))

$$\sum_{i,j,m,n,s,t} \langle i,j,m | U | s,t \rangle \alpha_i^\dagger \alpha_m^\dagger \alpha_s \alpha_t \quad (8.17)$$

Remembering that we write 4f orbitals of the Gd^{3+} ion as $a^i | 0 \rangle$ and an empty state near an Oxygen ion as $b^i | 0 \rangle$ let us examine the types of operator we can have in the positions of B_1 and B_2 of equation (8.13).

(i) Position B_1 : The only one electron excitation operators we can have here are :

$$a^i b \quad a^i a^j a b \quad a^i a^j b a$$

(ii) Position B_2 : Here we can only have :

$$b^i a \quad b^i a^j a a \quad a^i b^j a a$$

Since the excited state projected out by P , contains only one electron, the only second order processes involving the excitation of one electron are :

$$\begin{aligned} (1) & a^i b : b^i a \\ (2) & a^i b : b^i a^j a a \\ (3) & a^i b : a^j b^j a a \\ (4) & a^i a^j a b : b^i a \\ (5) & a^i a^j b a : b^i a \\ (6) & a^i a^j a b : b^i a^j a a \\ (7) & a^i a^j a b : a^j b^j a a \\ (8) & a^i a^j b a : b^i a^j a a \\ (9) & a^i a^j b a : a^j b^j a a \end{aligned} \quad (8.18)$$

8.4. An Effective Inter-site Operator

8.4.1. Second Quantised Effective Operators

To describe how an effective operator is obtained from the nine processes in (8.18) we take (2) as an example, writing it in shorthand as :

$$P_0 a_1^\dagger b_\alpha a_2^\dagger b_\beta a_3^\dagger a_4 P_0 \quad (8.19)$$

where the labels 1, 2, 3, and 4 are quantum labels for the 4f electrons and α and β are quantum numbers for empty orbitals near Oxygen neighbours. Because of the way H_0 is constructed (sections 2.5.2 and 8.2) one can write $P_r = b_\beta^\dagger a_2^\dagger a_3 a_4 P_0$. Since $P_r^2 = P_r$, the particular case of (8.19) becomes:

$$P_0 a_1^\dagger b_\alpha b_\beta^\dagger a_2^\dagger a_3 a_4 P_0 \quad (8.20)$$

Hence (8.19) may be replaced by (8.20). b_β may be anticommuted through the a operators to the right and similarly with b_α . When $\alpha = \beta$, as $b_\alpha b_\alpha^\dagger = 1 - b_\alpha^\dagger b_\alpha$ and α is empty in P_0 , only unity remains. If $\alpha \neq \beta$ then the whole ME will vanish. The operator in (8.20) therefore reduces to:

$$P_0 a_1^\dagger a_2^\dagger a_3 a_4 P_0 \quad (8.21)$$

and although the states $b_\alpha^\dagger |0\rangle$ have apparently disappeared they are still very much present in the MEs associated with (8.21). The operator in (8.21) only acts within the ground family and is strongly suggestive of a two-body operator. If we use this same procedure on case (1) in (8.18) we can clearly only obtain a one-body-like effective operator which will not contribute to a SCCF.

The one-electron excitations, after using the above, reduce to the eight contributions below:

$$\begin{aligned} (2) - \sum & \frac{\langle \frac{\sigma}{m_1} | X | \frac{\sigma}{m_2} \rangle \langle \frac{\sigma'}{m_2} | U | \frac{\sigma'}{m_4} \frac{\sigma'}{m_5} \rangle}{\Delta} P_0 a_{m_1, \sigma}^\dagger a_{m_2, \sigma}^\dagger a_{m_4, \sigma} a_{m_5, \sigma} P_0 \\ (3) + \sum & \frac{\langle \frac{\sigma}{m_1} | X | \frac{\sigma}{m_2} \rangle \langle \frac{\sigma'}{m_3} | U | \frac{\sigma'}{m_4} \frac{\sigma'}{m_5} \rangle}{\Delta} P_0 a_{m_1, \sigma}^\dagger a_{m_2, \sigma}^\dagger a_{m_3, \sigma} a_{m_4, \sigma} P_0 \\ (4) - \sum & \frac{\langle \frac{\sigma}{m_1} | U | \frac{\sigma}{m_2} \frac{\sigma'}{m_4} \rangle \langle \frac{\sigma'}{m_3} | X | \frac{\sigma'}{m_5} \rangle}{\Delta} P_0 a_{m_1, \sigma}^\dagger a_{m_2, \sigma}^\dagger a_{m_3, \sigma} a_{m_5, \sigma} P_0 \\ (5) + \sum & \frac{\langle \frac{\sigma}{m_1} | U | \frac{\sigma}{m_3} \frac{\sigma'}{m_4} \rangle \langle \frac{\sigma'}{m_2} | X | \frac{\sigma'}{m_5} \rangle}{\Delta} P_0 a_{m_1, \sigma}^\dagger a_{m_2, \sigma}^\dagger a_{m_3, \sigma} a_{m_5, \sigma} P_0 \quad (8.22) \\ (6) - \sum & \frac{\langle \frac{\sigma}{m_1} | U | \frac{\sigma}{m_3} \frac{\sigma'}{m_4} \rangle \langle \frac{\sigma'}{m_2} | U | \frac{\sigma'}{m_5} \frac{\sigma'}{m_6} \frac{\sigma'}{m_7} \rangle}{\Delta} P_0 a_{m_1, \sigma}^\dagger a_{m_2, \sigma}^\dagger a_{m_3, \sigma}^\dagger a_{m_4, \sigma}^\dagger a_{m_5, \sigma} a_{m_6, \sigma} a_{m_7, \sigma} P_0 \\ (7) + \sum & \frac{\langle \frac{\sigma}{m_1} | U | \frac{\sigma}{m_3} \frac{\sigma'}{m_4} \rangle \langle \frac{\sigma'}{m_2} | U | \frac{\sigma'}{m_5} \frac{\sigma'}{m_6} \frac{\sigma'}{m_7} \rangle}{\Delta} P_0 a_{m_1, \sigma}^\dagger a_{m_2, \sigma}^\dagger a_{m_3, \sigma}^\dagger a_{m_4, \sigma}^\dagger a_{m_5, \sigma} a_{m_6, \sigma} a_{m_7, \sigma} P_0 \\ (8) + \sum & \frac{\langle \frac{\sigma}{m_1} | U | \frac{\sigma}{m_3} \frac{\sigma'}{m_4} \rangle \langle \frac{\sigma'}{m_2} | U | \frac{\sigma'}{m_5} \frac{\sigma'}{m_6} \frac{\sigma'}{m_7} \rangle}{\Delta} P_0 a_{m_1, \sigma}^\dagger a_{m_2, \sigma}^\dagger a_{m_3, \sigma}^\dagger a_{m_4, \sigma}^\dagger a_{m_5, \sigma} a_{m_6, \sigma} a_{m_7, \sigma} P_0 \end{aligned}$$

$$(9) = \sum \frac{\langle \sigma' m_1' | U | \sigma m_1 \rangle \langle \sigma' m_2' | U | \sigma m_2 \rangle}{\Delta} P_{\sigma' m_1' \sigma' m_2' \sigma m_1 \sigma m_2}$$

In (8.22) the sign of each contribution is made up of the minus already present in second order in equation (8.13) together with any sign changes when the b 's are commuted through to the right of the operator. In (2) to (5) of (8.22) the summation is over the components of angular momentum m_1, m_2, m_3, m_4, m_5 , and the spin components σ and σ' . In (6) to (9) of (8.22) the summation is now over $m_1, m_2, m_3, m_4, m_5, m_6, m_7$ and $\sigma, \sigma', \sigma''$. The positive energy splitting Δ , denotes the energy difference between the ground state (with neighbouring 3s states empty) and an excited state in which a 4f electron is transferred to one 3s on a neighbouring Oxygen ion. The 3s state is denoted by a horizontal bar in MEs.

8.4.2. Conversion to Effective Spin and Orbital Operators

In this section we show how the operators between the projectors of (8.22) may be represented as a linear combination of operators of the type $a^\dagger a$ and those of the form $a^\dagger a a^\dagger a$ and hence how they can be rewritten in terms of spin and orbital angular momentum operators by using Stevens's equivalences of equation (2.17).

We now use the anticommutation rules to change each operator in (8.22) into the requisite form. It turns out, however, that there are two distinct ways of doing this, with two-body operators (for a full discussion see Dixon et al 1984). We choose the particular method which results in a form $a_{\sigma' m_1' \sigma' m_2'}^\dagger a_{\sigma m_1 \sigma m_2}$ plus additional terms which involve orbitals only. The reason for doing this is to produce an SCFF-like operator of the form $O_q^{(\sigma)}(L) \cdot \mathbf{L}_i \cdot \mathbf{L}_j, i \neq j$ so that our results may be compared with other authors who have also used operators of this type (Newman 1970, Dixon and Chatterjee 1980a,b, TDC1, TDC2). In fact the additional terms which appear are one-body like and purely orbital or are two-body like and describe orbit-orbit interactions. We have retained only the spin-spin terms above. The orbit-orbit terms can be shown to be *equivalent* to spin-spin terms, for the interactions we have used, (see Dixon et al 1984) and when both orbit-orbit and spin-spin contributions are retained the coefficient μ (see equation (8.28)) is merely multiplied by a factor of 4/3 (Dixon 1987, private communication) and so can be easily

incorporated in our calculations. The purely orbital one-body terms produce very small contributions to the ZFS, within the intermediate coupling ground state, for reasons given in the subsequent paragraph.

As an example we consider (2) of (8.22). Writing :

$$a_{m,\sigma}^\dagger a_{m,\sigma}^\dagger a_{m,\sigma}^\dagger a_{m,\sigma}^\dagger = a_{m,\sigma}^\dagger (\delta_{m,\sigma} - a_{m,\sigma}^\dagger a_{m,\sigma}^\dagger) a_{m,\sigma}^\dagger \quad (8.23)$$

When the first term in (8.23) is summed over σ , from equivalences (2.17), a purely orbital operator will result and its MEs will be very small within the intermediate coupling ground state (Wybourne 1966) which is:

$${}^1S_{7/2} > = 0.987 {}^1S_{7/2} > + 0.162 {}^1P_{7/2} > - 0.012 {}^1D_{7/2} > + 0.001 {}^1F_{7/2} > + \dots$$

The reason is not difficult to find since it will either vanish or contribute to the mean energy of the ground state for ${}^1S_{7/2} >$ and ${}^1P_{7/2} >$ (see our discussion in section 7.1). We therefore neglect MEs of purely orbital operators. Notice that equation (8.23) will introduce yet another minus sign.

After regrouping second quantised operators in (2) to (5) of (8.22) using the methodology of (8.23), the same net sign results for each effective operator. Furthermore if in (3) $m_4 \rightarrow m_5, m_5 \rightarrow m_4$, since $\langle a, b | U | c, d \rangle = \langle b, a | U | d, c \rangle$ (Raimes 1972, p.33), operators (2) and (3) becomes identical. In a similar way we can show that (4) and (5) of (8.22) are also equal. The result is that (2), (3), (4) and (5) give in total:

$$+ 4 \sum \frac{\langle m_1 | X | \bar{m}_1 \rangle \langle \bar{m}_2, m_2 | U | m_4, m_5 \rangle}{\Delta} a_{m,\sigma}^\dagger a_{m,\sigma}^\dagger a_{m,\sigma}^\dagger a_{m,\sigma}^\dagger \quad (8.24)$$

(Actually (4) = (3)* but as we take an equal Hermitian component from (2), (3), (4) and (5) to get our result eventually, equation (8.24) is correct as given).

In a similar way we can demonstrate that (6), (7), (8) and (9) are equal so we concentrate on the operator in (6) and manipulate it into the form $a^\dagger a a^\dagger a a^\dagger a$ so the relationships of Stevens given by (2.17) may be used. Thus we can write :

$$\begin{aligned} a_{m,\sigma}^\dagger a_{m,\sigma}^\dagger a_{m,\sigma}^\dagger a_{m,\sigma}^\dagger a_{m,\sigma}^\dagger a_{m,\sigma}^\dagger &= \delta_{m,\sigma} \delta_{\sigma',\sigma} a_{m,\sigma}^\dagger (\delta_{m,\sigma} \delta_{\sigma',\sigma} - a_{m,\sigma}^\dagger a_{m,\sigma}^\dagger) a_{m,\sigma}^\dagger \\ &+ \delta_{m,\sigma} a_{m,\sigma}^\dagger a_{m,\sigma}^\dagger a_{m,\sigma}^\dagger a_{m,\sigma}^\dagger - a_{m,\sigma}^\dagger a_{m,\sigma}^\dagger a_{m,\sigma}^\dagger a_{m,\sigma}^\dagger a_{m,\sigma}^\dagger \end{aligned} \quad (8.25)$$

On the RHS of (8.25), the first three terms are purely orbital from the first two relations in (2.17) i.e. when the sums over σ , σ' and σ'' are carried out. Hence they will either give zero or rotationally invariant MEs within $|^4S_{7/2}\rangle$, $|^6P_{7/2}\rangle$ and be very small (compared with those we retain) within $|^4S_{7/2}\rangle$ so we drop these terms. The last term is approximated in (8.25) by summing over σ'' , to produce a purely orbital operator, from $a_{\sigma,\sigma'}^\dagger a_{\sigma,\sigma''}$, and retaining only the $n=0$ contribution (otherwise we obtain a three-body contribution) when the equivalences in (2.17) are used. As $N_0^2 = 7$

$$\sum_{\sigma,\sigma'} a_{\sigma,\sigma'}^\dagger a_{\sigma,\sigma'} \rightarrow \text{unity operator}$$

since for Gd^{3+} , $\sum_i 1 = 7$.

We therefore have, when (6), (7), (8) and (9) of (8.22) are combined :

$$+ 4 \sum \frac{\langle m_1, m_2 | U | \bar{m}_1, \bar{m}_2 \rangle \langle \bar{m}_1, \bar{m}_2 | U | m_1, m_2 \rangle}{\Delta} a_{\sigma,\sigma'}^\dagger a_{\sigma,\sigma'}^\dagger a_{\sigma,\sigma'} a_{\sigma,\sigma'} \quad (8.26)$$

When the spin component summations are carried out over σ , σ' in (8.24) and (8.26) and the equivalences of (2.17) are used we find, for example, that:

$$\sum_{\sigma,\sigma'} a_{\sigma,\sigma'}^\dagger a_{\sigma,\sigma'}^\dagger a_{\sigma,\sigma'} a_{\sigma,\sigma'} = 2 \sum_{n=0} \Delta_{m,n,n} \Delta_{m,n,n} O_{m,-n,n}^{(n)}(U) O_{m,-n,n}^{(n)}(U) \left[\frac{1}{4} + \frac{1}{2} U_z \right] \quad (8.27)$$

Clearly if $i = j$ a purely orbital operator will result so we assume we can take only $i \neq j$ for reasons given earlier. Furthermore, for comparison with SCCF operators in the literature, we seek an operator of the form (notice that we concentrate our studies on second-order CFPs since it has been found that their contribution to the ZFS is by far the dominant (Dagg et al 1969)):

$$\mu \sum_{i,j} C_0^{(2)}(\theta, \phi) \mathcal{L}_i \mathcal{L}_j \quad (8.28)$$

In (8.27), if we choose $n=2$, $n'=0$, $m_1=m_2, m_2=m_4$ or $n'=2$, $n=0$, $m_1=m_2, m_2=m_4$ then operators of the form (8.28) are obtained since $O_0^{(2)} = -(45/2) C_0^{(2)}$. We can therefore write, in total,

$$\mu = \mu_1 + \mu_2 + \mu_3 + \mu_4$$

where :

$$\mu_1 = - \frac{8 \times 45}{2} \sum_{m_1, m_2, m_3} \frac{\langle m_1 | X | \bar{m}_2 \rangle \langle \bar{m}_2, m_3 | U | m_1, m_3 \rangle \langle m_1 | O_0^{(2)} | m_1 \rangle}{\Delta N_0 N_2^2}$$

$$\begin{aligned}
 \mu_2 &= -\frac{8 \times 45}{2} \sum_{\mathbf{R}} \frac{\langle m_1 | X | \bar{m}_2 \rangle \langle \bar{m}_3 m_3 | U | m_3 m_1 \rangle \langle m_3 | O_0^{(2)} | m_3 \rangle}{\Delta N_0 N_2^2} \\
 \mu_3 &= -\frac{8 \times 45}{2} \sum_{\mathbf{R}} \frac{\langle m_1 m_2 | U | \bar{m}_3 m_1 \rangle \langle \bar{m}_3 m_3 | U | m_3 m_2 \rangle \langle m_1 | O_0^{(2)} | m_1 \rangle}{\Delta N_0 N_2^2} \\
 \mu_4 &= -\frac{8 \times 45}{2} \sum_{\mathbf{R}} \frac{\langle m_1 m_2 | U | \bar{m}_3 m_1 \rangle \langle \bar{m}_3 m_3 | U | m_2 m_3 \rangle \langle m_2 | O_0^{(2)} | m_2 \rangle}{\Delta N_0 N_2^2}
 \end{aligned} \quad (8.29)$$

where the sum over \mathbf{R} is over the positions of the nine neighbouring water molecules to the Gd^{3+} ion.

8.5. Evaluation of the Coefficient μ

The 4f-wavefunction of Gd^{3+} is written in the separable form:

$$f_{4f}(\mathbf{r}) = \psi_{4f}(r) Y_3^m(\theta, \phi) \quad (8.30)$$

and a 3s-wavefunction at a neighbouring Oxygen site \mathbf{R} as :

$$g_{3s}(\mathbf{r} - \mathbf{R}) = (4\pi)^{-1/2} 2A^{3/2} \left(1 - 2A | \mathbf{r} - \mathbf{R} | + \frac{2}{3} A^2 | \mathbf{r} - \mathbf{R} |^2\right) e^{-A|\mathbf{r} - \mathbf{R}|} \quad (8.31)$$

where :

$$| \mathbf{r} - \mathbf{R} |^2 e^{-2|\mathbf{r} - \mathbf{R}|} = \sum_{l=0}^{\infty} \beta_l(\lambda, \mathbf{r}, \mathbf{R}) P_l(\cos \theta) \quad (8.32)$$

and $\beta_l(\lambda, \mathbf{r}, \mathbf{R})$ is defined in Appendix D. By using standard properties of 3j-symbols (equations (1.43) and (2.20) of Rotenberg et al 1959), we finally obtain :

$$\begin{aligned}
 \mu_1 &= - \sum_{\mathbf{R}} \bar{R}(3, L) \frac{Y_2^0(0_R, \phi_R)}{7 \times 5^3} P(R) Q(3, L, R) \\
 \mu_2 &= - \sum_{\mathbf{R}} \bar{R}(1, L) \frac{Y_2^0(0_R, \phi_R)}{5^3} P(R) Q(1, L, R) \left\{ \frac{3}{2} \frac{L}{L+1} \right\} \frac{(2L+1)}{7} \\
 \mu_3 &= - \sum_{\mathbf{R}} \bar{R}(1, L) \frac{7 Y_2^0(0_R, \phi_R)}{5^3} \frac{Q(3, 0, R)}{2} Q(1, L, R) \left\{ \frac{3}{2} \frac{L}{L+1} \right\} \frac{(2L+1)}{7} \\
 \mu_4 &= - \sum_{\mathbf{R}} \bar{R}(3, L) \frac{Y_2^0(0_R, \phi_R)}{5^3} \frac{Q(3, 0, R)}{2} Q(3, L, R)
 \end{aligned} \quad (8.33)$$

where :

$$\begin{aligned}
 P(R) &= \int_0^{\infty} \Psi_{4f}(r) \left[\frac{-R^2}{2m} \left(\frac{1}{r} \frac{d^2}{dr^2} r - \frac{12}{r^2} \right) - \frac{Z_{eff} e^2}{r} \right] \\
 &\quad \times (4\pi)^{-1/2} \left\{ 2A^{3/2} \beta_3(0, A, r, R) - 4A^{3/2} \beta_3(1, A, r, R) + \frac{4}{3} A^{3/2} \beta_3(2, A, r, R) \right\} r^2 dr \\
 Q(I, L, R) &= \int_0^{\infty} \int_0^{\infty} (4\pi)^{-1/2} \left\{ 2A^{3/2} \beta_3(0, A, r_1, R) - 4A^{3/2} \beta_3(1, A, r_1, R) + \frac{4}{3} A^{3/2} \beta_3(2, A, r_1, R) \right\} \\
 &\quad \times \Psi_{4f}(r_2) \frac{r_2^2}{r_1^{L+1}} \Psi_{4f}(r_1) \Psi_{4f}(r_2) r_1^2 r_2^2 dr_1 dr_2
 \end{aligned}$$

and

$$\dot{R}(I, L) = -7 \left(\begin{smallmatrix} 3 & 3 & 3 \\ 0 & 0 & 0 \end{smallmatrix} \right) (4\pi)^{-1/2} \left(\frac{4\pi}{2L+1} \right)^2 \frac{\pi}{2L+1} \frac{\langle 3110^2113 \rangle \langle 111Y_L113 \rangle \langle 311Y_L113 \rangle \times 8 \times 45}{\Delta N_0^2 N_z^2}$$

where $\langle 3110^2113 \rangle = 30.74085$ (Smith and Thornley 1966), $N_0^2 = 7$ and $N_z^2 = 189$ (Stevens 1974).

For the purpose of our numerical calculations we have used the 4f radial wavefunction of Freeman and Watson (1962) which takes the form :

$$\Psi_{4f}(r) = r^3 \sum_{i=1}^8 B_i e^{-W_i r} \quad (8.34)$$

The parameters W_i, B_i , for Gd^{3+} , are displayed in Table F.1 of Appendix F and have dimension a_0^{-1} and $a_0^{-6/2}$ respectively. The 6j-symbols we have used are given in Table F.2 of Appendix F and the reduced MEs of Y_L in Table F.3 of Appendix F. Using the technique described in Appendix D, we have obtained an analytical expression for $\beta_i(\lambda, Z, r, R)$, substituted this into the integrals above for $P(R)$ and $Q(I, L, R)$ and evaluated them using the computer. The values of $P(R)$ are given for the two values of R , $R_1 = 4.4785 a_0$ and $R_2 = 4.7619 a_0$, in Tables F.4 and F.5 of Appendix F when A varies between 1.4 and 1.9. Table F.6 of Appendix F lists the values of $\dot{R}(I, L)$ for the nine pairs (I, L) , and only for $Z_{eff} = 0.0$ since other cases can be trivially calculated, that arise in the calculation of μ . Tables F.7 and F.8 of Appendix F display the radial integrals $Q(I, L, R)$ over the range $A=1.4$ to $A=1.9$. Table F.9 of Appendix F displays the 3s-3s overlap for $R_{12}, R_{17}, R_{19}, R_{45}, R_{14}$ and R_{15} where R_{ij} in general denotes the distance between the sites i and j . Finally, Table F.10 of Appendix F lists the radial part of the 4f-3s overlap for $R_1 = 4.4785 a_0$ and $R_2 = 4.7619 a_0$.

8.6. The Effect of Overlaps

So far calculations have been performed using free-ion wavefunctions, whereas the second quantisation technique of Stevens should employ an orthonormal basis set, including the 3s functions near the nine neighbouring Oxygen ions. As the overlap between the 4f orbitals and each of the 3s orbitals is small a convenient set of orthonormal functions can be generated using the method of Löwdin (1950) (see section 5.4 for a brief description of the method). Thus, if we describe a 4f orbital by $|4fm\rangle$, where m is the associated magnetic quantum number and a 3s orbital at a site R by $|3sR\rangle$ then:

$$|4\tilde{f}m\rangle = |4fm\rangle - \frac{1}{2} \sum_R S_{m,R} |3sR\rangle \quad (8.35)$$

and

$$|3\tilde{s}R\rangle = |3sR\rangle - \frac{1}{2} \sum_m S_{m,R} |3sR\rangle - \frac{1}{2} \sum_m S_{m,R} |4fm\rangle \quad (8.36)$$

where the tildes above the kets on the left-hand side of (8.35) and (8.36) denote the new orthogonalised orbitals and we have expanded equation (5.7) and retained only those terms linear in the overlaps.

In μ_3 and μ_4 of (8.29) we should have used the orthogonalised orbitals in (8.35) so a typical Coulomb element containing three 4f orbitals and a 3s neighbouring orbit becomes :

$$\begin{aligned} \langle 4\tilde{f}m_1, 4\tilde{f}m_2 | U | 4\tilde{f}m_3, 3\tilde{s}Rm \rangle &= \langle 4f m_1, 4f m_2 | U | 4f m_3, 3sRm \rangle \\ &- \frac{1}{2} \sum_R S_{Rm} \langle 4f m_1, 4f m_2 | U | 4f m_3, 4f m \rangle + O(S^2) \end{aligned} \quad (8.37)$$

In (8.37) we have neglected all terms quadratic in overlaps i.e. $O(S^2)$ or the product of an overlap and an integral containing a non-central site orbital with on site ones (Dixon and Wardlaw 1986a). We have neglected all terms smaller than these and to make clear the magnetic quantum number part of $3sR$, when expanded in spherical harmonics related to the central site, we have written $3sRm$ rather than $3sR$. In a similar way, we find :

$$\langle 4\tilde{f}m_1 | X | 3\tilde{s}Rm \rangle = \langle 4f m_1 | X | 3sRm \rangle - \frac{1}{2} S_{Rm} \langle 4f m_1 | X | 4f m \rangle + O(S^2) \quad (8.38)$$

and

$$\langle 4f m_1 | O_0^{(2)} | 4f m_1 \rangle = \langle 4f m_1 | O_0^{(2)} | 4f m_1 \rangle + O(S^2) \quad (8.39)$$

It may also be shown that the denominators of the expressions in (8.29) will, to a good approximation, be unchanged by the effect of overlaps since the 4f and 3s energies are not modified up to the square of an overlap. That is :

$$\begin{aligned} \langle 4f m_1 | H_0 | 4f m_1 \rangle &= \langle 4f m_1 | H_0 | 4f m_1 \rangle + O(S^2) \\ \langle 3s \bar{g} | H_0 | 3s \bar{g} \rangle &= \langle 3s \bar{g} | H_0 | 3s \bar{g} \rangle + O(S^2) \end{aligned} \quad (8.40)$$

The product of MEs which appears in (8.29) for μ_3 , for example, when the effects of overlaps are incorporated, becomes :

$$\begin{aligned} & [\langle 4f m_1, 4f m_2 | U | 3s \bar{g} m_3, 4f m_1 \rangle \langle 3s \bar{g} m_3, 4f m_1 | U | 4f m_2, 4f m_3 \rangle \\ & - \frac{1}{2} S_{s, m_1} \langle 4f m_1, 4f m_2 | U | 3s \bar{g} m_3, 4f m_1 \rangle \langle 4f m_3, 4f m_1 | U | 4f m_2, 4f m_3 \rangle \\ & - \frac{1}{2} S_{s, m_1} \langle 4f m_1, 4f m_2 | U | 4f m_3, 4f m_1 \rangle \langle 3s \bar{g} m_3, 4f m_1 | U | 4f m_2, 4f m_3 \rangle \\ & + \frac{1}{4} |S_{s, m_1}|^2 \langle 4f m_1, 4f m_2 | U | 4f m_3, 4f m_1 \rangle \langle 4f m_3, 4f m_1 | U | 4f m_2, 4f m_3 \rangle] \\ & \times \langle m_1 | O_0^{(2)} | m_1 \rangle \end{aligned} \quad (8.41)$$

The first term in (8.41) is that appearing in (8.29) and the second, third and fourth are additional contributions due to overlaps. The angular part from the first and fourth terms are identical and result in two harmonics $Y_{10}^{m_1}(\theta_R, \phi_R)$ and $Y_{10}^{m_2}(\theta_R, \phi_R)$ coupled to form the harmonic $Y_2^0(\theta_R, \phi_R)$ in (8.33). However the second and third terms, linear in overlaps produce either the pair of harmonics $Y_{10}^{m_1}(\theta_R, \phi_R)$ and $Y_{10}^{m_2}(\theta_R, \phi_R)$ or $Y_{10}^{m_1}(\theta_R, \phi_R)$ and $Y_{10}^{m_2}(\theta_R, \phi_R)$ which are also coupled to form $Y_2^0(\theta_R, \phi_R)$ (Rotenberg et al 1959, eq. 1.15).

8.7. Results and Comparison with Experiment

In this section we use the results of a recent paper, which discussed contributions to the ZFS from a number of intra-site mechanisms (TDC2), and combine them with our qualitative estimate of splittings due to the inter-site mechanisms we have described. Suppose we denote the value of μ in TDC2 by μ_{int} and the net value of μ calculated from our inter-site mechanism μ_{eff} . μ_{int} was made up of two parts μ_1^{int} and μ_2^{int} where $\mu_1^{\text{int}} = +88.4 \text{ cm}^{-1}$ and $\mu_2^{\text{int}} = +59.9 \text{ cm}^{-1}$ so

$\mu_{\text{int}} = \mu_1^{\text{int}} + \mu_2^{\text{int}} = +148.3 \text{ cm}^{-1}$. From the TDC2 intra-site mechanism the total ZFS was $+0.853 \text{ cm}^{-1}$ and was proportional to μ_{int} . Therefore we have :

$$\xi \mu_{\text{int}} = +0.853 \text{ cm}^{-1} \quad (8.42)$$

for some constant ξ obtained by calculating the MEs of $C_0^{(2)}(\theta, \phi) \hat{L}_1 \hat{L}_2$ between the intermediate coupling many-electron states of Gd^{3+} . Hence, as μ_{int} is known, ξ is determined. To compare with experiment we must add contributions from all other mechanisms (Smith et al 1977) which give -0.432 cm^{-1} ($= \eta$ say). We require that the net μ multiplied by ξ when added to η should give the experimental ZFS of $+0.236 \text{ cm}^{-1}$. Hence :

$$(\mu_{\text{int}} + \mu_{\text{eff}}) \times \xi + \eta = +0.236 \text{ cm}^{-1} \quad (8.43)$$

and so :

$$\mu_{\text{eff}} = -32.16 \text{ cm}^{-1} \quad (8.44)$$

is required from our inter-site mechanism. Careful inspection of Table 8.4,

A	$Z_{\text{eff}}^{3/2} = 0.0$	$Z_{\text{eff}}^{3/2} = 3.0$	$Z_{\text{eff}}^{3/2} = 3.5$	$Z_{\text{eff}}^{3/2} = 4.0$	$Z_{\text{eff}}^{3/2} = 4.5$
1.4	-3.43	-9.85	-14.32	-26.21	-154.28
1.5	-14.42	-34.84	-45.60	-65.98	-119.33
1.6	-11.78	-24.97	-30.70	-39.83	-56.70
1.7	-0.30	-0.58	-0.69	-0.83	-1.07
1.8	+14.95	+26.33	+30.15	+35.28	+42.50
1.9	+30.64	+50.43	+56.51	+64.26	+74.48

where changes due to overlaps and the factor $4/3$ mentioned earlier have been taken into account, shows that a value of μ_{eff} of the magnitude and sign in (8.44) may be obtained for $Z_{\text{eff}}^{3/2} = 3.5$ and for $1.6 < A < 1.7$ which is very close to the region of values of A which make the $3s$ wavefunction most nearly orthogonal to the $1s$ and $2s$ orbitals of an Oxygen neighbour.

8.8. Conclusion and Discussion of Chapter 8

In this chapter we gave an account of how inter-site one-electron excitations can make contributions to ZFS of Gd^{3+} in lanthanum ethylsulphate. Our treatment has of necessity being *qualitative* at the outset in view of the uncertainties in the exact nature of excited states near neighbouring Oxygen sites. However, we have tried to make the model as physically plausible as possible by making the 3s wavefunction satisfy *five* boundary conditions as close as possible. We might expect an s-state near a neighbour to be 3s-like since 1s and 2s are already occupied. The choice of an s-state is principally for simplicity. Given that the wavefunction is 3s-like we have demanded firstly that it should have two nodes and secondly be normalised. Hence we chose the hydrogenic form involving only one unknown parameter. Thirdly we have tried to make the 3s wavefunction orthogonal to the 1s and fourthly orthogonal to the 2s wavefunction of Oxygen, the 1s and 2s being accurately known for a free ion. In addition we have demanded that the 3s state should be an unbound state and be the s-state which has the lowest energy consistent with the orthogonality boundary conditions.

Two-electron excitations can also be invoked to produce a SCCF but the angular integrals are more complicated than for our one-electron excitation mechanisms. For excitations involving two electrons the energy denominator appearing in the second order projector formalism will be much larger so we expect contributions from these processes to be small relative to the result of one-electron processes.

We have stated earlier (see section 8.2) that we have used the wavefunctions of Clementi and Roetti (1974) for a neutral Oxygen ion as we felt that each Oxygen would share two electrons with the two hydrogen ions forming the water molecule. Our results do not depend critically on the use of the neutral ion wavefunctions since we have repeated the orthogonality calculations using wavefunctions for the positively charged Oxygen ion given by Clementi and Roetti (1974). We find that the range of A for which the 3s was most orthogonal to the 1s and 2s was the same, the minimum of the sum of squares appearing for a slightly larger value of A . This is not too surprising as the 1s and 2s wavefunctions are very tightly bound within each atom or ion.

We conclude that the inter-site mechanism can produce a μ that is of the right sign and magnitude in order to compensate the intra-site mechanism (TDC1, TDC2). Even though our calculations have been qualitative, they suggest that the resultant ZFS is a delicate balance between a contribution from the paramagnetic Gd^{3+} ion itself (the intra-site mechanism) and one from the host in which it is embedded (the inter-site mechanism). We emphasise that the inter-site mechanism should be treated speculatively because of the various uncertainties involved in the problem. For example, a possible source of error in our model is that s-like wavefunctions were used near the nine neighbouring water molecules. Without a detailed knowledge of the host ion wavefunctions which participate in inter-site interactions it is very difficult to modify this procedure although a molecular orbital calculation for water could be useful. The mechanism also used three effective charges and an average distance in the calculation of the result and all terms quadratic or higher order in overlaps were neglected (see section 8.6).

We finally conclude that although there are a number of uncertainties in the numerics of the inter-site mechanism, the idea of a host contribution to the ZFS *must be important* since there are hosts in which Gd^{3+} has a relative ZFS that is opposite in sign even though the hosts have the same point symmetry and similar structure (Newman and Urban 1972). Such inter-site processes could be very important when calculating ZFSs of Gd^{3+} in other hosts, particularly where the sign of the splitting is opposite to that discussed in this chapter.

CHAPTER 9

CONCLUDING REMARKS

9.1. CFP's for $Er^{3+}Au$

In Table 9.1 we summarise our results, obtained in the first and dominant part of this thesis, for the CFPs of $Er^{3+}Au$, calculated within the first order perturbation theory of the DW model. We see that DW's first order perturbation theory gives a value of 60% of the experimentally determined C_4 CFP. The major contribution to the C_4 CFP derived using DW, originates from the $4f/5d(vbs)$ component which varies considerably with the screening constant k_c (see Table 5.2). We have already discussed the uncertainty of k_c (see section 2.6.3) and by fitting to a small number of experimental results (Table 2.2) we have found that $k_c^{Au} = 0.78a_0^{-1}$. As we have already pointed out earlier, great weight should not be attached to this value, since we used only three experimental data points in the fitting procedure. Nevertheless it suggests that perhaps the screening is larger than the one used throughout our calculations (i.e. $k_c^{Au} = 0.713a_0^{-1}$), and this is supported by many-body calculations which go beyond the RPA (see discussion in section 2.6.3). From Table 5.2 it becomes apparent that if $k_c^{Au} = 0.78a_0^{-1}$ then the contribution of the $4f/5d(vbs)$ mechanism is significantly modified to give $\approx -34cm^{-1}$ while simultaneously the $4f/ligand$ penetration mechanism becomes less important ($\approx 11.5cm^{-1}$ by inspection of Figure 11). The $4f/c_0$

contribution will be insignificantly modified (see Tables 6.4, 6.6) to give slightly smaller contributions and therefore a total value of $\approx -20\text{cm}^{-1}$ is obtained, in excellent agreement with experiment.

Table 9.1 : The CFPs from the three components of DW's first order perturbation theory, in comparison with an unscreened PCM with all neighbouring charges equal to +1, and experiment.

	C_4		C_6	
	$k_z = 0.0a_0^{-1}$	$k_z = 0.713a_0^{-1}$	$k_z = 0.0a_0^{-1}$	$k_z = 0.713a_0^{-1}$
4f/ligand penetration	10.67	12.62	1.54	1.63
4f/5d(vbs)	- 18.09	- 28.53	4.94×10^{-3}	$= 4.94 \times 10^{-3}$
4f/ c_0	2.69	2.68	0.21	$= 0.21$
SUM	- 4.73	- 13.23	1.76	1.85
PCM	8.3		0.83	
Experiment	$- 22.24 \pm 2.78$		4.17 ± 0.35	

Unfortunately, the situation is different for Er^{3+}Ag . According to the DW model the value of the screening constant k_z for Silver is virtually the same as that for Gold, the two being related by $k_z^{\text{Ag}} = \left(\frac{3.01}{3.02}\right)^{1/2} k_z^{\text{Au}}$. Since Er^{3+}Ag is a similar compound (e.g. fcc structure, similar nearest neighbour distance) to the Er^{3+}Au we expect that by applying the DW model in it's first order perturbation theory a similar value for the C_4 CFP of Er^{3+}Ag will result i.e. a value about two times smaller than the experimental one and so the DW model, in it's first order and within the assumptions invoked in our calculations, cannot explain the large C_4 CFP for Er^{3+}Ag . Let us examine each one of the three DW's first order contributions to the C_4 CFP and try to find if there is a decisive difference (at least as far as CFs is concerned) between the Er^{3+}Ag and Er^{3+}Au

dilute alloys. The 4f/ligand penetration mechanism although it plays an important role in determining the C_4 CFP for $Er^{3+}:Au$ cannot be very different for $Er^{3+}:Ag$. The reason is that the main factors which determine the magnitude of the contribution to the C_4 CFP from this particular mechanism are very alike for both systems. In particular, both systems form a fcc structure with nearest neighbour distances $R_{Au}^{Ag} = 5.471a_0$ and $R_{Au}^{Au} = 5.452a_0$. Also there is evidence (Samsonov 1968 p.102,p.106) that the metallic radius of Gold and Silver is virtually the same (i.e. $\approx 1.44 \text{ \AA}$). The final important factor for determining the magnitude of the 4f/ligand penetration contribution is the structure of the ligand wavefunctions themselves. This is expected different for Gold and Silver but we can easily see, by comparing the PCM value and the pseudo-PC value for C_4 in $Er^{3+}:Au$, that this difference cannot be the crucial factor determining the observed differences, in the values of the C_4 CFP, between the two dilute alloys. The 4f/5d(vbs) mechanism is virtually host-independent (the only relatively important dependence on the host comes through the screening constant k_s , which is similar for Gold and Silver) and so cannot be significantly different for the two systems. Finally, the part of the 4f/ ϵ_0 mechanism which has been examined in Chapter 6 of this thesis, for similar reasons as those given for the 4f/ligand penetration mechanism, does not qualify one system against the other. It is clear that the mechanism which will explain the difference in magnitude of the C_4 CFP for $Er^{3+}:Ag$ and $Er^{3+}:Au$ has to be host dependent. There are two main sources from which this can arise. The first is the interaction of the 4f(RE) electrons with the localised ligand electrons and nuclei. The second is due to the conduction electrons. From the above discussion of the 4f/ligand mechanism, whichever type of wavefunction we use, whether atomic or the appropriate one for the metallic phase, large difference of the C_4 CFP for $Er^{3+}:Ag$ and $Er^{3+}:Au$ cannot come about via this mechanism. We therefore believe that the 4f/conduction electron interaction is the most possible candidate to explain the above discrepancy. This interaction should be studied in more detail. One of its components i.e. the 4f/ ϵ_0 interaction has been estimated in this thesis, using parts of the first order DW model, and its contribution to C_4 and C_6 has been found small and of the wrong sign, as far as the C_4 CFP is concerned, with respect to experiment for both the Gold and Silver alloys (at least within the approximations made in section 6.1). Band structure calculations imply that the conduction

band has an appreciable orbital character (i.e. electrons of orbital angular momentum different from zero). In particular it has been found that in Silver and Gold pure metals apart from the majority s-like conduction band there is a set of five narrow d-bands (Christensen and Seraphin 1971, Christensen 1972), not too far below the Fermi energy, which influence the metallic properties of these substances (Ashcroft and Mermin 1976 p.289). By comparison of Figure 5 of Christensen and Seraphin (1971), which shows energy bands of Gold, and Figure 1 of Christensen (1972), which shows energy bands of Silver (see Appendix G), both calculated by the relativistic-augmented-wave-method, it becomes apparent *firstly* that the d-band width is broader in Gold than in Silver, *secondly* that the conduction band of Gold has more d-character than the corresponding conduction band of Silver and *finally* that the conduction band of Gold is broader in total than the one of Silver.

From equation (6.1) we see that $|c_0\rangle$ is also composed of a further correction, which involves other conduction band states coupled to $|c_0\rangle$. This correction is proportional to the inverse of the energy difference between a conduction band state and $|c_0\rangle$ (see equation 6.1). As we have discussed above the d-band width of Gold is larger than the corresponding one in Silver, so these electrons are more delocalised in Gold (for instance Lacueva et al 1982). This suggests that in Gold the average energy the conduction d-band is higher in energy relative to $|c_0\rangle$ than in Silver. Note that the $|c_0\rangle$ lies about half of the band width from the bottom of the band (Dixon and Wardlaw 1986b). Thus the contributions in the further correction term, for sufficiently small denominators, could make the d-like mixing into $|c_0\rangle$ very much more substantial in Silver than Gold. The larger average energy difference, principally due to the larger band width in Gold, could reduce such mixing to small proportions in $Er^{3+}:Au$.

As far as the less important C_4 CFP (at least to determine CF splittings for $Er^{3+}:Ag$ and $Er^{3+}:Au$) we see from Table 9.1 that it is formed mainly from the 4f/ligand penetration mechanism. If we use the above discussion of the penetration interaction this should be modified in the same order for both $Er^{3+}:Ag$ and $Er^{3+}:Au$ so this cannot explain the double size of the C_4 CFP in $Er^{3+}:Ag$ than in $Er^{3+}:Au$. From Table 9.1 it is clear that none of the 4f/5d(vbs) and 4f/ c_0 parts, at least within the approximations invoked in our calculations, can explain the double size of the C_4

CFP for $Er^{3+}Ag$ compared with $Er^{3+}Au$ unless there is strong mixing of f -like character into $|c_0\rangle$ from the conduction band. We might expect the amount of this f -character, arising from the RE ion, mixed with the host conduction states to be small since the resulting $4f$ /conduction mixture states have to be orthogonal. The $4f$ -electrons are known from experiment to be very well localised in Er^{3+} and hence the mixing with conduction states is very small (Anderson 1961). Thus we would expect the conduction band, with the RE present, to be mostly s and d -like as in the pure host. The complex orbital character of the conduction band as well as the band widths and energy differences between $|c_0\rangle$ and conduction band states should be investigated further in detail in order to account for the experimental values. Thus further systematic studies are needed to clarify the role of conduction electrons in CF splittings for these alloys.

Phenomenological models (Das and Ray 1970, Dixon and Dupree 1973) have already pointed out the importance of the inclusion of d and f -character within the conduction band for dilute RE noble metal alloys and pure heavy RE metals.

In the OPW model of Dixon and Dupree (1971a,b,1973) an empirical formula for CFPs was arrived at which describes very well a number of distinctly different experimental results (for instance electric field gradients-Devine and Dixon 1973, susceptibility data-Keller and Dixon 1976, CFs-Kikkert 1980). The first order DW theory, when examined in detail, surprisingly can be put into a similar form :

$$C_2(DW) = C_2(PCM)(1 + P_a)(1 - \sigma_a) + D_a + F_a \quad (9.1)$$

From the investigations undertaken in this thesis (Chapter 3) we see that the P_a arises from the $4f$ /ligand penetration effects and tends to enhance the naive PCM CFPs in the case of positively charged ligands. Actually the P_a 's can be identified by noting that $(1 + P_a)$'s are the pseudo-PCs defined in Chapter 3. For the case of negatively charged ligands we expect that P_a decreases the PCM CFPs (in agreement with *ab initio* calculations by Garcia and Faucher 1984). As the $4f$ electron penetrates the ligand electronic charge distribution it effectively "sees" less of this latter charge and hence a more positive (negative) charge in the case of positively (negatively) charged ligands.

σ_a comes about from the interaction of the 4f electrons with the E_r^{3+} filled cores. This is the well known Sternheimer parameter (Sternheimer 1968). It is negligible for the fourth and sixth order CFPs but important for the second order CFP (Ahmad 1981).

D_a includes components mainly from the 5d(vbs) but also any extra d -like contributions e.g. from an $s-d$ hybridised band.

The F_a parameter has to be introduced to account for the experimental value of the C_4 CFP. From our calculation we cannot provide all contributions which determine it. However, one factor seems to arise from the $4f/c_a$ mechanism. The mixing of the 5d(vbs) with neighbouring orbitals can also add to its value.

Remarkably the formula of equation (9.1), which comes about from the first principles DW model, agrees in form with the OPW one given by equation (2.1) apart from minor differences. For instance by comparison of equations (2.1) and (9.1) we see that the enhancement factor ($\xi/2$) of the PCM CFPs was common for all CFPs whereas in our formula is *order*-dependent. We can therefore understand the successful use of (2.1) in calculating CFPs, electric field gradients and susceptibility data (for a review see Dixon 1974).

9.2. ZFS for Gd^{3+} in Lanthanum Ethylsulphate

In Chapter 8 we calculated the contribution to the ZFS of Gd^{3+} in lanthanum ethylsulphate using an inter-site mechanism whereby an electron was excited to empty 3s-orbitals on nine neighbouring ligands in turn and then back to the RE. We found that, within the approximations used, the results of such a model when combined with all intra-site mechanisms could give excellent agreement with experiment. This calculation involved a number of approximations. The first was that excitation was to a 3s-like orbital on ligands which was described in a hydrogenic form with one parameter (see equation 8.11). This orbital is supposed to be empty so there is considerable uncertainty as to its form. In particular, it may have considerable overlap with similar orbitals on other sites and the RE orbitals and this we tried to incorporate by using Löwdin's technique (see section 8.6). We did however try to incorporate the fact that this was orthogonal to the filled $1s$ and $2s$ states of Oxygen (see section 8.8) A more suitable orbital possibly would be

obtained from a full molecular orbital calculation for water not Oxygen. Whether the Oxygen has a charge of unity or is uncharged or even negatively charged does not appear to affect the calculations significantly.

Following other authors we completely neglected the ethylsulphate radicals and it is not known how good an approximation this is. We also neglected any movement of the water-molecules, in particular their "rocking" motion.

The perturbation method of Stevens we have used to get a SCCF we believe is the best we can hope for since it automatically incorporates all the symmetries involved in *each order*. It is possible to excite electrons to two different sites to produce a two-body anisotropic interaction like the SCCF (Dixon and Tuszyński 1987a) but in this thesis there have not been considered nor have relativistic effects been included explicitly (although we have in a sense done so by putting Wybourne's relativistic result in "other" mechanisms which can be shown to be the most important as far as magnitude is concerned (Dixon and Tuszyński 1987b).

It is interesting to note that there are hosts as similar as YVO_4 and YPO_4 in which the second order CFP, found from experiment, is opposite in sign for Gd^{3+} (Newman and Urban 1972 and references therein). This strongly suggests that the host, in this case at any rate, will play a leading role in the determination of this parameter. In fact it has been suggested in the literature that covalency could play an important role (for instance Smith et al 1977). Hence intra-site mechanisms have been modified in the new host via the CF interaction and not the intra-site states used in the perturbation scheme. However the inter-site contributions involve not only the magnitude of the CF but also excitations from states on the RE to empty sites on *host* ions. We might therefore expect that inter-site contributions will be modified even more than intra-site ones when a different host is present.

APPENDIX A: Generalised Wannier Functions

It is well known that the solutions of the Schrödinger equation for a periodic potential are the Bloch functions $B_{k,n}$ which are plane waves modulated by a periodic factor (Bloch 1928). The quantum number k determines how much the phase changes if we propagate by a lattice vector and the quantum number n (which is called band index) takes integer values. It is worthwhile to stress that the Bloch functions imply propagation without any resistance so they should be a more appropriate description for metals or semiconductors than insulators (Ziman 1972). In an insulator where the electrons are well localised about particular sites a "localised" representation seems desirable. Such a set of localised functions, which are called Wannier functions, are defined as follows:

$$W_n(\underline{r}-\underline{L}) = \frac{1}{N^{1/2}} \sum_{\underline{k}} e^{-i\underline{k}\cdot\underline{L}} B_{k,n}(\underline{r}) \quad (\text{A.1})$$

where the sum over \underline{k} is over those \underline{k} vectors in the first Brillouin zone.

The $W_n(\underline{r}-\underline{L})$ have the following properties:

- (i) they are exponentially localised about particular sites i.e. $W_n(\underline{r}-\underline{L})$ is localised about the site \underline{L} .
- (ii) $W_n(\underline{r}-\underline{L})$ is orthogonal to any $W_{n'}(\underline{r}-\underline{L})$ for $n \neq n'$.
- (iii) Wannier functions centred at different sites are always orthogonal.
- (iv) they are orthogonal to Bloch functions of different bands.

When the periodicity of the potential is lost, as for instance by the presence of an isolated defect, it has been shown (Kohn and Offroy 1973, Gay and Smith 1974) that there exists a set of orthonormal Wannier-like functions, called *generalised* Wannier functions, for the perturbed lattice which have the following properties:

- (i) all the above mentioned properties of the perfect-lattice Wannier functions.
- (ii) similar degree of localisation as the perfect-lattice Wannier functions.
- (iii) as the \underline{L} recedes from the defect site they approach the perfect-lattice Wannier functions.

It is interesting to note that there is a similarity between the generalised (or perfect-lattice Wannier functions) and Löwdin's orthogonalised atomic orbitals (Löwdin 1950) in that they are both localised about ion sites and form an orthonormal set of functions.

APPENDIX B: Analytical Expressions for the Radial Wavefunctions used in Chapter 3

1. Radial Wavefunctions of Neutral-Gold Electronic Orbitals

1s-orbital

$$P_{1s}(r) = C_1 r e^{-Z_1 r}$$

Table B.1 The parameters C_1 and Z_1 which define the 1s radial wavefunction of Gold.

i	C_i	Z_i
1	1388.3661	78.401179

2s-orbital

$$P_{2s}(r) = C_1 r e^{-Z_1 r} + C_2 r^2 e^{-Z_2 r} + C_3 r^3 e^{-Z_3 r}$$

Table B.2 The parameters C_i and Z_i which define the 2s radial wavefunction of Gold.

i	C_i	Z_i
1	464.579	55.931155
2	-10689.9932	35.623429
3	-1631.5514	29.88598

2p-orbital

$$P_{2p}(r) = C_1 r^2 e^{-Zr} + C_2 r^3 e^{-Zr}$$

Table B.3 The parameters C_i and Z_i which define the 2p radial wavefunction of Gold.

i	C_i	Z_i
1	10195.172	43.052115
2	40222.666	36.934307

3s-orbital

$$P_{3s}(r) = C_1 r e^{-Zr} + C_2 r^3 e^{-Zr} + C_3 r^5 e^{-Zr}$$

Table B.4 The parameters C_i and Z_i which define the 3s radial wavefunction of Gold.

i	C_i	Z_i
1	217.1427	34.16282
2	-9496.303	34.57121
3	16936.268	19.29905

3p-orbital

$$P_{3p}(r) = C_1 r^2 e^{-Zr} + C_2 r^3 e^{-Zr} + C_3 r^4 e^{-Zr}$$

Table B.5 The parameters C_i and Z_i which define the 3p radial wavefunction of Gold.

i	C_i	Z_i
1	5122.258	37.84581
2	-6525.176	17.5993
3	-121514.37	26.34928

3d-orbital

$$P_{3d}(r) = C_1 r^2 e^{-Zr} + C_2 r^3 e^{-Zr} + C_3 r^4 e^{-Zr}$$

Table B.6 The parameters C_i and Z_i which define the 3d radial wavefunction of Gold.

i	C_i	Z_i
1	128.30763	12.357452
2	13010.166	20.844903
3	206523.1	44.880613

4s-orbital

$$P_{4s}(r) = C_1 r e^{-Z_1 r} + C_2 r^2 e^{-Z_2 r} + C_3 r^3 e^{-Z_3 r} + C_4 r^4 e^{-Z_4 r}$$

Table B.7 The parameters C_i and Z_i which define the 4s radial wavefunction of Gold.

i	C_i	Z_i
1	105.92873	30.891892
2	-4858.9218	30.997396
3	17223.459	20.876819
4	-5942.6514	10.796395

4p-orbital

$$P_{4p}(r) = r^2 C_1 e^{-Z_1 r} + r^3 [C_2 e^{-Z_2 r} + C_3 e^{-Z_3 r}] + r^4 C_4 e^{-Z_4 r}$$

Table B.8 The parameters C_i and Z_i which define the 4p radial wavefunction of Gold.

i	C_i	Z_i
1	2513.2289	34.466733
2	-11315.234	18.621294
3	682.48	8.347137
4	4967.2254	13.330245

4d-orbital

$$P_{4d}(r) = r^2[C_1 e^{-Z_1 r} + C_2 e^{-Z_2 r}] + r^3[C_3 e^{-Z_3 r} + C_4 e^{-Z_4 r}]$$

Table B.9 The parameters C_i and Z_i which define the 4d radial wavefunction of Gold.

i	C_i	Z_i
1	-12492.83	20.0354
2	12582.8	18.3056
3	-12375.857	17.86026
4	-641.475	7.965333

4f-orbital

$$P_{4f}(r) = r^4 \sum_{i=1}^3 C_i e^{-Z_i r}$$

Table B.10 The parameters C_i and Z_i which define the 4f radial wavefunction of Gold.

i	C_i	Z_i
1	2600.5631	10.40398
2	9780.7777	18.10517
3	108.3835	5.877722

5s-orbital

$$P_{5s}(r) = C_1 r^2 e^{-Zr} + r^3 [C_2 e^{-Zr} + C_3 e^{-2Zr}] + r^4 [C_4 e^{-2Zr} + C_5 e^{-3Zr}] + r^5 C_6 e^{-3Zr}$$

Table B.11 The parameters C_i and Z_i which define the 5s radial wavefunction of Gold.

i	C_i	Z_i
1	12792.106	172.513
2	-36473.673	36.8776
3	10094.765	21.9082
4	-3292.5318	9.86521
5	69.44265	4.31412
6	1665.0793	8.308174

5p-orbital

$$P_{5p}(r) = C_1 r^3 e^{-Zr} + r^4 [C_2 e^{-Zr} + C_3 e^{-2Zr}] + r^5 [C_4 e^{-2Zr} + C_5 e^{-3Zr}]$$

Table B.12 The parameters C_i and Z_i which define the 5p radial wavefunction of Gold.

i	C_i	Z_i
1	82241.64	67.8148
2	-44481.7	21.972091
3	5490.0474	12.26333
4	-7.167242	3.558108
5	-270.58143	5.658748

5d-orbital

$$P_{5d}(r) = r^4 \sum_{i=1}^5 C_i e^{-Z_i r} + r^3 \sum_{i=1}^5 C_i e^{-Z_i r}$$

Table B.13 The parameters C_i and Z_i which define the 5d radial wavefunction of Gold.

i	C_i	Z_i
1	121964.87	41.626691
2	-1937.607	10.517553
3	20910.1	24.970535
4	14.501	2.9096991
5	0.54861442	1.5034575

2. The 4f Radial Wavefunction of Er^{3+}

$$P_{4f}^{Er^{3+}} = r^4 \sum_{i=1}^4 C_i e^{-Z_i r}$$

Table B.14 The parameters C_i and Z_i which define the 4f radial wavefunction of Er^{3+} .

i	C_i (in a_0^{-3})	Z_i (in a_0^{-1})
1	3141.6112	14.375
2	601.33500	8.015
3	71.845565	5.343
4	3.4191078	2.944

3. The 5d(vbs) Radial Wavefunction of Er^{3+}

$$P_{5d(vbs)}^{Er^{3+}} = r^{3.5} \sum_{i=1}^5 C_i e^{-Z_i r} + r^3 \sum_{i=1}^5 C_i e^{-Z_i r}$$

Table B.15 The parameters C_i and Z_i which define the 5d(vbs) radial wavefunction of Er^{3+} .

i	C_i	Z_i
1	6529.53	25.8263
2	- 723.6	8.1395
3	271.377	7.88832
4	3.09486	1.93227
5	0.127524	0.933536

APPENDIX C: Expansion of the Screened Coulomb Interaction in Legendre Polynomials

In this Appendix an analytical technique is developed for the expansion of a screened Coulomb interaction in Legendre polynomials i.e.

$$\frac{F(k_e | \underline{r}_1 - \underline{r}_2 |)}{|\underline{r}_1 - \underline{r}_2|} = \sum_{n=0}^{\infty} a_n(r_1, r_2) P_n(\cos \gamma) \quad (C.1)$$

where \underline{r}_1 and \underline{r}_2 refer to the same origin and γ is the angle between \underline{r}_1 and \underline{r}_2 . By using orthogonality properties of the Legendre polynomials, $a_n(r_1, r_2)$ is given by (see, for instance, Arfken 1970, p.547):

$$a_n(r_1, r_2) = \frac{2n+1}{2} \int_{-1}^1 \frac{F(k_e | \underline{r}_1 - \underline{r}_2 |)}{|\underline{r}_1 - \underline{r}_2|} P_n(x) dx \quad (C.2)$$

where $x = \cos \gamma$. The $|\underline{r}_1 - \underline{r}_2|$ is now written as:

$$r_s (1 + h^2 - 2hx)^{1/2} \quad (C.3)$$

where $h = r_e/r_s$, $r_e = \min(r_1, r_2)$ and $r_s = \max(r_1, r_2)$. We have previously (Christodoulos 1985) determined the following series expansion for the screening function:

$$F(x) = 1 - \frac{2}{\pi} \sum_{t=0}^{\infty} \frac{(-1)^t x^{2t+1}}{(2t+1)(2t+1)!} \quad (C.4)$$

By using equations (C.3) and (C.4) we obtain:

$$a_n(r_1, r_2) = \frac{2n+1}{2r_s} \int_{-1}^1 \left[\frac{1}{(1+h^2-2hx)^{1/2}} - \frac{2}{\pi} \sum_{t=0}^{\infty} \frac{(-1)^t x^{2t+1}}{(2t+1)(2t+1)!} (1+h^2-2hx)^t \right] P_n(x) dx \quad (C.5)$$

where $\lambda = k_e r_s$. Equation (C.5) can be easily rearranged to give:

$$a_n(r_1, r_2) = \frac{2n+1}{2r_s} \left[I_n^*(x) - \frac{2}{\pi} \sum_{t=0}^{\infty} \frac{(-1)^t \lambda^{2t+1}}{(2t+1)(2t+1)!} I_n^t(x) \right] \quad (C.6)$$

where $I_n^t(x)$ is defined as:

$$I_n^t(x) = \int_{-1}^1 (1+h^2-2hx)^t P_n(x) dx \quad (C.7)$$

By using the Legendre polynomials of Arfken (1970 p.541) and integration by parts we finally establish the relations (C.9) for $I_n^t(x)$, $n = 0, 1, 2, 3, 4, 5, 6$. To present our results in a compact form we define the following quantity:

$$f(\kappa, \pm) = - \frac{1}{(i+1) \cdots (i+\kappa)(2h)^{\kappa}} \left[(1-h)^{2(i+\kappa)} \pm (1+h)^{2(i+\kappa)} \right] \quad (\text{C.8})$$

where κ is an integer and the \pm of the LHS is related only to the \pm of the RHS. We finally obtain:

$$\begin{aligned} I_i^0(x) &= f(1, -) \\ I_i^1(x) &= f(1, +) + f(2, -) \\ I_i^2(x) &= f(1, -) + 3f(2, +) + 3f(3, -) \\ I_i^3(x) &= f(1, +) + 6f(2, -) + 15f(3, +) + 15f(4, -) \\ I_i^4(x) &= f(1, -) + 10f(2, +) + 45f(3, -) + 105f(4, +) + 105f(5, -) \\ I_i^5(x) &= f(1, +) + 15f(2, -) + 105f(3, +) + 420f(4, -) + 945f(5, +) + 945f(6, -) \\ I_i^6(x) &= f(1, -) + 21f(2, +) + 210f(3, -) + 1260f(4, +) + 4725f(5, -) \\ &\quad + 10395f(6, +) + 10395f(7, -) \end{aligned} \quad (\text{C.9})$$

We have developed SUBFUNCTIONS, in FORTRAN 77, for the calculation of the $a_n(r_1, r_2)$ for $n = 0, \dots, 6$. To check our programmes, we calculated successfully (in the limit of no screening i.e. $k_c = 0a_0^{-1}$) Slater integrals which appear in the literature.

APPENDIX D: A method for the expansion of Off-Site Functions

A method to calculate multi-center integrals is to express all functions involved in the integrand with respect to a common origin. We wish to develop a method for expanding a function sited at a point \mathbf{R} from the origin, with respect to the origin.

Suppose the off-site wavefunction takes the form:

$$f(|\mathbf{r} - \mathbf{R}|) Y_L^M(\hat{\mathbf{r}}) \quad (\text{D.1})$$

where \mathbf{r} , \mathbf{R} referred to the origin and $(\hat{\mathbf{r}})$ represent the orientation of $\mathbf{r} - \mathbf{R} = \mathbf{r}'$, \mathbf{r}' referred to the off-site point. Using Brink and Satchler (1968 p.151) we may write:

$$|\mathbf{r} - \mathbf{R}|^{-1/2} Y_L^M(\hat{\mathbf{r}}) = \sum_{\lambda, \mu} B(L, \lambda, \mu, R) (-1)^\mu \begin{pmatrix} L-\lambda & \lambda & L \\ M-\mu & \mu & -M \end{pmatrix} Y_{L-\lambda}^{M-\mu}(\hat{\mathbf{r}}) Y_\lambda^\mu(\hat{\mathbf{R}}) \quad (\text{D.2})$$

where:

$$B(L, \lambda, \mu, R) = (-1)^{L-\lambda} (2L+1) \left[\frac{(2L)!}{(2\lambda)!} \frac{4\pi}{[2(L-\lambda)+1] (2\lambda+1)} \right]^{1/2} r^{L-\lambda} R^\lambda \quad (\text{D.3})$$

By writing (D.1) as:

$$\frac{f(|\mathbf{r} - \mathbf{R}|)}{|\mathbf{r} - \mathbf{R}|^{1/2}} [|\mathbf{r} - \mathbf{R}|^{1/2} Y_L^M(\hat{\mathbf{r}})] \quad (\text{D.4})$$

we may use (D.2) and the fact that we may write:

$$\frac{f(|\mathbf{r} - \mathbf{R}|)}{|\mathbf{r} - \mathbf{R}|^{1/2}} = \sum_{\lambda=0}^{\infty} \beta_\lambda(r, R) P_\lambda(\cos\theta) \quad (\text{D.5})$$

to expand (D.1) as a product of spherical harmonics involving $(\hat{\mathbf{r}})$ and $(\hat{\mathbf{R}})$ (by using the Addition Theorem of Spherical Harmonics - Arfken 1970 p.581 - for D.5)

For the specific case, when:

$$f(|\mathbf{r} - \mathbf{R}|) = |\mathbf{r} - \mathbf{R}|^{-1/2} e^{-Z|\mathbf{r} - \mathbf{R}|} \quad (\text{D.6})$$

(i.e. Slater-like orbital) we derive an explicit formula for $\beta_\lambda(r, R)$ as follows:

$$\frac{|\mathbf{r} - \mathbf{R}|^{-1/2}}{|\mathbf{r} - \mathbf{R}|^{1/2}} e^{-Z|\mathbf{r} - \mathbf{R}|} = |\mathbf{r} - \mathbf{R}|^{-1/2} e^{-Z|\mathbf{r} - \mathbf{R}|} = \sum_{\lambda=0}^{\infty} \beta_\lambda(\lambda, Z, r, R) P_\lambda(\cos\theta) \quad (\text{D.7})$$

where:

$$\beta_\lambda(\lambda, Z, r, R) = \frac{2\lambda+1}{2} \int_{-1}^1 |\mathbf{r} - \mathbf{R}|^{-1/2} e^{-Z|\mathbf{r} - \mathbf{R}|} P_\lambda(x) dx \quad (\text{D.8})$$

(see, for instance, Arfken 1970 p.547). The $|L - R|^\lambda$ can be written as :

$$R^\lambda (1 + h^2 - 2hx)^{\lambda/2} \quad (D.9)$$

where $h = \frac{r}{R}$ and $x = \cos(\theta)$. By using standard analytical techniques (equation 12.8 from Arfken 1970 and Gradshteyn and Ryzhik 1965 p.21) we finally obtain :

$$\beta_l(\lambda, Z, r, R) = \frac{(2l+1)R^\lambda}{2h} \sum_{i=0}^{[l/2]} \frac{(-1)^i (2l-2s)!}{2^s l! (l-s)! 2h^{l-2s}} \sum_{q=0}^{l-2s} \frac{(-1)^q (1+h^2)^{l-2s-q}}{(l-2s-q)! q!} \left[e^{-2R(h-1)} \sum_{p=0}^{\lambda+2q+1} \frac{(h-1)^{\lambda+2q+1-p}}{(ZR)^{p+1}} \frac{(l+2q+1)!}{(\lambda+2q+1-p)!} - e^{-2R(h+1)} \sum_{p=0}^{\lambda+2q+1} \frac{(h+1)^{\lambda+2q+1-p}}{(ZR)^{p+1}} \frac{(l+2q+1)!}{(\lambda+2q+1-p)!} \right] \quad (D.10)$$

The notation $[l/2]$ denotes the integer part of the argument $l/2$.

We now wish to define the function $\Lambda_R^{\text{Au}}(r, R)$ used in equation (5.15). The 5d radial wavefunction of Gold, assumed at a site R from the origin, is written as (note that $L = 2$ and the radial wavefunction is given in Appendix B):

$$\frac{R(|L-R|)}{|L-R|^2} = \sum_{i=1}^3 C_i |L-R| e^{-Z_i |L-R|} + \sum_{i=4}^5 C_i e^{-Z_i |L-R|} \quad (D.11)$$

which, by using equation (D.7) and replacing $|L-R|$ by \bar{r} , becomes:

$$\sum_{s=0}^{\infty} A_{ls}(r, R) P_s(\cos\theta) \quad (D.12)$$

where:

$$A_{ls}(r, R) = \sum_{i=1}^3 C_i \beta_s(1, Z_i, r, R) + \sum_{i=4}^5 C_i \beta_s(0, Z_i, r, R) \quad (D.13)$$

We have developed a SUBFUNCTION for the expansion of equation (D.10), in FORTRAN 77. We checked the validity of our expansion very carefully. For instance we successfully reproduced overlaps given by Sharma (1976).

APPENDIX E: Values of the $F_{\lambda}^{n,k}(4f, 5d^{L_n}, 5d^{A_n})$ radial integrals of Chapter 5, in (e^2/a_0) units, for $n=4, 6$.

Table E.1: $F_{\lambda}^{n,k}(4f, 5d^{L_n}, 5d^{A_n})$ radial integrals defined by (5.15) in units of (e^2/a_0) .					
	$n = 4$			$n = 6$	
(\bar{n}, λ)	$k_c = 0.0a_0^{-1}$	$k_c = 0.713a_0^{-1}$	$k_c = 1.0a_0^{-1}$	(\bar{n}, λ)	$k_c = 0.0a_0^{-1}$
(0,0)	0.4224 $\times 10^{-3}$	0.408 $\times 10^{-3}$	0.265 $\times 10^{-3}$	(2,0)	0.3309 $\times 10^{-3}$
(0,1)	0.1263 $\times 10^{-3}$	0.1238 $\times 10^{-3}$	0.924 $\times 10^{-4}$	(2,1)	0.102 $\times 10^{-3}$
(0,2)	0.4643 $\times 10^{-4}$	0.4595 $\times 10^{-3}$	0.376 $\times 10^{-4}$	(2,2)	0.3781 $\times 10^{-4}$
(1,0)	0.1133 $\times 10^{-2}$	0.1091 $\times 10^{-2}$	0.687 $\times 10^{-3}$	(3,0)	0.3588 $\times 10^{-3}$
(1,1)	0.317 $\times 10^{-3}$	0.3095 $\times 10^{-3}$	0.225 $\times 10^{-3}$	(3,1)	0.101 $\times 10^{-3}$
(1,2)	0.1084 $\times 10^{-3}$	0.1071 $\times 10^{-3}$	0.852 $\times 10^{-4}$	(3,2)	0.3283 $\times 10^{-4}$
(2,0)	0.1607 $\times 10^{-2}$	0.1541 $\times 10^{-2}$	0.924 $\times 10^{-3}$	(4,0)	0.3598 $\times 10^{-3}$
(2,1)	0.4154 $\times 10^{-3}$	0.4036 $\times 10^{-3}$	0.281 $\times 10^{-3}$	(4,1)	0.9382 $\times 10^{-4}$
(2,2)	0.1264 $\times 10^{-3}$	0.124 $\times 10^{-3}$	0.962 $\times 10^{-4}$	(4,2)	0.274 $\times 10^{-4}$
(3,0)	0.1885 $\times 10^{-2}$	0.1799 $\times 10^{-2}$	0.102 $\times 10^{-2}$	(5,0)	0.3473 $\times 10^{-3}$
(3,1)	0.4554 $\times 10^{-3}$	0.4403 $\times 10^{-3}$	0.291 $\times 10^{-3}$	(5,1)	0.855 $\times 10^{-4}$
(3,2)	0.1242 $\times 10^{-3}$	0.121 $\times 10^{-3}$	0.903 $\times 10^{-4}$	(5,2)	0.2292 $\times 10^{-4}$
(4,0)	0.2021 $\times 10^{-2}$	0.1922 $\times 10^{-2}$	0.103 $\times 10^{-2}$	(6,0)	0.326 $\times 10^{-3}$
(4,1)	0.4645 $\times 10^{-3}$	0.447 $\times 10^{-3}$	0.279 $\times 10^{-3}$	(6,1)	0.7693 $\times 10^{-4}$
(4,2)	0.1165 $\times 10^{-3}$	0.1133 $\times 10^{-3}$	0.803 $\times 10^{-4}$	(6,2)	0.194 $\times 10^{-4}$
(5,0)	0.2054 $\times 10^{-2}$	0.194 $\times 10^{-2}$	0.982 $\times 10^{-3}$	(7,0)	0.2987 $\times 10^{-3}$
(5,1)	0.4556 $\times 10^{-3}$	0.433 $\times 10^{-3}$	0.258 $\times 10^{-3}$	(7,1)	0.6852 $\times 10^{-4}$
(5,2)	0.1078 $\times 10^{-3}$	0.103 $\times 10^{-3}$	0.702 $\times 10^{-4}$	(7,2)	0.1653 $\times 10^{-4}$
(6,0)	0.201 $\times 10^{-2}$	0.19 $\times 10^{-2}$	0.908 $\times 10^{-3}$	(8,0)	0.2702 $\times 10^{-3}$
(6,1)	0.435 $\times 10^{-3}$	0.413 $\times 10^{-3}$	0.233 $\times 10^{-3}$	(8,1)	0.6034 $\times 10^{-4}$
(6,2)	0.98 $\times 10^{-4}$	0.944 $\times 10^{-4}$	0.609 $\times 10^{-4}$	(8,2)	0.1408 $\times 10^{-4}$
(7,0)	0.191 $\times 10^{-2}$	0.18 $\times 10^{-2}$	0.817 $\times 10^{-3}$	(9,0)	0.2397 $\times 10^{-3}$
(7,1)	0.404 $\times 10^{-3}$	0.384 $\times 10^{-3}$	0.206 $\times 10^{-3}$	(9,1)	0.5266 $\times 10^{-4}$
(7,2)	0.8904 $\times 10^{-4}$	0.855 $\times 10^{-4}$	0.524 $\times 10^{-4}$	(9,2)	0.1092 $\times 10^{-4}$
(8,0)	0.1774 $\times 10^{-2}$	0.167 $\times 10^{-2}$	0.719 $\times 10^{-3}$	(10,0)	0.2101 $\times 10^{-3}$
(8,1)	0.37 $\times 10^{-3}$	0.351 $\times 10^{-3}$	0.179 $\times 10^{-3}$	(10,1)	0.4382 $\times 10^{-4}$
(8,2)	0.7988 $\times 10^{-4}$	0.765 $\times 10^{-4}$	0.447 $\times 10^{-4}$	(10,2)	0.946 $\times 10^{-5}$

APPENDIX F: Data Used for the Calculations of Chapter 8

Table F.1: Parameters of the 4f-radial wavefunction for Gd³⁺

i	W_i (in a_0^{-1})	B_i (in $a_0^{-3/2}$)
1	12.554	1923.8151
2	7.046	329.66724
3	4.697	43.274827
4	2.578	1.5047469

Table F.2: Values of the 6j-symbol $\left\{ \begin{matrix} 3 & 2 & 1 \\ L & L & L \end{matrix} \right\}$

l	$L=0$	$L=2$	$L=4$	$L=6$
1	0	$+\left(\frac{2^2}{5 \times 7^2}\right)^{1/2}$	$+\left(\frac{11}{2 \times 3^2 \times 7^2}\right)^{1/2}$	0
3	$\frac{1}{7}$	$+\left(\frac{192}{2 \times 3^2 \times 5^2 \times 7^2}\right)^{1/2}$	$-\left(\frac{1}{2^2 \times 7^2}\right)^{1/2}$	$+\left(\frac{5^2}{2 \times 3^2 \times 7^2}\right)^{1/2}$
5	0	$+\left(\frac{1}{2^2 \times 3^2 \times 7^2}\right)^{1/2}$	$+\left(\frac{13}{5 \times 7^2 \times 11}\right)^{1/2}$	$+\left(\frac{1}{2 \times 9 \times 11}\right)^{1/2}$

Table F.3: Values of the $\langle l11Y_L113 \rangle$

l	$L=0$	$L=2$	$L=4$	$L=6$
1	0	$+\left(\frac{9}{4\pi}\right)^{1/2}$	$-\left(\frac{3}{\pi}\right)^{1/2}$	0
3	$+\left(\frac{7}{4\pi}\right)^{1/2}$	$-\left(\frac{7}{3\pi}\right)^{1/2}$	$+\left(\frac{9 \times 7}{2 \times 11 \times \pi}\right)^{1/2}$	$-\left(\frac{7 \times 25}{3 \times 11 \times \pi}\right)^{1/2}$
5	0	$+\left(\frac{25}{6 \times \pi}\right)^{1/2}$	$-\left(\frac{5 \times 9}{13 \times \pi}\right)^{1/2}$	$+\left(\frac{49}{12 \times \pi}\right)^{1/2}$

Table F.4 : Values of Δ , KE and PE components of $P(R_1)$ for $Z_{eff} = 10$ varying with A for $R_1 = 4.4785a_0$

A	Δ in 10^8cm^{-1} independent of R ($Z_{eff} = 0$)	KE in e^2/a_0 $\times 10^{-2}$	PE in e^2/a_0 $\times 10^{-2}$	$P(R_1)$ in e^2/a_0 $\times 10^{-2}$
1.4	2.187	0.3311	+ 0.9046	+ 1.2360
1.5	2.432	0.5631	- 0.5400	+ 0.0231
1.6	2.699	0.7548	- 1.8920	- 1.1370
1.7	2.988	0.8970	- 3.0800	- 2.1830
1.8	3.299	0.9872	- 4.0640	- 3.0770
1.9	3.632	1.0280	- 4.8320	- 3.8040

Table F.5 : Values of KE and PE components of $P(R_2)$ for $Z_{eff} = 10$ varying with A for $R_2 = 4.7619a_0$

A	KE in e^2/a_0 $\times 10^{-2}$	PE in e^2/a_0 $\times 10^{-2}$	$P(R_2)$ in e^2/a_0 $\times 10^{-2}$
1.4	0.4432	- 0.4489	- 0.0057
1.5	0.5929	- 1.6170	- 1.0240
1.6	0.6988	- 2.6310	- 1.9320
1.7	0.7593	- 3.4520	- 2.6920
1.8	0.7774	- 4.0690	- 3.2920
1.9	0.7590	- 4.4910	- 3.7320

Table F.6 : Values of $R(I, L)$ in cm as A varies and for $Z_{eff} = 0$. Columns headed (I, L)

A	$\times 10^{-3}$ (3,0)	$\times 10^{-3}$ (5,2)	$\times 10^{-3}$ (3,2)	$\times 10^{-4}$ (1,2)	$\times 10^{-4}$ (5,4)	$\times 10^{-5}$ (3,4)	$\times 10^{-5}$ (1,4)	$\times 10^{-4}$ (5,6)	$\times 10^{-5}$ (3,6)
1.4	-8.313	1.199	-2.217	1.1853	6.733	-1.512	8.424	6.889	-1.938
1.5	-7.476	1.079	-1.994	1.0660	6.004	-1.360	7.575	6.196	-1.743
1.6	-6.736	0.972	-1.796	0.9605	5.452	-1.225	6.826	5.580	-1.571
1.7	-6.086	0.878	-1.623	0.8676	4.928	-1.107	6.166	5.041	-1.418
1.8	-5.511	0.796	-1.470	0.7857	4.461	-1.002	5.584	4.567	-1.284
1.9	-5.007	0.723	-1.335	0.7137	4.050	-0.911	5.073	4.149	-1.167

Table F.7 : Values of $Q(I, L, R)$ in e^2/a_0 for $R_1 = 4.4785a_0$ as A varies. Columns headed (I, L) .

A	$\times 10^{-3}$ (3,0)	$\times 10^{-4}$ (5,2)	$\times 10^{-4}$ (3,2)	$\times 10^{-3}$ (1,2)	$\times 10^{-5}$ (5,4)	$\times 10^{-4}$ (3,4)	$\times 10^{-5}$ (1,4)	$\times 10^{-5}$ (5,6)	$\times 10^{-4}$ (3,6)
1.4	-0.925	-2.429	0.305	8.00	-7.234	0.550	4.540	-3.760	0.441
1.5	0.497	-2.138	3.307	8.04	-5.995	1.913	4.535	-3.017	1.300
1.6	1.829	-1.711	5.993	7.76	-4.338	3.105	4.353	-2.054	2.048
1.7	3.000	-1.190	8.227	7.26	-2.421	4.069	4.050	-0.9628	2.644
1.8	3.978	-0.6195	9.944	6.62	-0.4	4.780	3.670	0.1693	3.076
1.9	4.741	-0.0375	11.14	5.92	1.590	5.240	3.260	1.267	3.348

Table F.8 : Values of $Q(I, J, R)$ in $e^2 a_0$ for $R_2 = 4.7619 a_0$ as A varies. Columns headed (I, J) .

A	$\times 10^{-3}$ (3,0)	$\times 10^{-4}$ (5,2)	$\times 10^{-4}$ (3,2)	$\times 10^{-3}$ (1,2)	$\times 10^{-3}$ (5,4)	$\times 10^{-4}$ (3,4)	$\times 10^{-3}$ (1,4)	$\times 10^{-3}$ (5,6)	$\times 10^{-4}$ (3,6)
1.4	0.418	-1.511	2.551	6.98	-4.144	1.446	3.93	-2.070	0.978
1.5	1.570	-1.177	4.800	6.72	-2.890	2.436	3.76	-1.350	1.595
1.6	2.572	-0.768	6.645	6.25	-1.434	3.221	3.48	-0.534	2.079
1.7	3.385	-0.3225	8.020	5.64	0.0902	3.780	3.12	0.309	2.417
1.8	3.999	0.1262	8.926	4.98	1.569	4.119	2.73	1.113	2.614
1.9	4.421	0.5508	9.410	4.32	2.915	4.262	2.35	1.832	2.687

Table F.9 : The $\langle g_{11}(r) | g_{11}(|r - R|) \rangle$ overlap. All R_{ij} are in a_0 units.

A	$\times 10^{-1}$ $R_{12}=4.986$	$\times 10^{-1}$ $R_{17}=6.861$	$\times 10^{-2}$ $R_{10}=8.482$	$\times 10^{-2}$ $R_{45}=8.248$	$\times 10^{-2}$ $R_{14}=7.924$	$\times 10^{-1}$ $R_{13}=6.537$
1.4	3.1498	1.7033	6.978	8.074	9.7936	1.962
1.5	2.9113	1.3413	4.675	5.538	6.2412	1.594
1.6	2.6442	1.0269	3.040	3.688	4.7769	1.260
1.7	2.3581	0.7667	1.926	2.392	3.2025	0.972
1.8	2.0653	0.5595	1.191	1.516	2.0976	0.733
1.9	1.7775	0.3999	0.722	0.941	1.3456	0.541

Table F.10 : Radial integral of the $\langle f_{4f}(r) | g_{2s}(1r - R) \rangle$ overlap.

A	$\times 10^{-3}$	$\times 10^{-3}$
	$R_1 = 4.4785a_0$	$R_2 = 4.7619a_0$
1.4	- 3.6988	- 0.4367
1.5	- 0.6250	2.1914
1.6	2.3407	4.5583
1.7	5.0397	6.5682
1.8	7.3759	8.1810
1.9	9.3048	9.3974

APPENDIX G: RAPW energy bands of Silver and Gold

1. RAPW band structure of Gold

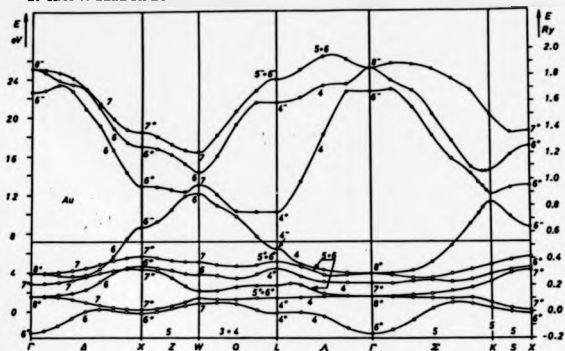


FIG. 5. RAPW energy bands of gold (normal volume). $E_F = 0.530$ Ry. Energies are measured from the muffin-tin zero.

2. RAPW band structure of Silver

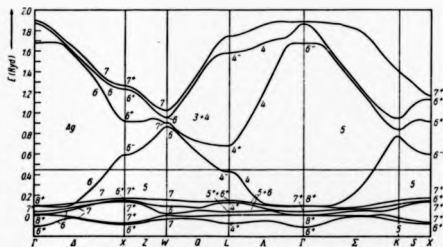


Fig. 1. RAPW band structure of silver along symmetry lines. (Note that the labels of the irreducible representations at L are not the 'conventional'). Energies are in Ryd above the muffin-tin zero (MTZ). The Fermi level lies 0.444 above MTZ.

REFERENCES

International Conferences on Crystal Field Effects

- [1] "*Crystalline Electric Field Effects in Metals and Alloys*" edited by R A B Devine-held in Montreal/CANADA 1974 (Universite de Montreal 1974)
 - [2] "*Crystal Field Effects in Metals and Alloys*" edited by A Furrer-held in Zurich/SWITZERLAND 1976 (New York: Plenum Press 1977)
 - [3] "*Crystalline Electric Field and Structural Effects in f-Electron Systems*" edited by J E Crow, R P Guertin and T W Mihalasin-held in Philadelphia/USA 1979 (New York: Plenum Press 1980)
 - [4] "*Crystalline Electric Field Effects in f-Electron Magnetism*" edited by R P Guertin, W Suski and Z Zolnierak-held in Wroclaw/POLAND 1981 (New York: Plenum Press 1982)
 - [5] "*Crystalline Field and Anomalous Mixing Effects in f-electron Systems*" edited by T Kasuya-held in Sendai/JAPAN 1985 (published in *J Magn Magn Mater* **52**, 1985)
- Abragam A and Bleaney B 1970, "*Electron Paramagnetic Resonance of Transition Ions*", (Oxford: Oxford University Press)
- Ahmad S 1981, *J Phys C: Solid State Phys* **14**, 2759-69
- Arfken G 1970, "*Mathematical Methods for Physicists*", (New York: Academic Press)
- Anderson P W 1961, *Phys Rev* **124**, 41-53
- Ashcroft N W and Mermin N D 1976, "*Solid State Physics*", (Philadelphia: Saunders College)
- Atkins P W 1983, "*Molecular Quantum Mechanics*", (Oxford: Oxford University Press)
- Baberschke K 1982, "*Crystalline Electric Field Effects in f-Electron Magnetism*", edited by R P Guertin, W Suski and Z Zolnierak (New York: Plenum), 101-12
- Bates C A, Dixon J M, Fletcher J R and Stevens K W H 1968, *J Phys C: Solid State Phys* **1**, 859-71

- Ballhausen C J 1962, *"Introduction to Ligand Field Theory"*, (New York: McGraw-Hill Book Company, Inc)
- Batson P E, Chen C H and Silcox J 1976, *Phys Rev Lett* **37**, 937-40
- Becquerel J 1929, *Z. Physik* **58**, 205-16
- Belorisky E, Berthier Y and Devine R A B 1984, *J Magn Magn Mater* **44**, 313-28
- Bethe H 1929, *Ann Physik* **3**, 133-206 (English Translation "Splitting of Terms in Crystals" by Consultants Bureau Inc: New York)
- Bishton S S and Newman D J 1970, *J Phys C:Solid State Phys* **3**, 1753-61
- Bleaney B, Scovil H E D and Trenam R S 1954, *Proc Roy Soc A (London)* **223**, 15-29
- Bleaney B and Stevens K W H 1953, *Rept Prog Phys* **16**, 108-59
- Bloch F 1928, *Z. Physik* **52**, 555-600
- Bohm D and Pines D 1953, *Phys Rev* **92**, 609-25
- Buckmaster H A, Chatterjee R and Shing Y H 1972, *Can J Phys* **50**, 991-1001
- Buehler R J and Hirschfelder J O 1951, *Phys Rev* **83**, 628-33
- Buehler R J and Hirschfelder J O 1952, *Phys Rev* **85**, 149
- Chatterjee R, Smith M R and Buckmaster H A 1976, *Can J Phys* **54**, 1228-33
- Chow H C 1973, *Phys Rev B* **7**, 3404-5
- Christensen N E 1972, *Phys Stat Sol (b)* **54**, 551-63
- Christensen N E and Seraphin B O 1971, *Phys Rev B* **4**, 3321-44
- Christodoulos F 1985, *"Screening effects on Crystalline Electric Fields for Er^{3+} in Gold"*, MSc thesis, University of Warwick, UK
- Clementi E and Roetti C 1974, *"Atomic Data and Nuclear Data Tables - Roothaan-Hartree-Fock Atomic Wavefunctions"* **14**, Numbers 3-4, (New York: Academic Press)
- Condon E V and Shortley G H 1935, *"The Theory of Atomic Spectra"*, (Cambridge: Cambridge University Press)

- Dagg I R, Kemp R C and Symmons H F 1969, *J Phys C: Solid State Phys* **2**, 1098-101
- Daniel E and Friedel J 1965, "9th International Conference on Low Temperature Physics", edited by J Daunt, P Edward, F Milford and M Yaqub (New York: Plenum), 933-54
- Daniels J, Festenberg C V, Raether H and Zeppenfeld K 1970, *Springer Tracts in Modern Physics* **54**, 78-135
- Das K C and Ray D K 1970, *Solid State Commun* **8**, 2025-8
- Devine R 1974, *J Phys F: Met Phys* **4**, 1447-53
- Devine R A B and Dixon J M 1973, *Phys Rev B* **7**, 4902-7
- Dieke G H 1968, "Spectra and Energy Levels of Rare Earth Ions in Crystals", (New York: Interscience Publishers)
- Dirac P A M 1958, "The Principles of Quantum Mechanics", (Oxford: Clarendon Press)
- Dixon J M 1973, *Solid State Commun* **12**, 789-94
- Dixon J M 1974, "Crystalline Electric Field Effects in Metals and Alloys", edited by R A B Devine (Montreal: Universite de Montreal 1974), 322-48
- Dixon J M and Chatterjee R 1980a, *Phys Status Solidi (b)* **99**, 313-7
- Dixon J M and Chatterjee R 1980b, *Phys Lett A* **76**, 147-8
- Dixon J M, Chatterjee R and McInnes J A 1982, *Phys Status Solidi (b)* **111**, 155-60
- Dixon J M and Dupree R 1971a, *J Phys F: Metal Phys* **1**, 539-48
- Dixon J M and Dupree R 1971b, *J Phys F: Metal Phys* **1**, 549-53
- Dixon J M and Dupree R 1973, *J Phys F: Metal Phys* **3**, 118-24
- Dixon J M and Tuszyński J A 1987a, *J Phys C: Solid State Phys*, to be published
- Dixon J M and Tuszyński J A 1987b, *Physica A*, to be published
- Dixon J M and Wardlaw R S 1986a, *Physica A* **135**, 105-38
- Dixon J M and Wardlaw R S 1986b, *J Phys C: Solid State Phys* **19**, 943-61

- Dixon J M, Wardlaw R S and Stevens K W H 1984, *Physica B* **124**, 149-55
- Dunlap B D, Hall L N, Behroozi F, Crabtree W G and Niarchos D G 1984, *Phys Rev B* **29**, 6244-51
- Duthie J C and Heine V 1979, *J Phys F: Metal Phys* **9**, 1349-55
- Economou E N 1979, "*Green's Functions in Quantum Physics*", (Berlin: Springer-Verlag)
- Eisenberger P, Platzman P M and Schmidt P 1975, *Phys Rev Lett* **34** 18-20
- Elliott R J and Stevens K W H 1952, *Proc Roy Soc A (London)* **215**, 437-53
- Elliott R J and Stevens K W H 1953a, *Proc Roy Soc A (London)* **218**, 553-66
- Elliott R J and Stevens K W H 1953b, *Proc Roy Soc A (London)* **219**, 387-404
- Fert A and Levy P M 1977, *Phys Rev B* **16**, 5052-67
- Fitzwater D R and Rundle R E 1959, *Z Kristallogr* **112**, 362
- Freed S 1931, *Phys Rev* **38**, 2122-30
- Freeman A J and Desclaux J P 1979, *J Magn Magn Mat* **12**, 11-21
- Freeman A J and Watson R E 1962, *Phys Rev* **127**, 2058-75
- Frick B and Loewenhaupt M 1986a, *Z Phys B: Cond Matter* **63**, 213-30
- Frick B and Loewenhaupt M 1986b, *Z Phys B: Cond Matter* **63**, 231-40
- Fulde P 1979, "*Handbook of the Physics and Chemistry of Rare Earths*", edited by K A Gschneider and L Eyring (Amsterdam: North-Holland Publishing Company), 295-386
- Fulde P and Loewenhaupt M 1986 *Advn Phys* **34**, 589-661
- Gajek Z and Mulak J 1985, *Int J Quant Chem* **XXVIII**, 889-94
- Garcia D and Faucher M 1984, *Phys Rev B* **29**, 1703-7
- Gay J G and Smith J R 1974, *Phys Rev B* **9**, 4151-64
- Gerloch M 1986, "*Orbitals, Terms and States*", (Chichester: John Wiley & Sons)
- Gibbons P C, Schnatterly S E, Riisko J J and Field J R 1976, *Phys Rev B* **13**, 2451-60

- Gorter C J 1932, *Phys Rev* **42**, 437-8
- Gradshteyn I S and Ryzhik I M 1965, *Tables of Integrals, Series and Products*, (London: Academic Press)
- Griffiths D and Coles B R 1966, *Phys Rev Lett* **16**, 1093-5
- Heine V 1960, *"Group Theory"*, (New York: Pergamon Press)
- Heiniger F, Purwins H G and Walker E 1974, *Phys Lett A* **47**, 53-4
- Hellwege K H 1939a, *Z. Physik* **113**, 192-202
- Hellwege K H 1939b, *Ann. Physik* **34**, 521-40
- Hellwege K H 1947, *Nachr. Akad. Wiss. Göttinger, Math-Phys. Kl.*, 58-66
- Herman F and Skillman S 1963, *"Atomic Structure Calculations"*, (Englewood Cliffs, New Jersey: Prentice Hall Inc)
- Hirst L L, Williams G, Griffiths D and Coles B R 1968, *J Appl Phys* **39**, 844-6
- Hoenig H E, Mappel H, Njoo H K and Seim H 1974, *"Crystalline Electric Field Effects in Metals and Alloys"*, edited by R A B Devine (Université de Montréal), 298-324
- Hüfner S 1978, *"Optical Spectra of Transparent Rare Earth Compounds"*, (New York: Academic Press)
- Hutchings M T 1964, *Solid State Phys* **16**, 227-73
- Hutchison C A, Judd B R and Pope D F D 1957, *Proc Phys Soc B* **70**, 514-20
- Joos G 1939, *Ergeb. Exakt Naturwiss* **18**, 78-98
- Jordahl O 1934, *Phys Rev* **45**, 87-97
- Judd B R 1955, *Proc Roy Soc A (London)* **232**, 458-74
- Judd B R 1967, *"Second Quantisation and Atomic Spectroscopy"*, (Baltimore: The John Hopkins Press)
- Judd B R 1977, *Phys Rev Lett* **39**, 242-4
- Judd B R 1985, *Rep Prog Phys* **48**, 907-54

- Kasuya T 1966, "*Magnetism II B*", edited by G T Rado and H Suhl (New York: Academic Press), 271
- Keller G and Dixon J M 1976, *J Phys F: Metal Phys* **6**, 819-28
- Ketelaar J A A 1937, *Physica* **4**, 619
- Kikert P J W 1980, "*Crystal Field of Dy in non-magnetic Metals*", PhD thesis, University of Croningen, The Netherlands
- Kittel C 1976, "*Introduction to Solid State Physics*", (New York: John Wiley & Sons, 5th edition)
- Kohn W and Offroy J R 1973, *Phys Rev B* **8**, 2485-95
- Kramers H A 1930, *Proc Acad Sci (Amsterdam)* **23**, 959-72
- Lacueva G, Levy P M and Fert A 1982, *Phys Rev B* **26**, 1099-124
- Lea K R, Leask M J M and Wolf W P 1962, *J Phys Chem Solids* **23**, 1381-405
- Löwdin P O 1950, *J Chem Phys* **18**, 365-75
- Lucken E A C 1961, *Encyclopaedic Dictionary of Physics* **1**, 324-6
- Lulek T 1969, *Acta Phys Polon* **26**, 551-69
- del Moral A 1984, *J Phys F: Metal Phys*, **14**, 1477-90
- Morin P, Pierre J, Schmitt D and Drexel W 1976, *J Phys (France)* **37**, 611-6
- Morin P, Rouchy J and du Tremolet de Lacheisserie E 1977, *Phys Rev B* **16**, 3182-93
- Morrison J C, Fields P R and Carnall W T 1970, *Phys Rev B* **2**, 3526-32
- Newman D J 1970, *Chem Phys Lett* **6**, 288-90
- Newman D J 1971, *Advn Phys* **20** 197-256
- Newman D J and Urban W 1972, *J Phys C: Solid State Phys* **5**, 3101-9
- Orton J W 1968, "*Electron Paramagnetic Resonance*", (London: Iliffe Books Ltd)
- Oseroff S, Passeggi M, Wohlleben D and Schultz S 1977, *Phys Rev B* **15**, 1283-90

- Pal R K and Tripathy D N 1985, *Pramāna* **24**, 905-10
- Pal R K, Tripathy D N and Mandal S S 1980, *Phys Stat Sol (b)* **100**, 651-8
- Parker F T, Oesterreicher H and Eno H 1977, *Phys Rev B* **16**, 4382-4
- Pines D 1964, *"Elementary Excitations in Solids"*, (New York: W A Benjamin, Inc)
- Post K and Niesen L 1984, *J Phys F: Metal Phys* **14**, 2203-12
- Praether J L 1961, *"Atomic Energy in Crystals"*, (Nat Bur Stand Monograph, No 19)
- Prokhorov A M 1986, *Sov Phys Usp* **29**, 3-19
- Pryce M H L 1950, *Phys Rev* **80**, 1107-8
- Racah G 1942a, *Phys Rev* **61**, 186-97
- Racah G 1942b, *Phys Rev* **62**, 438-62
- Racah G 1943, *Phys Rev* **63**, 367-82
- Racah G 1949, *Phys Rev* **76**, 1352-65
- Raether H 1980, *Springer Tracts in Modern Physics* **88**
- Raimes S 1957, *Rep Prog Phys* **20**, 1-37
- Raimes S 1961, *"The Wave Mechanics of Electrons in Metals"*, (Amsterdam: North-Holland Publishing Company)
- Raimes S 1972, *"Many Electron Theory"*, (Amsterdam: North-Holland Publishing Company)
- Rainford B D, Turberfield K G, Busch G and Vogt O 1968, *J Phys C: Solid State Phys* **1**, 679-83
- Rajnak K and Krupke W F 1967, *J Chem Phys* **46**, 3532-42
- Rajnak K and Wybourne B G 1964, *J Chem Phys* **41**, 565-9
- Rotenberg M, Bivins R, Metropolis N and Wooten J K Jr 1959, *"The 3-j and 6-j symbols"*, (Cambridge, Mass: The Technology Press, MIT)
- Russell H N and Saunders F A 1925, *Astrophys J* **61**, 38
- Samsonov G V 1968, *"Handbook of the Physicochemical Properties of the Elements"*, (London: Oldbourne Book Co. Ltd)

- Sandars P G H and Beck J 1965, *Proc Roy Soc A* **282**, 97-107
- Schiff L I 1968, "*Quantum Mechanics*", (New York: McGraw-Hill Inter Book Company)
- Schlapp R and Penney W G 1932, *Phys Rev* **42**, 666-86
- Schmitt D, Morin P and Pierre J 1977, *Phys Rev B* **15**, 1698-705
- Sharma R R 1976, *Phys Rev A* **13**, 517-27
- Shenoy G K, Crabtree G W, Niarchos D, Behroozi F, Dunlap B D, Hinks D and Noakes D R 1982, "*Crystalline Electric Field Effects in f-Electron Magnetism*", edited by R P Guertin, W Suski and Z Zolnierak (New York: Plenum), 431-41
- Silver B R 1976, "*Irreducible Tensor Methods*", (New York: Academic Press)
- Slater J C 1953, *Rev Mod Phys* **25**, 199-210
- Smith D and Thornley J H M 1966, *Proc Phys Soc* **82**, 779-81
- Smith M R, Shing Y H, Chatterjee R and Buckmaster H A 1977, *J Magn Resonance* **26**, 351-63
- Spedding F 1940, *Phys Rev* **58**, 255-7
- Sternheimer R M, Blume M and Peierls R F 1968, *Phys Rev* **173**, 376-89
- Stevens K W H 1952, *Proc Phys Soc A (London)* **65**, 209-15
- Stevens K W H 1974, *Phys Lett A* **47**, 401-3
- Stevens K W H 1976, *Phys Lett C* **24**, 1-75
- Stevens K W H 1977, "*Crystal Field Effects in Metals and Alloys*" edited by A Furrer (New York: Plenum), 1-8
- Stevens K W H 1980, "*Crystalline Electric Field and Structural Effects in f-Electron Systems*", edited by J E Crow, R P Guertin and T W Mihalisin (New York: Plenum), 1-7
- Stewart G R 1984, *Rev Mod Phys* **56**, 755-87
- Tinkham M 1964, "*Group Theory in Quantum Mechanics*", (New York: McGraw-Hill Inter Book Company)
- Touborg P, Nevald R and Johansson T 1978, *Phys Rev B* **17**, 4454-60

- Touborg P 1979, "*Experimental Investigations of the Crystal Fields in Rare Earth Metals and their Alloys*" (Odense: Odense University Press)
- Tomaschek R and Deutschbein O 1933, *Physik Z* **34**, 373-6
- Tomaschek R 1942, *Ergeb Exakt Naturwiss* **20**, 268-302
- Tuszyński J A 1983, "*Applications of effective operator techniques in the Crystal Field Theory*", PhD thesis, University of Calgary, Canada
- Tuszyński J A, Dixon J M and Chatterjee R 1984, *Physica A* **127**, 228-40
- Tuszyński J A, Dixon J M and Chatterjee R 1986, *Physica A* **135**, 213-25
- Ulrich D L and Barnes R G 1967, *Phys Rev* **164**, 428-35
- Van Vleck J H 1932a, "*Theory of Magnetic and Electric Susceptibilities*", (Oxford: Oxford University Press)
- Van Vleck J H 1932b, *Phys Rev* **41**, 208-15
- Vogt O and Cooper B R 1968, *J Appl Phys* **39**, 1202-4
- Wannier G H 1937, *Phys Rev* **52**, 191-7
- Williams G and Hirst L L 1969, *Phys Rev* **183**, 407-15
- Woodgate G K 1983, "*Elementary Atomic Structure*", (Oxford: Oxford University Press, 2nd edition)
- Wybourne B G 1965a, "*Spectroscopic properties of Rare-earths*", (New York: Interscience Publishers-John Wiley & Sons, Inc)
- Wybourne B G 1965b, *J Chem Phys* **43**, 4506
- Wybourne B G 1966, *Phys Rev* **148**, 317-27
- Zacharias P 1975, *J Phys F: Metal Phys* **5**, 645-56
- Ziman J M 1972, "*Principles of the Theory of Solids*", (Cambridge: Cambridge University Press)
- Zirngiebl E, Hillebrands B, Blumenröder S, Güntherodt G, Loewenhaupt M, Carpenter J M, Winzer K and Fisk Z 1984, *Phys Rev B* **30**, 4052-54

Zolnierek Z 1984, *J Phys Chem Solids* 45, 523-8

Zolnierek Z 1985, *Solid St Commun* 56, 609-14